AN ABSTRACT OF THE THESIS OF

Timothy Joe Dodson for the degree of Master of Science in Civil Engineering presented on July 12, 1983

Title: Influence of Geotextile Permeability on Stability of Rubble Shore Protection Structures

Redacted for Privacy

Abstract approved: Dr. J.R. Bell

The effect of geotextile permeability on the stability of rubble shore protection structures was investigated by conducting large-scale wave tank tests on a revetment. Pore pressure within the sandy gravel core of the revetment were measured in one phase of the experiment, and stability of armor units on the structure face were measured in a second phase.

During application of waves to the test structure, mean pore pressures within the core, called "residual pore pressures," are observed to rise in a specific pattern which is relatively insensitive to geotextile permeability. The transinet pore pressure response pattern corresponds well to the qualitative pattern predicted by analytic models of pore pressure response in cohesionless soils below an ocean floor subjected to wave loading. Stability of armor units is observed to be independent of geotextile permeability.

A qualitative descriptive model is proposed as a means of explaining the measured pore pressure response. The model combines a theorized pore pressure gradient due to an "average" circulating flow in the core superimposed on a pattern of residual pore pressures generated as a response to cyclic shear stresses.

Results of the experimental tests show that, for the condition tested, a decrease in geotextile permeability does not lead to a decrease in structure stability. Residual pore pressures are not greater and armor units are not observably less stable when a less permeable or impermeable geotextile is used.

Influence of Geotextile Permeability on Stability of Rubble Shore Protection Structures

by

Timothy Joe Dodson

A THESIS

submitted to

Oregon State University

in partial fulfillment of
the requirements for the
degree of

Master of Science

Completed July 12, 1983

Commencement June 1984

APPROVED: Redacted for Privacy

Professor of Civil Engineering in charge of major

Redacted for Privacy

Head of department of Civil Engineering

Redacted for Privacy

Dean of Graduate School

Date thesis is presented July 12,1983

Typed by Laurie Campbell and Julie Womack for Timothy Joe Dodson

ACKNOWLEDGEMENT

Thank you Dr. J.R. Bell, Dr. T.S. Vinson, Dr. C.K. Sollitt, and Dr. W.G. McDougal for your advice and support. Thank you Larry Crawford and David Standly for your patient efforts in generating the data.

Special thanks go to my prayer warriors at Calvin United Presbyterian Church who were so faithful in their intercessory vigil. I love you and sincerely dedicate the words on these pages to you.

Praises be to you, my girl Friday and loving mate. No one but you and I will know how much of the credit belongs to you, Linda. Thank you from the bottom of my heart.

Finally, thanks go to Laurie Campbell and Julie Womack for their tireless efforts in typing and correcting my blunders.

This research was supported by the Oregon State University Sea Grant College Program, National Oceanic and Atmospheric Administration Office of Sea Grant, Department of Commerce, under Grant No., NA79AA-D-00106.

TABLE OF CONTENTS

TABLE OF CONTENTS (continued)

TABLE OF CONTENTS (continued)

LIST OF FIGURES

LIST OF TABLES

INFLUENCE OF GEOTEXTILE PERMEABILITY ON STABILITY OF RUBBLE SHORE PROTECTION STRUCTURES

1.0 INTRODUCTION

1.1 Background

Rubble structures are perhaps the most common method of protecting shorelines from the attack of waves. These structures are energy and protect the shoreline from erosion. Successive layers of stone must be sized such that the voids in an overlying layer are bridged by the stones in the underlying layer. In this manner, erosion of stones through the overlying layer is prevented. In the case of rubble seawalls and revetments, the final material that must be protected from erosion is the original beach soil or backfill that forms the core of the structure. Protection of the native material has historically been accomplished by placing a graded aggregate filter between the soil and the first layer of "armor" stone.

During the last 20 years, geotextiles--permeable fabrics made of synthetic polymers--have been increasingly used as substitutes for graded aggregate filters. The cost of properly graded geologic materials, the difficulty in controlling the quality of the aggregate gradation, and the difficulty in placing the graded filter under water without segregation have provided motivation for the substitution of geotextile filters.

In response to recent demand for fabrics to be used in geotechnical applications, the textile industry has produced a large

number of specific geotextiles with widely varying mechanical and hydraulic characteristics. In order to select the most appropriate geotextile from among the many available, an engineer must apply appropriate criteria to the geotextile characteristics.

Design authorities [U.S. Army Corps of Engineers CW-02215 (1977), Rankilor (1981), Heerten (1981)] all specify both a maximum allowable pore size and a minimum allowable permeability as the primary criteria for judging the suitability of a fabric to serve as a filter for the underlying soil. In addition to meeting the filter criteria, geotextiles for use in rubble structures must be strong enough to endure the construction process and durable enough to withstand the environment.

In examining geotextiles excavated from North Sea rubble shore protection structures, Heerten (1981) observed that many excavated fabrics had become considerably clogged with sediment during long-term use. Clogging, of course, reduces geotextile permeability. A geotextile selected for use based on a tested permeability may come to have a very different permeability in the long term. This motivates the question: what are the effects of geotextile permeability on the stability of rubble structures?

1.2 Purpose and Scope of Investigation

The purpose of this study is to investigate the influence of geotextile permeability on the stability of a rubble structure under wave attack. Two aspects of stability were considered: (1) stability of the core material against sliding, reduced effective

stress or liquefaction, and (2) stability of the armor units against the hydraulic forces working to remove or displace them.

The scope of activities included large-scale wave tank experiments conducted in two phases. An 18 ft (5.49 m) high, 3 to 1 sloping revetment, with a sandy gravel core and approximately 45 lb (20 kg) armor stone, was subjected to a variety of waves with periods between 1.77 and 8.84 sec and heights between 9 and 44 in (23 and 112 cm). During Phase I, in the summer of 1982, pore pressures within the core of the structure were monitored during wave attack. Geotextile layers with different permeabilities were incorporated in the structure and the effect on the pore pressure response recorded. Pore pressure patterns within the core may affect both the armor stability and stability of the core. The Phase II experiment, conducted during the spring of 1983, evaluated the change in response of armor units to wave attack for rubble structures incorporating geotextile layers with different permeabilities.

Observed pore pressure data are presented in a variety of plots that reveal response patterns. The response of both residual (accumulated mean) pore pressure and transient pore pressure amplitude at several locations within the core are plotted as function of geotextile permeability, wave height, and dimensionless wave length. A qualitative model is proposed that describes the pore pressure patterns observed as responses to wave-induced cyclic shear stresses with superimposed responses to circulating flow within the core. A conclusion is drawn that low geotextile permea-

bility does not adversely affect the stability of the core material.

Armor stability is observed to be virtually independent of the permeability of a geotextile incorporated in the rubble structure. It is suggested that, in cases of armor and bedding layers of high permeability overlying a much less permeable core, the permeability of a geotextile interposed between the core and the overlying layer does not have a significant effect on the wave-induced flow and resulting hydraulic forces acting on the armor.

2.0 BACKGROUND

2.1 Rubble-Mound Structures

2.1a Definition

As stated in the U.S. Army Corps of Engineers, Shore Protection Manual (1977), "the rubble-mound structure is a mound of stones of different sizes and shapes either dumped at random or placed in courses." In some cases, where the proper size geologic materials are not available, man-made concrete units are used in place of stone. A distinguishing characteristic of the rubble structure is that the stones or concrete units are not bound to each other by cables, adhesives, or other means other than interlocking between units and friction between units. Most concrete units are specially shaped to promote interlocking.

2.1b Performance

To protect the shoreline, a rubble structure must reflect or dissipate the energy of the attacking waves. The outermost units of the structure are called armor units. They must have sufficient mass to be held in place by gravity forces when subject to the lift and drag hydraulic forces associated with the waves. Interlocking and friction between armor units can also contribute to their stability.

There are many empirical formulas available for selection of the weight of the armor units. A comprehensive list of these is available in Günbak (1979). The parameters selected for use in the formulas are those most significant in defining the hydrodynamic

forces and gravity forces acting on the armor units. All formulas take into account the specific gravity of the armor, the slope of the face of the structure, and the height of wave at the structure. Almost all formulas also incorporate a stability coefficient to account for the shape of the armor unit. The stability coefficient is determined by model studies. Some formulas also directly incorporate wave period, friction between armor units, or water depth.

Stones underlying the armor layer must be large enough to bridge the pores in the armor layer. Typically, rubble structures are constructed of layers or courses, the materials of each course being smaller than that of the overlying course. Figure 2.1 shows a typical rubble-mound structure cross section taken from the Shore Protection Manual (1977).

The weight gradation of stone from layer to layer is consistent with the conventional geotechnical filter design. The openings in the overlying layer must have diameters no larger than the diameter of the smallest particle of the largest 15 percent of the underlying material. This criterion is met if the diameter of the largest particle of the smallest 15 percent of the overlying material has a diameter no more than five times that allowable opening size [Sowers (1979)]. This requirement is usually expressed as $5 \cdot D_{15}$ (filter) $\leq D_{85}$ (filtered material).

2.1c Advantages and Disadvantages

The primary advantage of a rubble structure is that it is quite flexible. Settlement of the structure results in readjust-

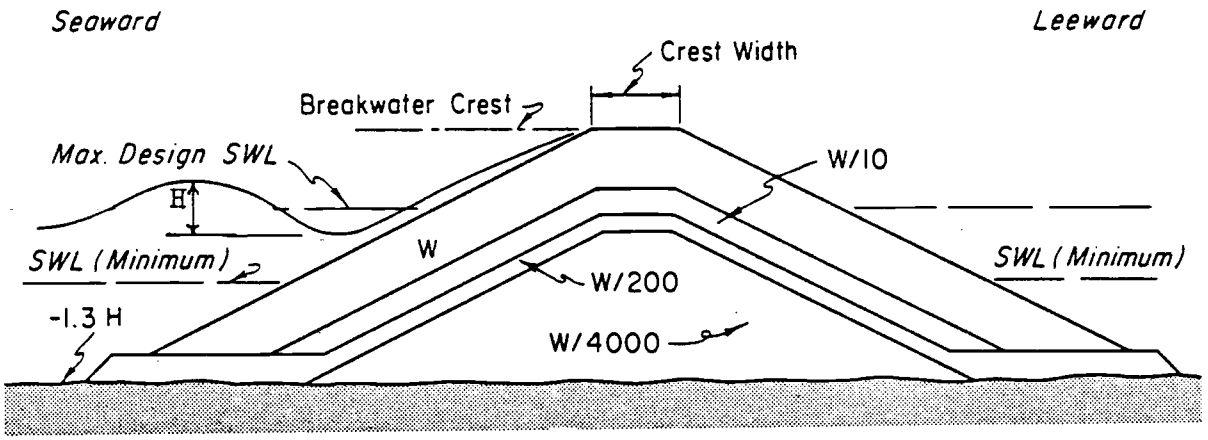

Idealized Multilayer Section

Rock Size	Layer	Rock Size Gradation (%)
W	Primary Cover Layer	125 to 75
W/10	First Underlayer	130 to 70
W/200	Second Underlayer	150 to 50
W/4000	Core and Bedding Layer	170 to 30

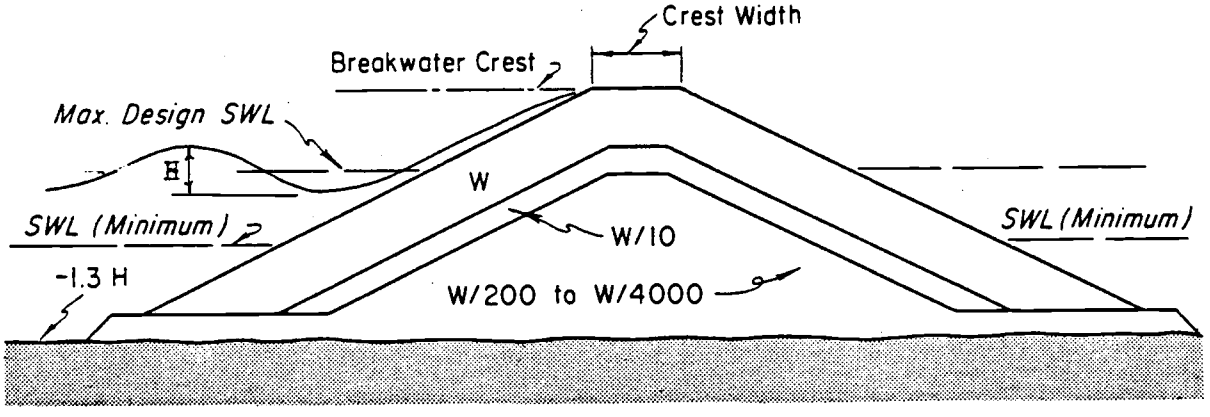

Recommended Three-layer Section

Figure 2.1. Typical U.S. Army Corps of Engineers rubble structure (from U.S. Army Corps of Engineers Shore Protection Manual)

ment of the component stones usually resulting in increased stability rather than in failure. Other advantages are: easy repair, relatively inexpensive materials, and wave energy is absorbed rather than reflected. The main disadvantage of rubble structures is the large quantities of materials required.

2.1d Summary of Previous Stability Research

Losada and Gimenez-Curto (1980) report 11 possible causes of failure or breaking of rubble-mound breakwaters as synthesized by Bruun in 1979:

1. Knock-outs of single armor units.
2. Lift-outs of single armor units.
3. Slides of the entire armor layer due to lack of friction with underlying material.
4. Breaking of armor units due to fatigue.
5. Scouring of the crown base or wave screen.
6. Damages to the inner slope due to overtop.
7. Damages due to excessive permeability in underlying layers which allows water to flow inside causing great lift-out forces on the crown and inner slope armor units.
8. Toe erosion.
9. Soil failure (bearing capacity).
10. Variation in the armor stone properties.
11. Poor construction.

Figure 2.2 from Losada and Gimenez-Curto (1980) shows the locations of these types of failures. Failure mechanisms Numbers 6 and 7 above for breakwater failure do not apply to revetment or

seawall failure. Also, many rubble structures are built without a special crown or wave screen. In the case of revetments or seawalls, the existing geologic material on the land side of the structure must be protected from erosion through the pores in the structure.

Sigurdsson (1962) reported on a laboratory investigation of actual forces exerted on idealized spherical armor units in a model rubble structure subject to water waves. The forces he measured suggested three possible causes of failure: (1) sliding of a section of the armor layer; (2) lifting out of individual armor units; and (3) impact of the breaker front pushing or rolling armor units over the top of the structure.

From his observations of an experimental rubble structure model, Font (1968) noted that initial damage was not dependent on duration of the wave attack. Long term attack by waves smaller than the size critical to armor stability did not degrade the structure. When attacking waves were of the critical size or larger, damage began to occur upon application of the first few waves. He also noted that initial damage was always in the form of displacement of individual armor units. A wave of sufficient size to initiate damage was also large enough to cause continued progressive destruction of the structure under further attack.

During large-scale tests of riprap stability by the U.S. Army Coastal Engineering Research Center in Washington, D.C., Saville (1966) observed that the armor layer of a riprap structure tends to be initially self-healing with individual armor units shifting to

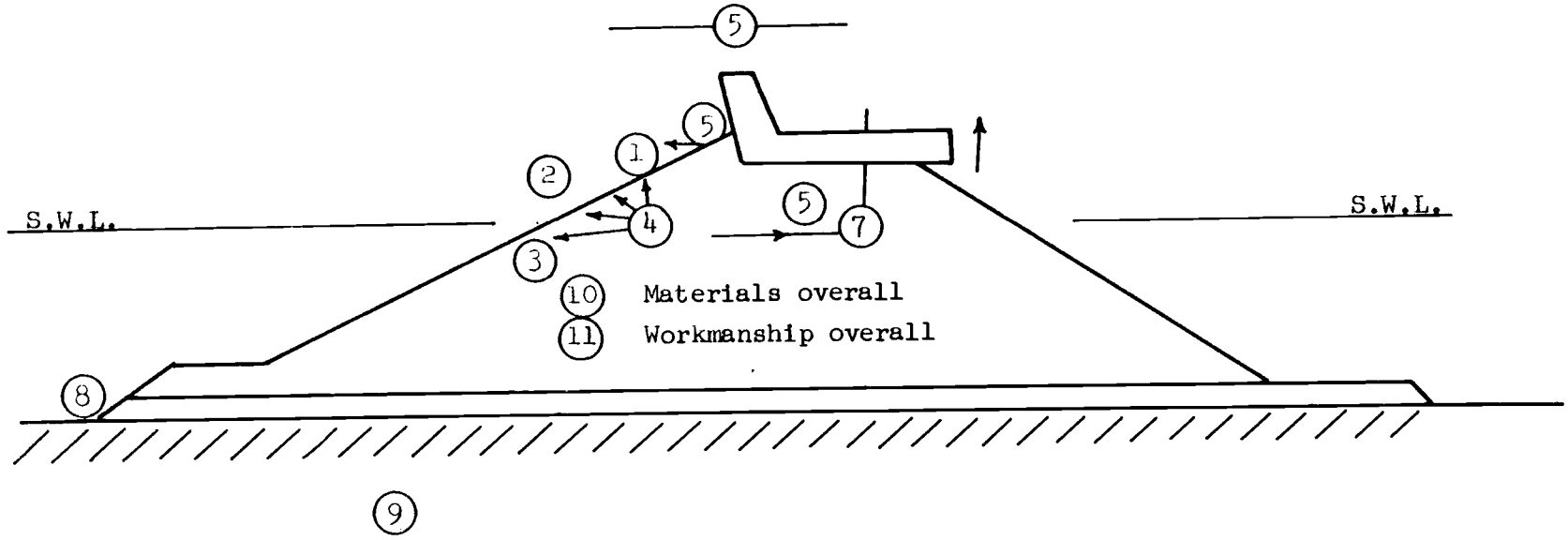

Figure 2.2. Location of failures in a rubble mound breakwater after Losada (1980)

fill holes created by removal of other individual units. Saville also noted considerable small-scale movement of armor units when under attack by waves much smaller than the size required to cause damage. Researchers in general seem to agree that the lifting out of individual armor units is an event which initiates destruction of rubble structures.

Once failure of a breakwater structure is initiated, materials of the structure are progressively rearranged by the wave forces. The forces tend to shape the structure into a profile of the same form as an equilibrium step profile of a natural beach [Bruun and Johannesson (1976)]. As illustrated in Figure 2.3, a typical equilibrium profile for a rubble mound subjected to "infinite" wave action has a nearly horizontal "step" or "bench" at an elevation near the still water level. "Infinite" wave attack is a long term attack by waves of sufficient size to cause degradation.

There has been considerable investigation of the hydraulic conditions which cause initial instability of armor units. Sigurdsson (1962) identified two zones of the structure slope that have different characteristic flow patterns during wave attack. A lower zone is characterized by high rotational accelerations near the face of the structure caused by the onrushing flow in the toe of an incipient breaker colliding with the downrushing flow from the previous wave. Higher on the slope, flows and flow accelerations tend to be more parallel to the slope. Figure 2.4 illustrates these two zones.

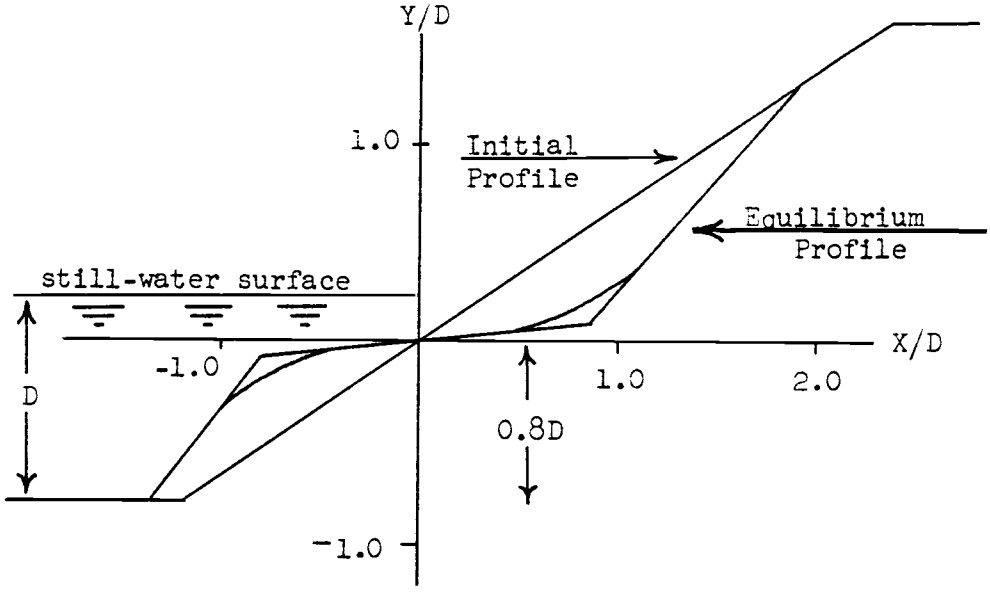

Figure 2.3. Equilibrium profile of a rubble structure under wave attack

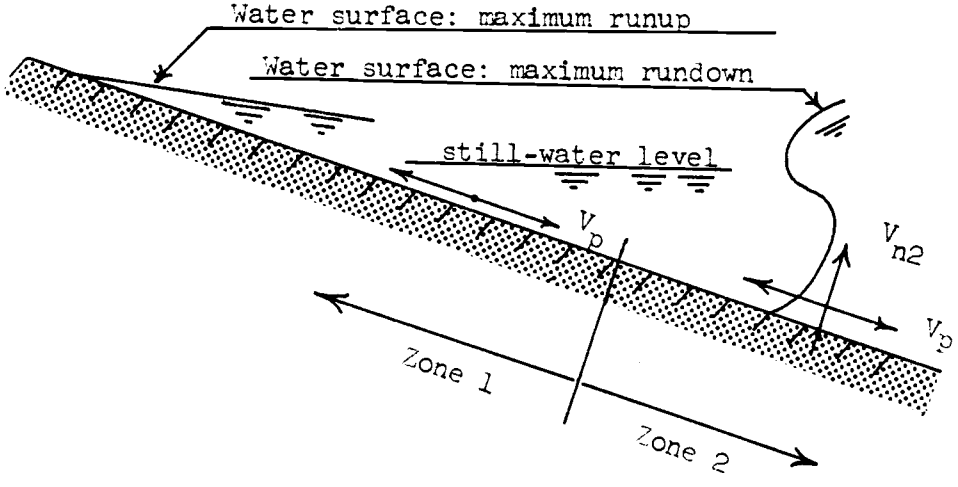

Figure 2.4. Zones of parallel and rotating flows

Sigurdsson discovered that the forces most critical to armor stability are normal forces that occur at the toe of the advancing breaker or when water is flowing out of the structure. His tests, conducted on idealized spherical armor units, demonstrated failures initiating at or below the lowest level of wave retreat. Extensive tests on rock slopes conducted by Kydland at the Norwegian Institute of Technology are reported by Bruun and Johannesson (1976) to have shown that damage was always initiated just below the still water level. Bruun and other Norwegian researchers [Bruun and Johannesson (1976); Bruun and Günbak (1976), Günbak (1979)] also agree with Sigurdsson that the high normal forces in the toe of the advancing breaker are the forces critical to armor unit stability. Günbak (1979) also points out that Hudson and Font showed that, in shallow water situations, waves breaking in front of the structure, such that wave impact from the breaking wave crest hits directly onto the breakwater slope, causes the most critical destabilizing forces.

Sigurdsson noted that outflow of water from the slope also contributed significantly to both maximum normal force and maximum downslope parallel forces on the armor units. He observed that outflow closely follows wave retreat and therefore contributes volume to the normal flows in the breaker toe.

Model investigations have suggested to some [Sigurdsson (1962), Bruun (1970)] that permeability of the core material has a significant effect on the stability of a rubble structure. These investigators have noted that reduced permeability of the core

leads to higher runup and higher hydrostatic pressures within the slope, both of which are considered to have destabilizing effects on the armor. In Sigurdsson's experiments, he noted higher outflow from the slope and an associated increased normal force in the case of an "infinitely permeable" core. In contrast, Carver (1980), in his model study, discovered that varying the size of rock underlying the armor units between the sizes of 1/5 and 1/20 the size of the armor units had no observable effect on the stability of the armor.

Associated with wave loadings on a soil surface are induced cyclic shear stresses within the soil. These cyclic shear stresses are not mentioned by researchers of rubble structure stability, but are an integral part of the analytic models of ocean bottom response to wave loadings such as the models by Seed and Rahman (1978) and Finn, Siddharthan, and Martin (1980).

Finn and Lee (1979) propose a method of slices for effective stress stability analysis of a submerged slope which takes into account loadings of gravity, wave pressures on the sloping surface, and transient and residual pore pressures on a trial failure surface. However, such an analysis assumes an uncoupling of the shear stress response and the pore pressure response within the soil. The wave pressures on a steep slope are very difficult to model analytically.

The situation for a rubble structure is further complicated by the free surface flow phenomena and a partially saturated soil. No analytic model exists for prediction of the wave-induced cyclic

shear stresses within a rubble structure core. However, it is possible that such stresses affect the stability of the core of rubble structures. A fairly extensive review of the literature addressing rubble structure stability revealed no mention of a deep-seated slide failure in the core.

2.2 Geotextiles in Rubble Structures

2.2a Function

The purpose of a geotextile in a rubble structure is to prevent material beneath the geotextile from penetrating or eroding through the material overlying the geotextile. This function relieves the designer from the strict gradation constraints imposed on the overlying material. Geotextiles are most appropriate for this function when the underlying materials are small particles such as sands and gravels.

2.2b General Description

A geotextile is a permeable fabric material constructed of synthetic polymer fibers and intended for use in geotechnical applications. Numerous specific fabrics with an extremely wide variety of properties, are available on the market. The fabrics are most commonly classified according to fabric structure and fiber polymer. They are formed by weaving, knitting, or bonding fibers together. Bonding is accomplished by needle punching, heat, or resins. Polymers most commonly used are polypropylene, polyester, and polyethylene. Lesser used polymers include nylon and polyvinyledene chloride. Extensive research by Bell and Hicks

(1980) has revealed the following salient features and geotextile characteristics.

Mechanical properties of geotextiles are strongly influenced by both construction technique and polymer type. While strength varies widely among fabrics, it is ultimately characterized by the strength of the plastic fibers. These plastics are also capable of large elongations and some are subject to creep. Woven fabrics typically have a higher modulus and lower elongation than non-wovens.

Geotextiles generally have moderately high permeabilities of 10^{-3} to 10^{-2} cm/sec (3.3×10^{-5} to 3.3×10^{-4} ft/sec). This is comparable to a clean, medium to fine sand. Coarse monofilament woven fabrics have permeabilities greater than fine gravels. In use, permeabilities can be reduced due to clogging or blinding of pores. Woven fabrics are not subject to clogging, but are subject to blinding.

All common fabrics are stable with respect to temperature within the range of normal climatic temperatures. Mechanical properties change with temperature changes within the climatic range, but not permanently. Biological and chemical stability of geotextiles is very good in most natural environments.

All geotextile polymers degrade severely over time when subjected to ultraviolet light. This susceptibility to ultraviolet light can be reduced considerably, but not eliminated, by the addition of carbon black or other pigmentation to the fibers or by chemical stabilizers.

2.2c History of Use

Geotextiles have been used as replacements for graded aggregate filters in shore protection structures for at least the past 20 years. Barrett (1966) reports on a rubble revetment constructed in Deerfield Beach, Florida in 1962 using a geotextile filter. Since that time, use of geotextiles in shore portection applications has increased dramatically. Many of these applications have been by federal government agencies including the Army Corps of Engineers, Department of Interior, Department of Navy, and Federal Highway Administration. Heerten (1980) reports the use of geotextiles has been standard practice in coastal engineering works on the North Sea coast since before 1970.

2.2d Design Criteria

Geotextiles used in shore protection structures are always considered to perform as filters. Therefore, suitability of a fabric is based on two criteria: the size of the openings in the fabric and the permeability of the fabric. Of course, the fabric must also be strong enough to endure the construction process and durable enough to endure exposure to the environment without degradation of its filter function. Geotextiles are rarely required to provide strength in a structure. Dunham and Barrett (1974) recommend that during installation, the fabric be gathered in loose folds to prevent development of tensile stresses.

The U.S. Army Corps of Engineers in CW02215 (1977) specifies that fabrics be chosen on the basis of their "equivalent opening size" (EOS) and their "gradient ratio." The EOS is a measure of

pore size established by sieving glass beads through the fabric, and the gradient ratio is a measure of the permeability of the fabric in conjunction with the soil it is intended to filter after allowing a time for clogging to occur.

Rankilor (1981) also recommends that a fabric be selected according to filter criteria which include both pore size and permeability. He provides the reader with a collection of criteria developed by a wide cross section of researchers. The criteria are categorized according to whether the fabric is woven or nonwoven and whether the flow is one way or reversing as in a wave environment.

Heerten (1980) also recommends selection based on permeability and pore size criteria. He develops the concept of a permeability reduction factor to account for blinding or clogging of fabric openings in situ. He provides design charts to use in determining the reduction factor based on tested fabric permeability and gradation of the soil to be filtered.

2.2e Advantages

Geotextiles have many advantages over graded aggregate as filters in shore protection structures. The filtering capability of the fabric is not subject to variability in materials and is much less subject to workmanship errors in installation, making quality control much easier. Filter design with fabrics is not limited by geographic availability of materials. The difficulties associated with placement of graded aggregates under water are eliminated. Another advantage is that failure of a structure due

to short-term localized deficiencies in the armor layer may possibly be avoided, owing to the tensile strength of the geotextile. In contrast, if a portion of rubble is removed in a revetment or seawall with an aggregate filter, loss of the filter will quickly follow.

2.2f Performance

Deerfield Beach, Florida provides an interesting case history illustrating the effectiveness of geotextiles used in rubble shore protection structures [Barrett (1966), Dunham and Barrett (1974)]. In 1962, a revetment was constructed on this beach with a polypropylene geotextile placed between the beach sands and the 500 to 5,000 lb armor stones. As of 1976, this structure had functioned without maintenance despite wave attack associated with numerous hurricanes and storms.

Heerten (1980) excavated geotextiles that were buried in revetment structures on the shores of the North Sea for periods of up to 21 years. He found no evidence of any fabric having failed to perform its function of preventing erosion of soils though the riprap, despite the fact that the opening sizes in the fabrics sometimes exceeded those recommended by modern design rules. Interestingly, he discovered that in all cases, deposition of fine particles in and on the fabrics occurred from the sea side. He also observed significant flattening of some of the revetment slopes and theorized that this flattening may have been "perhaps caused by soil-liquefaction under wave impact but certainly not by washout through the filter-fabrics."

Haliburton, Lawmaster, and McGuffey (1981) report on two revetment test sections at Holly Beach, Louisiana. In these test sections, interlocking concrete blocks 4 in thick and 8 in square were placed on a geotextile lying directly on medium to coarse clean sands. The section built using a fabric with an EOS equivalent to a No. 10 sieve and a five percent open area failed while the other section built with fabric of EOS No. 40 sieve and 30 percent open area was stable. The authors explain the failure of the former section as follows: "...the fabric, when a majority of the fabric openings were covered by the flat concrete blocks, was not able to drain as freely as the beach sand, thus excessive hydrostatic pressures were created in the slope, precipitating internal collapse of the revetment."

2.3 Summary Comments

All typical revetment design cross sections incorporating geotextiles [Shore Protection Manual (1977); Rankilor (1981); Barrett (1966)] call for a layer of smaller stones between the fabric and the armor to reduce mechanical loads on the fabric and to aid in drainage. Barrett (1966) emphasizes that in the case of interlocking block revetments, "the crushed rock layer is an absolute necessity as wave tank tests have shown that if the block is placed directly upon the filter cloth, seepage through the joints will not be fast enough to prevent a buildup of hydrostatic pressure." Although the Holly Beach case history is concerned with flat concrete blocks rather than rubble, it has been included in

the background to illustrate the concern designers have with build-up of hydrostatic pressures within shore protection structures.

Based on small-scale tests [Bruun and Johannesson (1974), Sigurdsson (1962), Günbak (1979)], permeability of the core of a rubble-mound structure is considered important to stability of the armor. Adequate permeability of geotextiles in the structure is also considered by most authorities to be important to avoid damaging buildup of interior hydrostatic pressures. However, a large-scale experimental investigation of the effect of geotextile permeability has never been reported. Such an investigation is especially appropriate considering Heerten's observation of fabric clogging in actual structures during long-term use.

3.0 THE EXPERIMENT

3.1 Purpose

The experiment was designed to investigate geotextile permeability effects in two primary areas of concern with respect to rubble structure stability against wave attack. The first area of concern was the possibility of instability of the structure arising from a wave-induced accumulation of pore pressure within the core of the structure. The second area of investigation was the stability of rubble armor units. The experiment was conducted in two phases so that each of these two areas of concern could be investigated independently.

3.2 Facility

The experiment was conducted in the Oregon State University Wave Research Facility. This is a large-scale channel measuring 12 ft (3.66 m) in width, 15 ft (4.57 m) in depth, and 342 ft (104.2 m) in length. The wave board is hinged and driven by an MTS hydraulic piston. Waves up to 5 ft (1.5 m) in height can be generated as either simple periodic wave trains or random waves in a specified spectrum. An on-site PDP-11 computer is used to control the generator and for data acquisition. Waves are measured using a sonic surface profiler.

3.3 Overview of Experiment

The experimental rubble structure consisted of a revetment 15

ft (4.57 m) high and 12 ft (3.66 m) wide with a still water level 8 ft (2.44 m) above the toe. The face of the structure had a slope of 3 horizontal to 1 vertical. The revetment consisted of three layers overlying a sandy gravel core: (1) a geotextile layer, (2) a bedding layer of 3 in (7.6 cm) concrete cubes, and (3) an armor layer of approximately 45 lb (20 kg) armor units. Figure 3.1 shows a typical cross section of the structure.

During Phase I, pore pressures within the core were measured by an array of pressure transducers and piezometers. During Phase II, armor stability was evaluated by visual and aural observation supplemented by photographs of the revetment above still water level following each run.

During Phase I, the structure was subjected to trains of simple periodic waves selected from Dean's Stream-Function cases. The wave cases provided a variety of wave periods and wave heights. The waves selected for use in Phase II were at three of the five wave periods used in Phase I. However, in Phase II, the wave height was increased in small increments rather than in the large steps associated with the Dean's Stream-Function cases.

3.4 Phase I: Core Pore Pressure Investigation

3.4a Geometry

Figure 3.1 shows the geometry of the revetment structure used in the Phase I investigation. A slope of 3 horizontal to 1 vertical was selected. A 3 to 1 slope constructed of the gravel used in this experiment is stable against a slope stability failure under

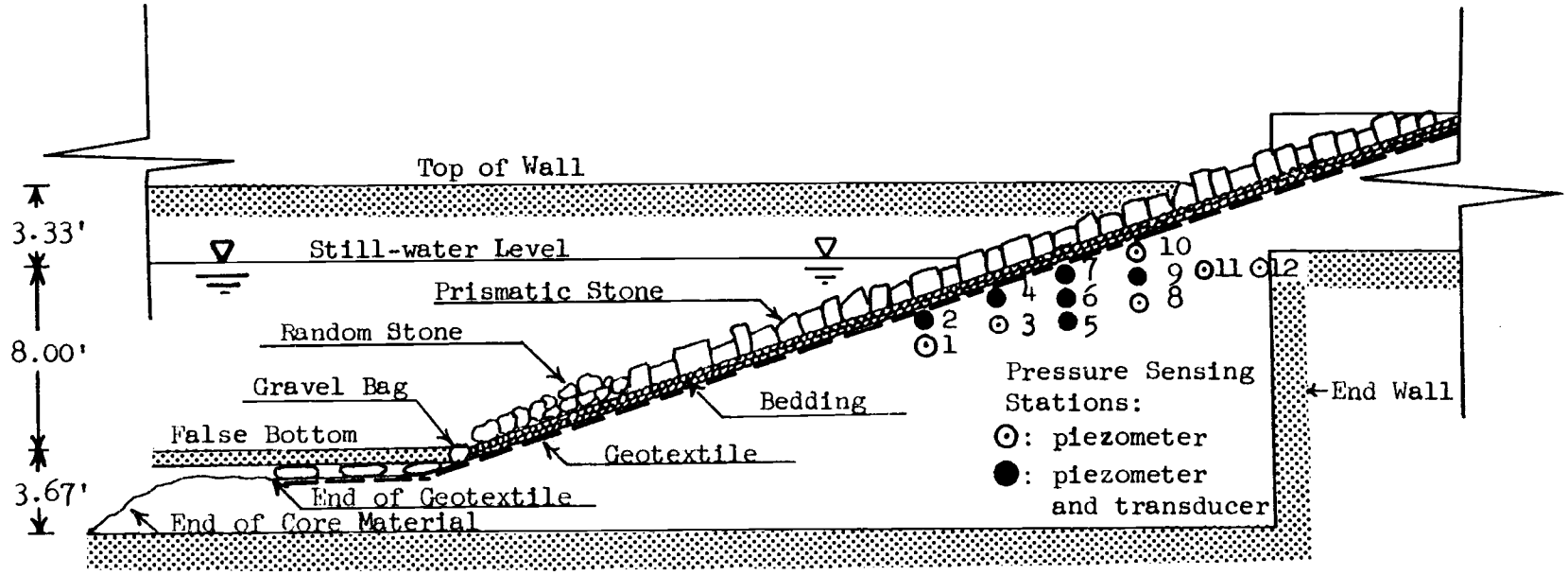

Figure 3.1. Cross section of Phase I experimental setup

normal static conditions. A 3 to 1 slope is within the range of slopes normally used in rubble shore protection structures, being near the shallow end of that range.

The bedding or "armor bridging" layer consisting of 3 in (7.6 cm) concrete cubes was designed to a 6 in (15.2 cm) thickness. This thickness is typical of those used in actual designs [Shore Protection Manual (1977); Rankilor (1981); Barrett (1966)], and provided a double-layer thickness of the 3 in (7.6 cm) conrete cubes. A double-layer thickness was considered minimum to ensure no gaps in the bedding layer.

The armor layer was constructed only 10 in (25 cm) thick. This was a single unit thickness of armor, in constrast to the minimum double-unit thicknesses recommended by design authorities. However, the single-unit thickness was sufficient for stability of the armor units against the waves selected for the experiment. A minimum thickness was considered an experimental advantage in two ways. First, maximum hydraulic energy could be applied to the geotextile and core by minimizing dissipation of energy in a thick armor layer. Second, confinement of the underlying layers was minimized by the thin armor layer, maximizing the possibility of instability in the core material. The portion of the slope deeper than 4 ft (1.2 m) below the still water level was covered with conventional rubble riprap which was stable in all experimental runs.

A false bottom of 12 ft (3.66 m) square, 8 in (20.3 cm) thick concrete slabs was installed during the experiment to accommodate a

concurrent experiment 72 ft (22 m) closer to the wave board. The surface of the false bottom was 3.67 ft (1.12 m) above the true bottom. The resulting water depth above the false bottom was 8 ft (2.44 m). There remained 3.33 ft (1.01 m) of wall above the still water level.

In Phase I, the toe of the slope was not sealed off from the water below the false bottom. The fabrics used in the experiment terminated 10 ft (3 m) from the toe of the slope on the horizontal bench of core material located below the false bottom.

Fabrics were anchored at the top of the slope by burial in a 2 ft (0.6 m) deep trench. This anchoring is typical of revetment designs. The anchor trench was located at an elevation above the highest wave runup anticipated during the experiment.

The pattern of pore pressure sensing devices was centered on the intersection of the still water level and the plane of the geotextile. The transducers and piezometers were anchored in place 3 ft (0.9 m) from the wall of the tank as shown in Figures 3.2 and 3.3. The anchors were 3 ft (0.9 m) long by 6 in (15.2 cm) wide aluminum bars. The transducer ports were screened from the core material by a patch of needle-punched nonwoven geotextile [Bidem C42 (Monsanto)]. The piezometer tips were buried with an approximate 1 in thickness of uniform medium sand surrounding each one to serve as bedding protection against the gravel core material.

3.4b Materials

The core material of the revetment was a coarse, rounded, 3 in minus sandy, river-run gravel with scattered cobbles up to 6 in in

Figure 3.2. Array of pressure sensing instruments

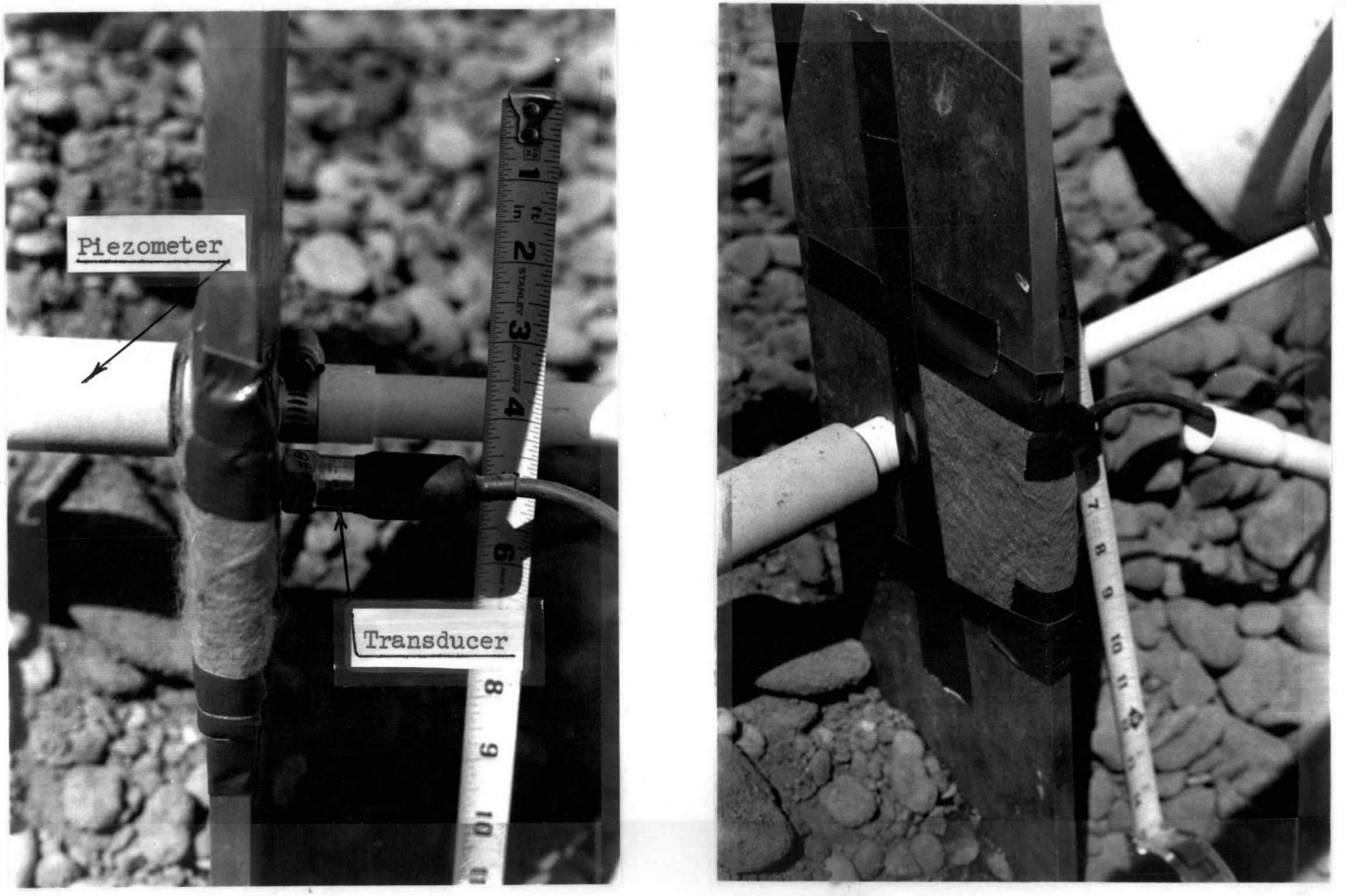

Figure 3.3. Piezometer and transducer installation

diameter. A grain size distribution of this material is shown in Figure 3.4. The permeability of the gravel was estimated to be approximately 2×10^{-2} cm/sec (6.6×10^{-4} ft/sec) based on the gradation [Cedergren (1975)].

The "armor bridging layer" or "bedding" material consisted of rough 3 in (7.6 centimeter) nominal cubes of concrete. These cubes met the Shore Protection Manual size criterion for first underlayer rock as shown in Figure 2.1.

The armor units selected for use on Phase I were prismatic units with typical dimensions as shown in Figures 3.5 and 3.6. The units have an exceptionally high Hudson stability coefficient [Sollitt and DeBok (1976)] and were selected to enable construction of a thin armor layer that would not be subject to damage by the waves to be used in the experiment.

The fabrics selected for use in Phase I were chosen to represent a range of permeabilities. An impermeable membrane, a low permeability fabric, and a high permeability fabric were selected. The extreme case of an impermeable fabric was represented by continuous polyethylene membrane placed between Typar and Synflex geotextiles for protection against mechanical damage from the core and bedding materials. Typar (spunbonded polypropylene by Dupont) with a permeability of 1.4×10^{-2} cm/sec (4.6×10^{-6} ft/sec) was chosen as a material with a permeability somewhat lower than that of the core material. Typar has an EOS of a 140 to 170 U.S. Standard sieve. Less than one percent of the core material is finer than this size. Poly-Filter GB (woven polypropylene by

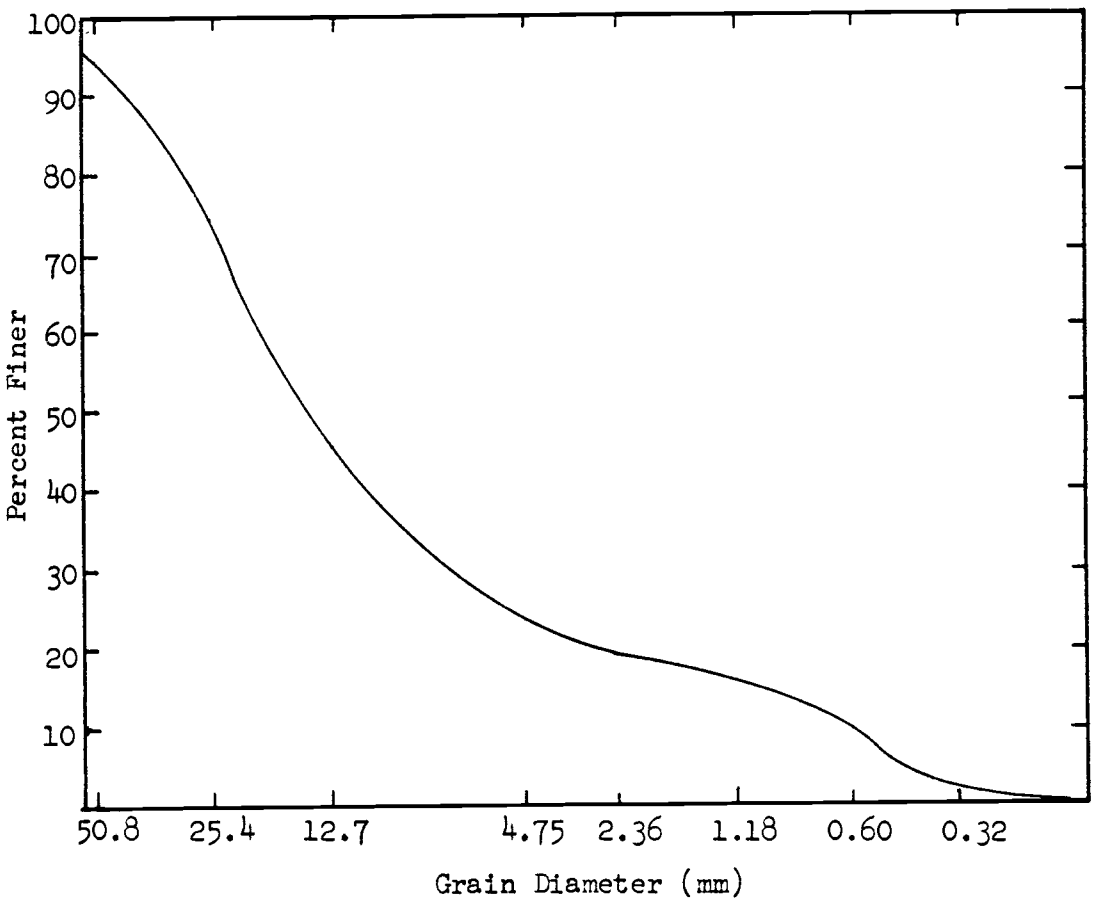

Figure 3.4. Grain size distribution of core material

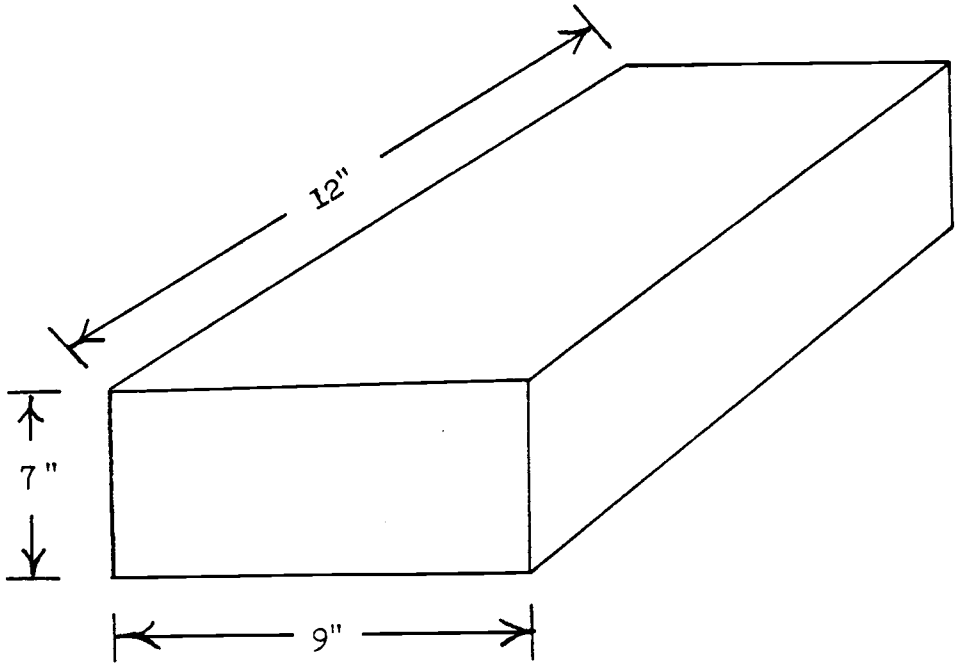

Figure 3.5. Phase I armor stone typical dimensions

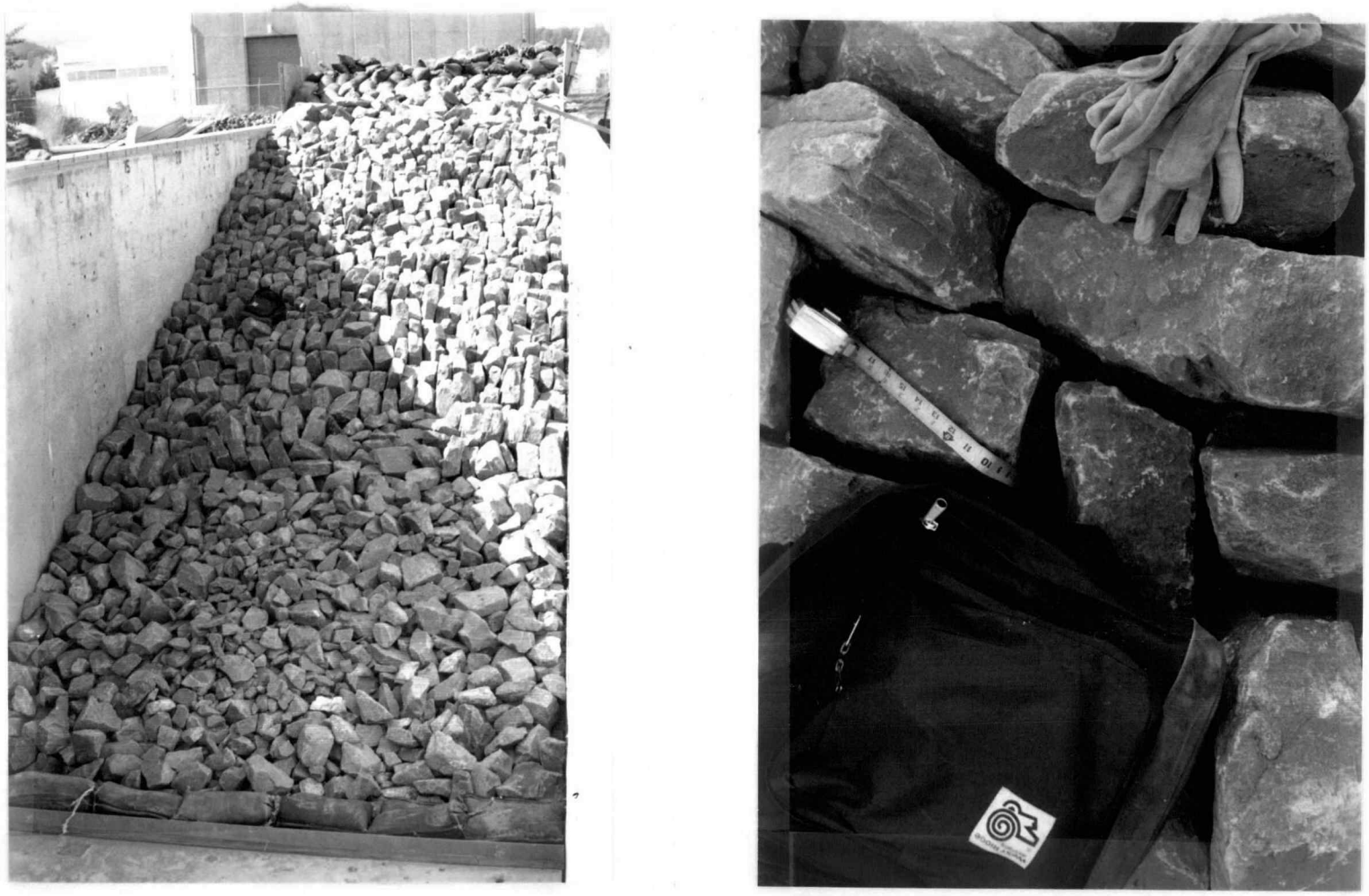

Figure 3.6. Phase I armor stone in place on slope

Carthage Mills) was chosen as a high permeability fabric. Although the permeability of Poly-Filter GB is not published, it has a percent open area of not less than 21 percent and an EOS of a 40 sieve. Compared to the similar Poly-Filter X, which has not more than 6 percent open area, an EOS of a 70 seive and a permeability of 3.5×10^{-2} cm/sec (1.1×10^{-3} ft/sec), Poly-Filter GB can be considered to have a permeability of at least 1.5×10^{-1} cm/sec (4.9×10^{-3} ft/sec). This is an order of magnitude greater permeability than the core material. Ten percent of the core material passed the No. 40 sieve. The geotextile characteristics are summarized in Table 3.1.

3.4c Measuring Devices

Pore pressures were measured with (1) Druck PDCR 10/D pressure transucers with a zero to 5 psi (34.5 kPa) pressure sensing range and, (2) 6 in (15.2 cm) long ceramic piezometer tips with inside diameters to fit 1/2 in (1.27 cm) PVC tubing. Voltages from the six transducers were fed through preamplifiers and power amplifiers to strip chart recorders and to the PDP 11 for recording on magtion 6 was not recorded on strip charts. The 1/2 in (1.27 cm) PVC tubing from the piezometer tips extended horizontally 3 ft (0.9 m) to the wall and vertically to 1 ft (0.30 m) above the top of the wall. Piezometric levels were manually measured in the vertical tubes by means of graduated dip sticks with exposed electric probes at the tips. Contact of the exposed probes with the water in the vertical tube was registered by a needle deflection on a galvanometer.

Table 3.1. Summary of geotextile characteristics

Geotextile Characteristic	Typar	Poly-Filter GB
Polymer	Polypropylene Monofilament	Polypropylene Monofilament
Structure	spunbonded continuous filament	Woven Monofilament
Permeability	1.4×10^{-2} cm/sec	estimate 1.5×10^{-1} cm/sec
Equivalent Opening Size (EOS)	No. 140 to 170 sieve	No. 40 sieve
Elongation at Break	63%	10% to 35%
Weight	6 oz/yd^2	6.6 oz/yd^2
Grab Tensile Strength (ASTM D 1682)	207 lbs.	200 lbs.
Puncture Strength (ASTM D 751)	75 lbs.	120 lbs.

A measuring tape was fastened horizontally along the top of the wall in the vicinity of the wave swash zone. This tape served as a reference for recording runup and rundown on the slope.

3.4d Selection of Waves

Waves were chosen for which direct entry could be made into Dean's Stream-function tables [Dean (1974)]. This facilitated any analysis of the experimental data requiring precise definition of the wave characteristics. Twelve different wave cases were investigated with periods between 1.77 and 8.84 sec and with heights between 15 and 44 in (38 and 112 cm). A summary of the waves used is given in Table 3.2.

3.4e Constructing the Test Revetment

The gravel cores used in the experiment had been in place several months prior to this experiment and had been subjected to many previous wave loadings. The gravels were excavated back by clamshell to ensure that a homogeneous core with a surface unwashed by previous waves was obtained. A 3.5 ft (1.1 m) wide trench 2.5 ft (0.76 m) deep was excavated next to the tank wall to provide for installation of the pressure sensing devices as shown in Figure 3.2. With instruments in place, the trench was backfilled by hand and hand tamped using shovels as tamping devices. Typar fabric was placed on the slope. The concrete cube bedding was dumped onto the slope near the top and rolled down the fabric-covered slope where it was adjusted into a nominal 6 in (15 cm) thickness. The Typar suffered some minor damage during placement of the bedding. Scat-

Table 3.2. Waves utilized in Phase I

Dean's Wave Case	H/L_o	T (sec)	H (ft)	L_o
8A	0.041995	1.77	0.68	16.04 ft
8B	0.083974	1.77	1.36	16.04 ft
8C	0.0125988	1.77	2.03	16.04 ft
7A	0.031267	2.80	1.28	40.14 ft
7B	0.062490	2.80	2.52	40.14 ft
7C	0.093785	2.80	3.76	40.14 ft
6A	0.018312	3.95	1.47	79.88 ft
6B	0.036631	3.95	2.92	79.88 ft
6C	0.054927	3.95	4.40	79.88 ft
5A	0.009752	5.59	1.55	159.99 ft
5B	0.019505	5.59	3.07	159.99 ft
4A	0.003902	8.84	1.56	400.11 ft

tered holes up to 0.04 in (1 mm) resulted from abrasion by the cubes. Finally, the armor units were hand-placed on the main body of the slope beginning at the toe and working upward. The prismatic armor stone placed on the main body of the slope required considerable care in hand placement to ensure the high stability required.

3.4f Data Collection

Each of the 12 wave cases were conducted for a period of approximately 20 min during which time data were collected. Piezometer readings were laborious because of the unexpectedly large dynamic component of water fluctuation within the piezometer tubes and because of the long period fluctuations in readings due to a traveling standing wave pattern in the wave tank. Piezometers were read sequentially during the runs. Transducer data were recorded on strip charts for the first 50 or more waves and the last 50 or more waves. Data for the first 30 and last 30 waves of each case were stored on magnetic tape and were output in digital and graphic form.

The data acquisition system continuously averaged the pressure readings over a two-wave period to give an average pressure readout with time representing the "residual" or "average static" pore pressure buildup associated with the wave case. Additional output from the digital data included a time plot similar to a strip chart output and a "pressure grid" composed of a 10-samples-per-wave readout of simultaneously measured transducer pressures for a span of four waves at the end of the first 30 waves and four waves at

the beginning of the last 30 waves.

The standing wave pattern in the tank was scanned with the sonic wave profiler as soon as possible after the reflected wave had passed the scanning reach. The profiler output was recorded on strip charts and magnetic tape enabling wave height and reflection coefficient computation.

Runup and rundown maxima were recorded referencing the horizontal scale. Determination of the maxima were somewhat subjective, but were, in every case, estimated by the same individual by eye.

3.4g Reconstructing the Revetment

After all 12 wave cases were conducted on the Typar fabric, the wave tank was drained and the armor and bedding layers were removed from the slope by hand. Some additional degradation of the Typar fabric had occurred due to abrasion. The fabric was replaced with Poly-Filter GB, the false bottom being temporarily removed during the change. The bedding and armor layers were replaced by hand as before.

Following the 12 wave cases with Poly-Filter GB, the rebuilding process was repeated with the impervious polyethylene sandwiched between Typar and Synflex. The final 12 wave cases were conducted using a highly permeable nominal 2 in (5 cm) thick layer of 1/4 in to 1 in (0.5 cm to 2.5 cm) clean rounded gravel placed between the core material and a double layer of Typar. The original 6-ounce Typar had been degraded by the first series, and so was augmented by a layer of new 4-ounce Typar for the final series.

3.5 Phase II: Armor Unit Stability

3.5a Geometry

Figure 3.7 shows that Phase II of the experiment was very similar to Phase I in geometry. Again a 3 to 1 slope was used and the false bottom and water depths were the same. The main differences were the toe of the slope and the armor layer. As shown in Figure 3.8, a fabric layer of Poly-Filter GB, Typar, polyethylene sheet, and Synflex sealed off the portion of the toe between the level of the false bottom and the true bottom of the tank for the entire experiment. The concrete false bottom did not extend all the way to intercept the slope as in Phase I. A bench constructed of bags of gravel overlying the stack of fabrics completed the false bottom between the concrete and the slope. Also underlying these bags was a 6 in (15 cm) deep layer of flat concrete 12 in (30.5 cm) square plates. These plates, plus a 10 in (25 cm) layer of gravel bags, also extended up the slope to an elevation 2 ft (0.61 m) above the false bottom.

The graded armor units in this phase were placed in a random manner. The armor layer was nominally 15 in (38 cm) thick.

The fabrics in this phase were anchored at the top of the slope by attachment to a steel bar rather than buried in a trench. The fabrics were wrapped several times around the bar located on the backside of the slope. The bar was secured in place with gravel bags attached to it by cables.

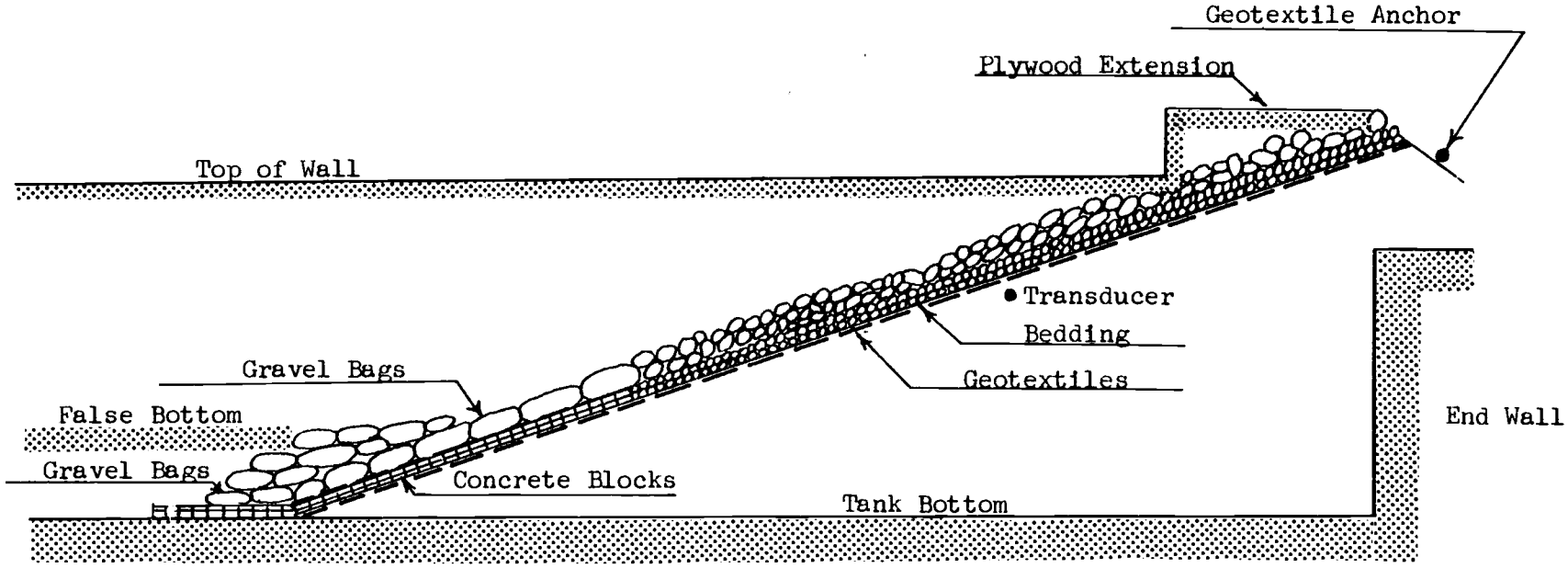

Figure 3.7. Cross section of Phase II experimental setup

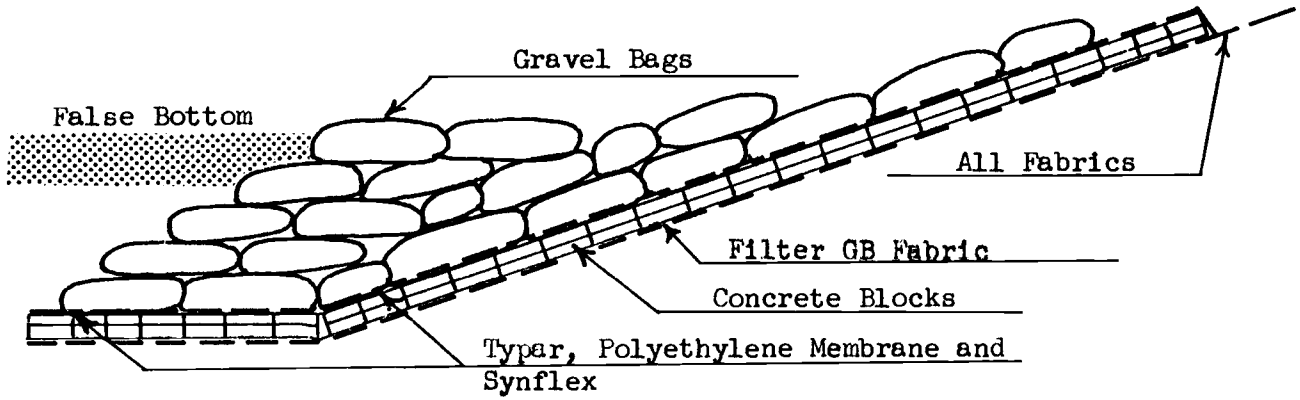

Figure 3.8. Toe detail, Phase II structure

3.5b Materials

The Phase I materials were used in the Phase II section except an armor was selected that was intended to fail under a 27 in (69 cm) high wave. Hudson's formula was used to select a median armor weight of 44 lb (20 kg) based on a stability coefficient of three. A U.S. Army Corps of Engineers' investigation [Thomsen, Wholt, and Harrison (1972)] has shown that the median weight of graded armor material is a satisfactory "effective size" with respect to stability. The gradation of the armor material used is shown in Figure 3.9. The armor was an angular diorite quarry stone with a specific gravity of 2.7. The stones were of a wide variety of shapes with no particular shape being most prevalent.

3.5c Measuring Devices

Initial failure of armor units is very difficult to quantitatively measure. Determination of the initial failure condition was accomplished by visual and aural observation of the slope by the same individual. The observations were supplemented by photographs of the slope after each wave case run. These photographs show only the portion of the slope above the still water level and were used to corroborate the observations made during wave attack.

A single pressure transducer was located on the centerline of the slope as shown in Figure 3.7. The output of this transducer was recorded only on a strip chart recorder.

3.5d Selection of Waves

Waves of periods used in Dean's Stream-function cases were

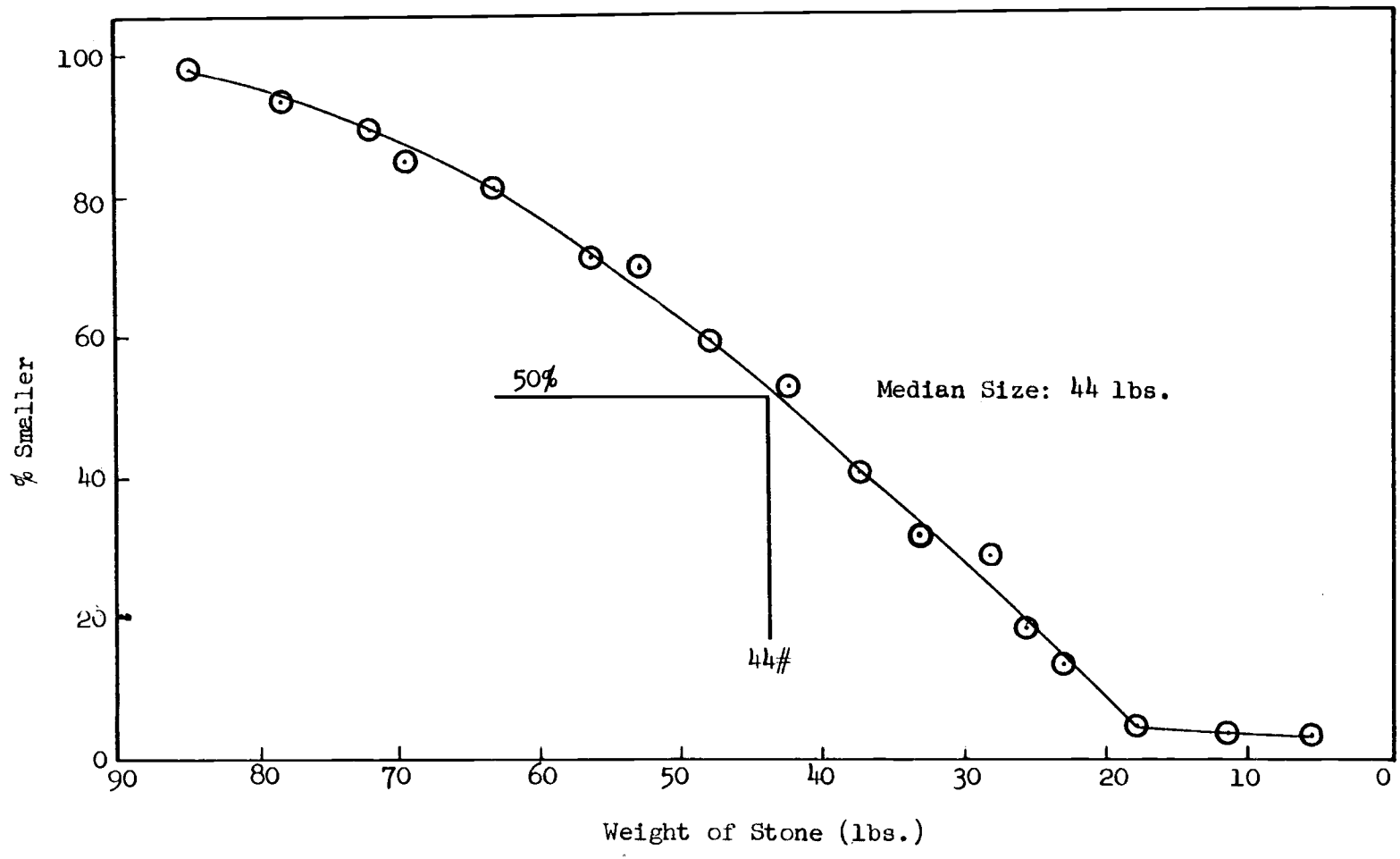

Figure 3.9. Distribution of stone weights in Phase II armor

chosen for the Phase II program. A period of 5.59 sec at a height of 27 in was anticipated to be the critical wave. This wave has an Iribarren's number, $\xi = (\tan\alpha)/(H/L_o)^{1/2}$, of 2.9 which is in the range between 2 and 3 considered to be critical to armor stability [Bruun and Johannesson (1976), Günbak (1979)]. In order to check the effect of wave length and Iribarren's number on stability, waves of 2.80 and 3.95 sec periods were also selected. Wave heights between 15 and 44 in (38 and 112 cm) in 2 to 4 in (5 to 10 cm) increments were employed.

3.5e Sequence of Tests

The tests were conducted with the impermeable geotextile case first, low permeability fabric second, high permeability fabric third and, finally, a control case with no geotextile. This was to facilitate conduct of the experiment as explained later in this section.

3.5f Constructing the Test Revetment

The gravel core material was in place several weeks prior to this experiment and had been subjected to many series of wave loadings while protected with a rubber tire armor layer. The Poly-Filter GB fabric and the layer of 12 in (30.5 cm) square concrete blocks at the toe of the slope were also in place during the previous wave loadings.

The Poly-Filter GB was rolled back off the slope above the concrete blocks. The upper few inches of gravel had been washed by previous waves and was removed by hand shovels in order to achieve a homogeneous slope similar to Phase I. The gravel slope was

groomed to an even 3 to 1 grade and the transducer buried.

Following burial of the transducer, the geotextiles were stacked on the slope. The Poly-Filter GB, extending beneath the concrete blocks, was replaced first. Next, the Typar was placed followed by the polyethylene sheet and Synflex. This stacking was done so that, during the experiment, fabrics could be removed one by one creating a progressively more permeable geotextile layer. The top three fabrics were placed over the top of the concrete blocks and extended down to and several feet along the bottom of the tank. The fabrics were anchored at the toe and the gravel bag bench at the toe of the slope was constructed on top of the fabric layers. The concrete cube bedding layer was placed as in Phase I and the armor material was dumped from trucks over the top of the wall onto the bedding layer. The armor was rearranged by hand in a random manner to achieve a 15 in (38 cm) nominal thickness of armor layer.

3.5g Data Collection

Waves were run against the slope in bursts of 60 waves for waves less than about 33 in (84 cm) in height and in bursts of 100 for larger waves. The wave cases were sequenced roughly in order of increasing height with the wave period being changed as necessary. Each wave case was run for one burst after which the next higher wave was run.

Visual and aural observation of the slope was made during each wave case. A strip chart recording of the transducer output was also made. The standing wave pattern was scanned with the sonic

profiler as soon as practical after formation of the standing wave pattern. The wave profile was recorded on a separate strip chart. Runup and rundown measurements were taken as in Phase I.

The tank was stilled for a period of 1 to 5 min between wave bursts. During the stilling period, and occasionally during the last few waves of a burst, a photograph was taken of the slope.

3.5h Rebuilding the Revetment

Following a full series of wave bursts against a slope with a given geotextile case, the slope served further as a wave absorber for another experiment in a different section of the tank. In no case was the armor layer damaged to the extent that the bedding layer was exposed. No movement occurred in the bedding layer or the gravel slope.

The armor, bedding layer, and the uppermost geotextile were removed from the slope between the elevation of the false bottom and the uppermost reach of runup. The bedding layer and the armor were replaced on the newly exposed geotextile layer. All work was done by hand.

The third series of wave runs were conducted on the slope with the Poly-Filter GB material. In this case, the waves for the concurrent experiment were applied before the waves of the Phase II experiment. Only minor damage was done to the armor layer by the pre-experiment waves. The damage was repaired using armor units from above maximum runup. Repair was done without draining the tank. As a consequence, some very minor "benching" below still water level was left in place for the third series of waves.

4.0 EXPERIMENTAL RESULTS

4.1 Analysis Method: Pore Pressure Data

Graphical data from the strip chart recorder were used as the primary source of data for pressure transducers at Stations 2, 4, 5, 7 and 9. The computer plots similar to the strip chart outputs were the primary data for the transducer at Station 6. Typical strip chart and computer plot outputs are shown in Figures 4.1 and 4.2.

A typical reduction of a graphical record is shown in Figures 4.1 and 4.2. The analysis was accomplished by visual averaging of the peaks and the troughs of the cyclic pressure readings. The main pressure was taken as the average pressure. No attempt was made to integrate the pressures with respect to time in order to arrive at a time-averaged pressure. The difference between the peak and trough pressure is called "transient amplitude" in this report. The difference between the mean pressure and the mean pressure prior to wave attack is called "residual pressure," a term used by Finn, Siddharthan, and Martin (1980) to describe excess pore pressures generated by cyclic shear stresses applied to a saturated cohesionless soil. In arriving at the residual pressure, long-term fluctuations in the mean pressure were taken into account. Those long-term fluctuations were due to a traveling standing wave pattern in the wave tank.

The number of wave cycles required to build a steady residual pressure was also evaluated visually as shown in Figures 4.1 and

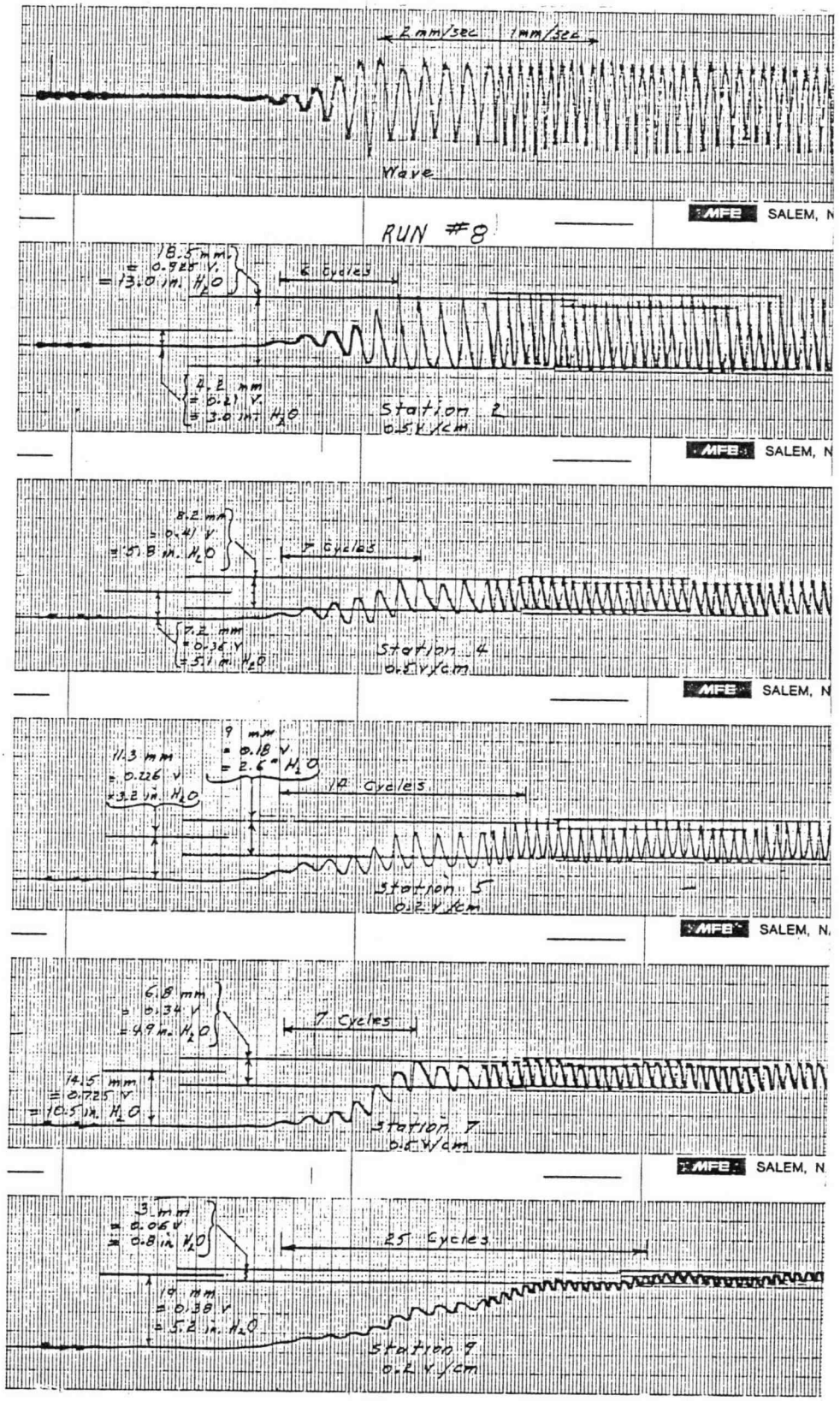

Figure 4.1. Typical strip chart of pore pressure data

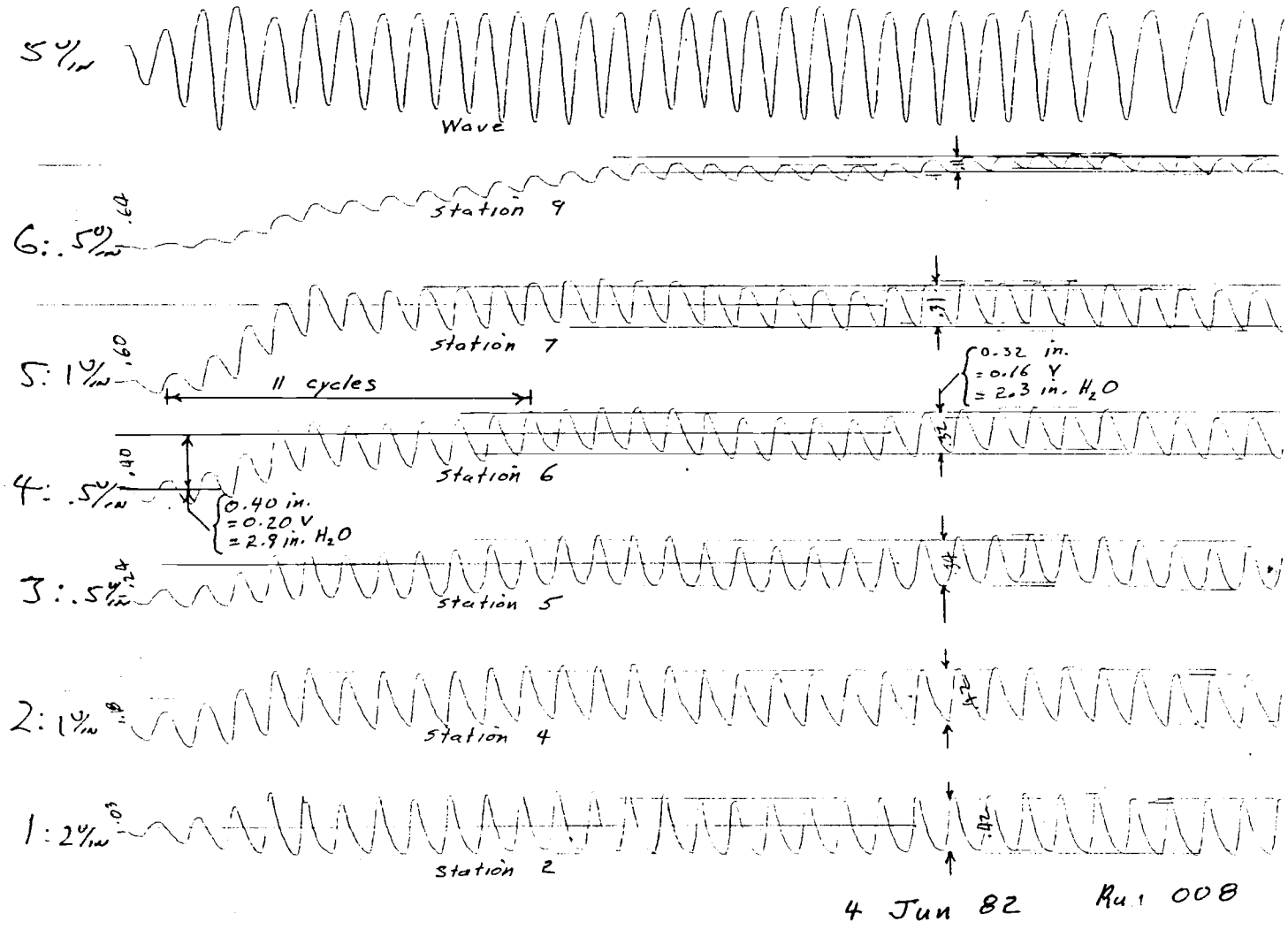

Figure 4.2. Typical computer plot of pore pressure data

4.2. In some cases, it was difficult to define the point at which the residual pressure became "steady." The "steady" point was chosen as the first point at which the pore pressure response met two criteria: (1) the transient response being steady in the long-term pattern, and (2) the mean pressure being equal to the long-term mean.

Digital computer output was used primarily to corroborate the graphical data. These data were most valuable for verifying transient amplitude since the initial pressures prior to wave attack were not adequately sampled in many cases. Close agreement between the digital data and the graphical analysis confirmed the accuracy of the graphical analysis.

The transient amplitude and residual pressures are normalized to the height of the attacking water wave for presentation in graphic form. The pressure values were converted to equivalent inches of water by dividing by the unit weight of water and non-dimensionalized by dividing the wave height in inches.

Several possible trends in the data were investigated by various graphic presentations of the data. The rate of generation of dimensionless residual pressure was checked for variation as a function of fabric permeability, of wave height, and wave period. The magnitudes of dimensionless residual pressure and dimensionless transient amplitude were investigated as a function of each of the same three variables.

Residual pressure and transient amplitude were plotted on a cross section of the revetment to demonstrate patterns of pressures

within the slope. Approximate contours of equal residual pressure were drawn on these plots. Examples of these plots are given in Figures 4.9 and 4.10. Data from the piezometers were used to extend the pattern of residual pressures. To aid in interpretation of the data, plots were made of (1) the number of wave cycles to build a steady residual pressure, (2) the dimensionless residual pressure, and (3) the transient pressure amplitude, each as a function of wave height at a given wave period. These plots were made for each transducer station and are attached to this report as Figures A.1 through A.12 of the Appendix.

4.2 Analysis Method: Armor Unit Stability

The stability of the armor units was evaluated by visual and aural observation by the author during testing. Colored stripes were painted across the slope to aid in identification of any stones that moved. Minor in-place movements of individual units were recorded as "adjustments." These were small movements that diminished as the unit adjusted to a more stable position. Initial damage was defined as the situation in which the nominal size 44 lb (20 kg) stones and larger were observed moving out of their original positions and rolling down the slope. Typically, when rock that size began to move, there was considerable continuing action throughout the 100-wave burst. These movements were distinct from the adjustment-type movements under smaller waves.

Observations of rock movements were verified where possible by photographs of the slope taken after each wave case. However, only

the portion of the slope above still water level was visible in the photographs, and failure typically was initiated in the portion of the slope between still water level and minimum draw down. Drainage of the large wave tank between wave cases was not practical.

Observations of armor stability are plotted on a fail/no-fail basis. The plot demonstrates the wave cases tested and reveals the failure wave height at each wave period for each of the fabric cases.

4.3 Results: Residual Pore Pressure

4.3a Rate of Residual Buildup

Steady residual pore pressure was reached in fewer than 40 wave cycles in every case. In the very few cases for which fabric permeability appeared to make a difference in the rate of rise of residual pressure, the most permeable fabric case required the fewest wave cycles to reach a steady residual pressure. The rate of buildup was slower for the 3.95 sec waves than for either the 2.80 or 5.59 sec waves. The number of cycles to achieve steady residual pore pressure was independent of wave height.

4.3b Magnitude of Residual Buildup

As indicated in Figures 4.3 through 4.7, the magnitude of the dimensionless residual pressure was sensitive to wave length and to distance into the slope, but generally quite insensitive to wave height. Varying the permeability of the geotextile affected the residual pressures. The effect was different at different locations within the core.

In general, the dimensionless pressure increased as wave length increased, for the shorter wave lengths tested, and remained approximately constant as wave length increased further. The deeper into the slope the transducer was located, the more definite the trend. The shallow transducers at Stations 2, 4, and 7 showed fluctuations of the dimensionless residual at the longer wave lengths. These results are shown in Figures 4.3 through 4.7.

The most consistent trend in the dimensionless residual pressure was a rapid decrease with distance into the slope. The plots in Figure 4.8 and the typical residual pressure contours shown in Figures 4.9 and 4.10 demonstrate this rapid decrease. The peak residual pressure appears to occur near the intersection of the still water level and the plane of the geotextile. This pattern did not change as geotextile permeability varied.

Associated with the pore pressure rise within the slope was an actual rise in the average phreatic surface. The piezometer at Station 10 was located 3 in (8 cm) above the still- water phreatic surface, but filled with water and recorded residual and dynamic pore pressures during experimental runs with waves of about 1.5 ft (0.5 m) height and larger.

The effect of geotextile permeability on the magnitude of dimensionless residual pressure is reversed between the shallow transducer stations located below portions of the slope below still water level and those located below portions of the slope at or above the still water level. The downslope stations show the largest residuals under the impermeable fabric and lowest residuals

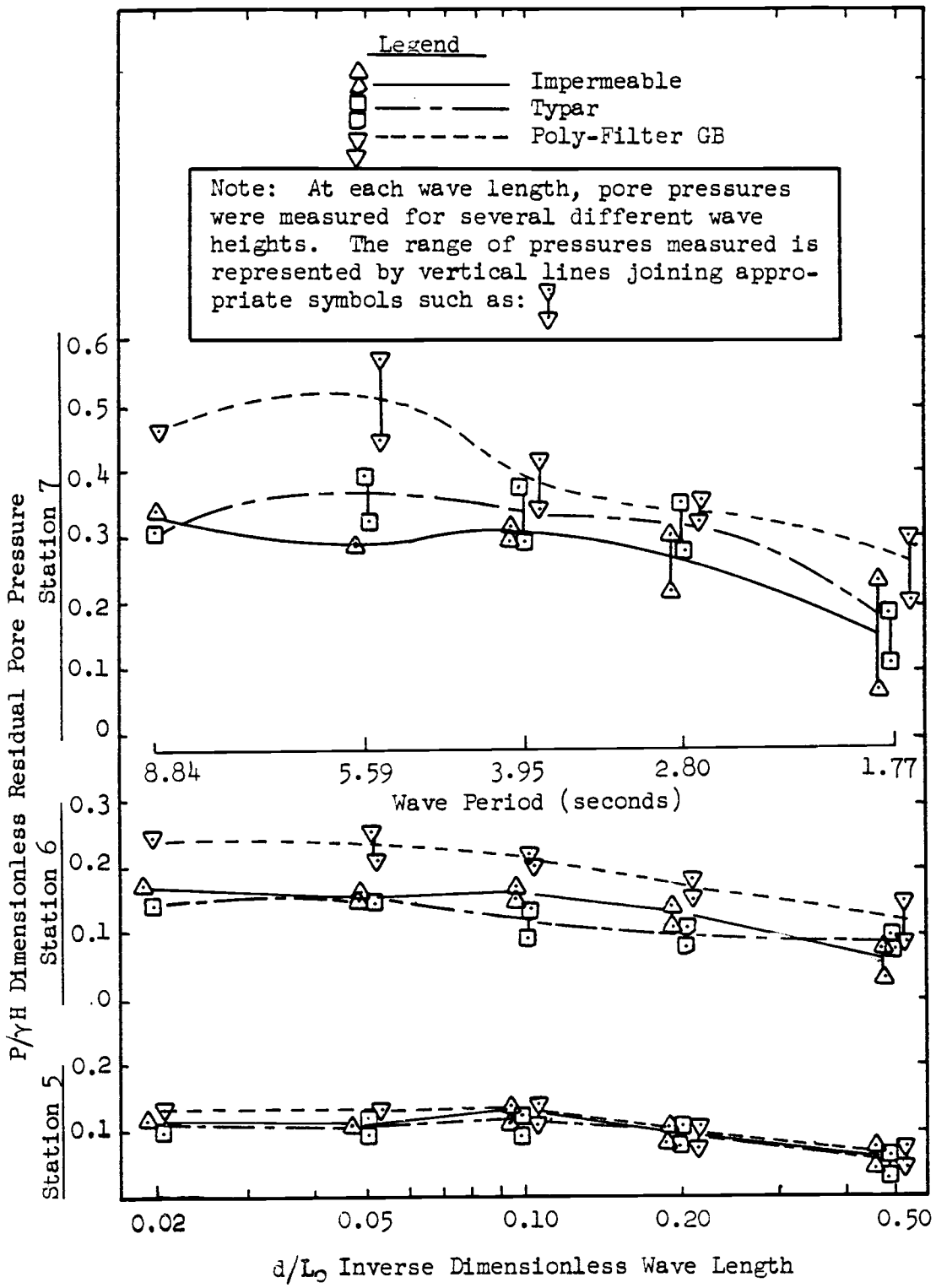

Figure 4.3. Dimensionless residual pore pressure as a function of inverse dimensionless wave length for Stations 5, 6, and 7

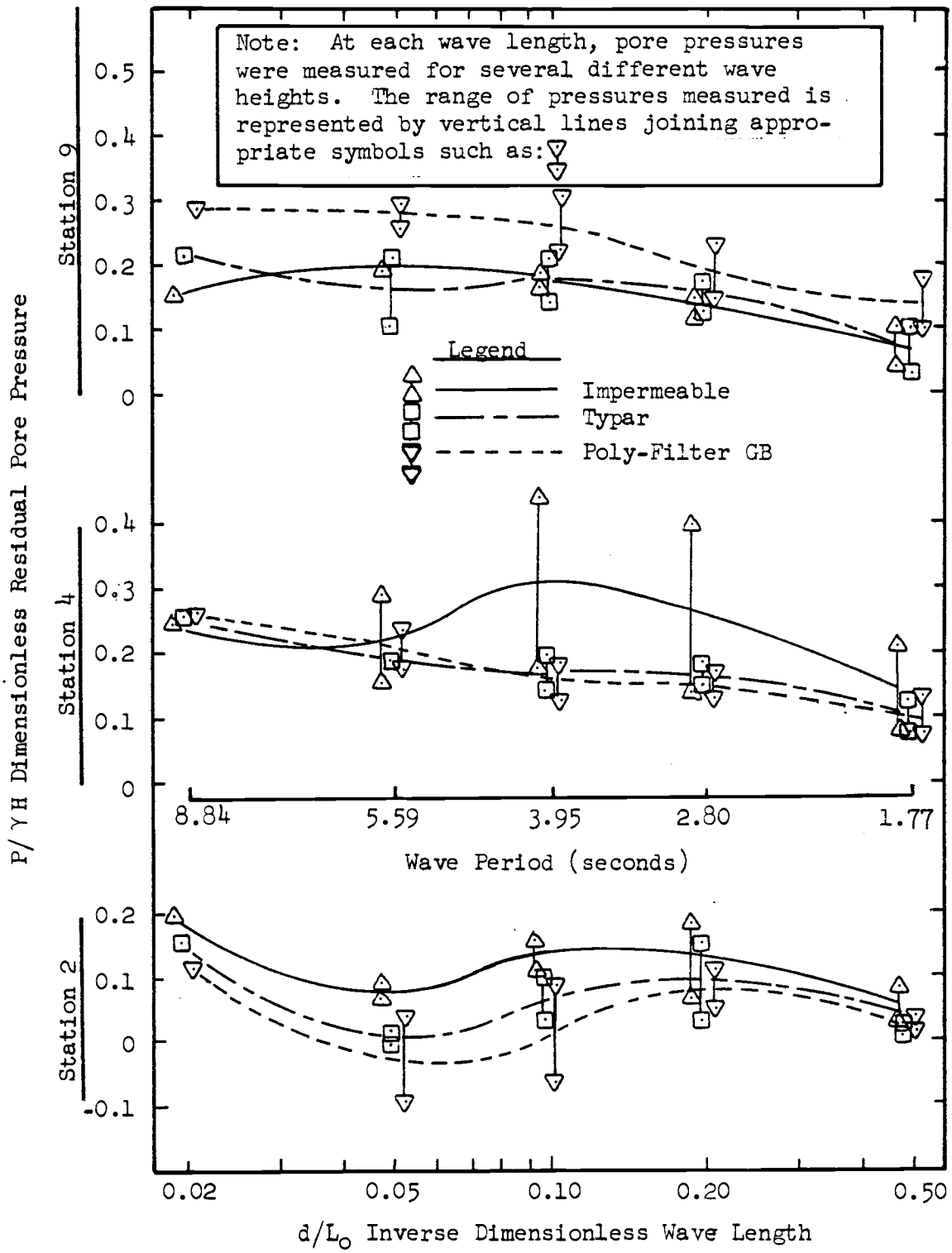

Figure 4.4. Dimensionless residual pore pressure as a function of inverse dimensionless wave length for Stations 2, 4, and 9

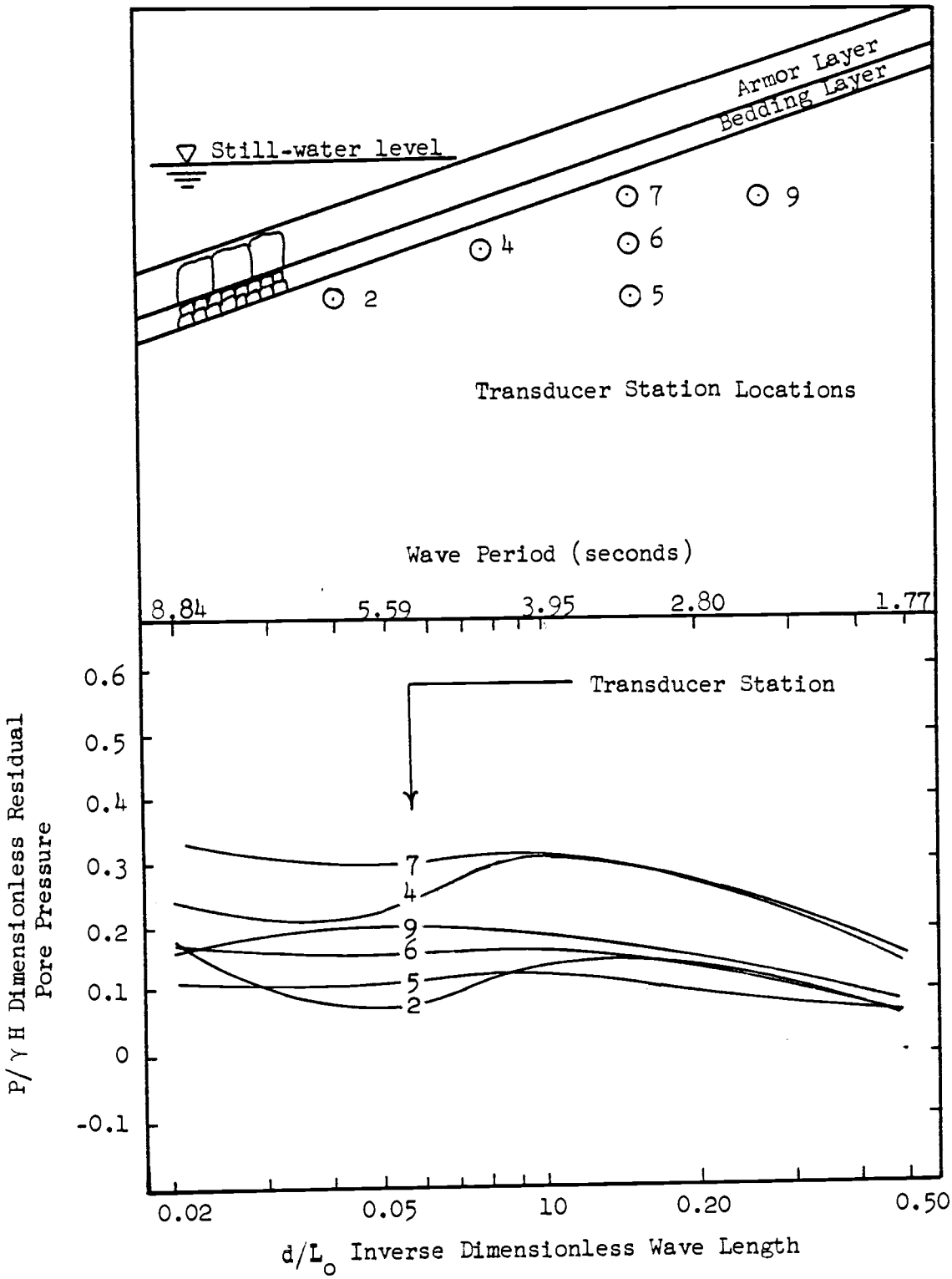

Figure 4.5. Dimensionless residual pore pressure as a function of inverse dimensionless wave length and location in the structure with Impermeable membrane

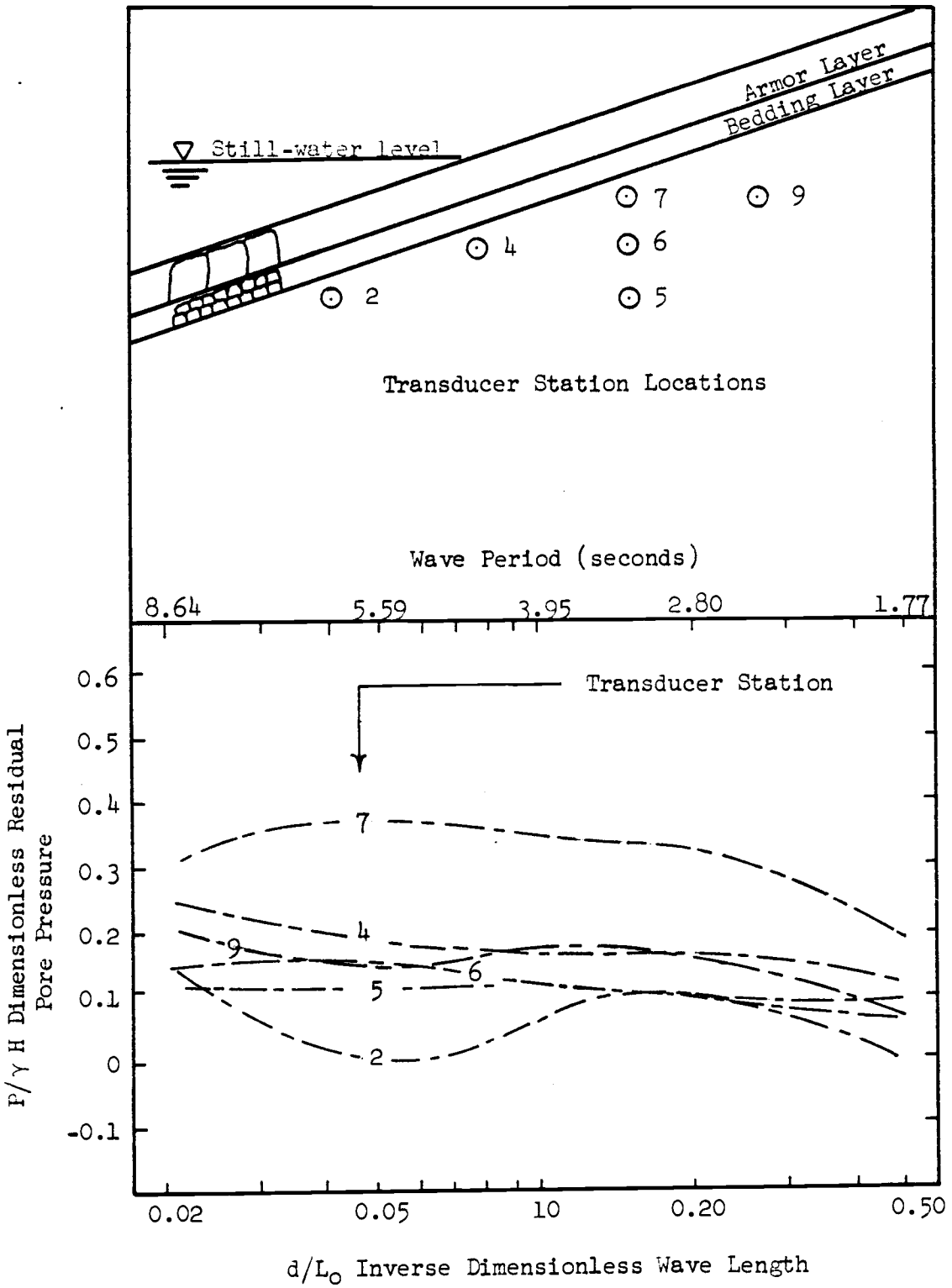

Figure 4.6. Dimensionless residual pore pressure as a function of inverse dimensionless wave length and location in the structure with Typar, low permeability geotextile

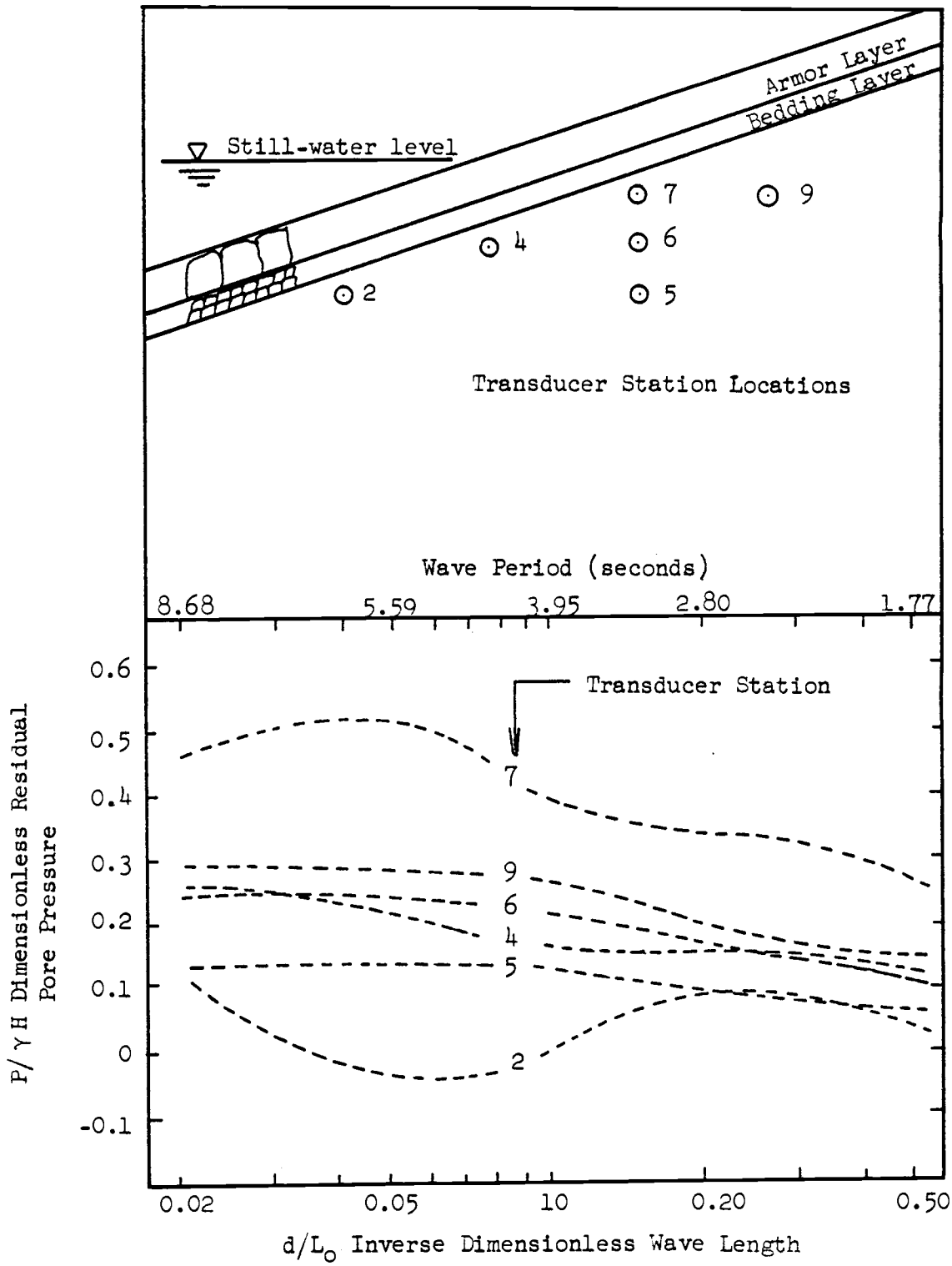

Figure 4.7. Dimensionless residual pore pressure as a function of inverse dimensionless wave length and location in the structure with Poly-Filter G.B., high permeability geotextile

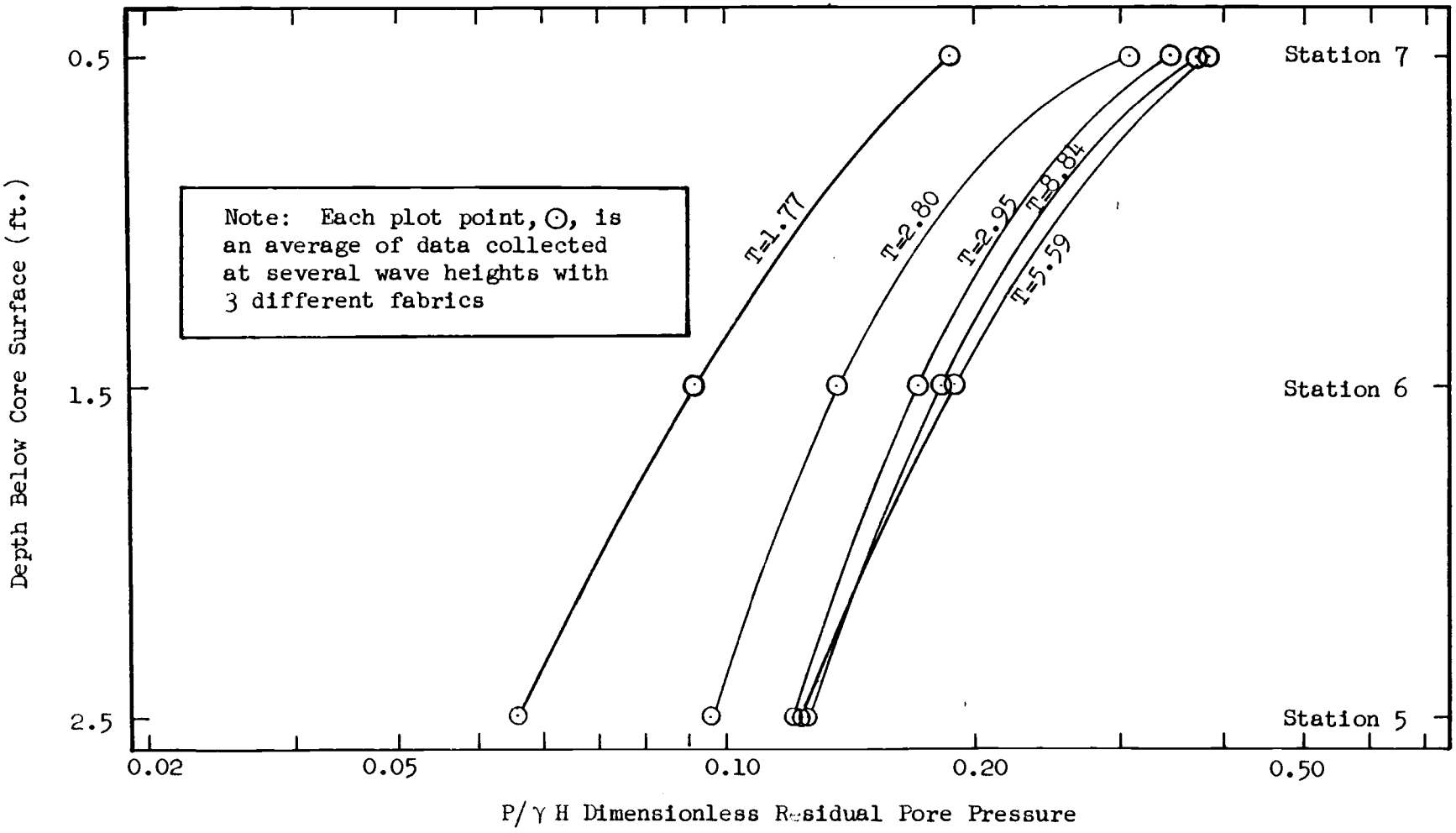

Figure 4.8. Dimensionless residual pore pressure as a function of depth below the core surface at Stations 5, 6, and 7

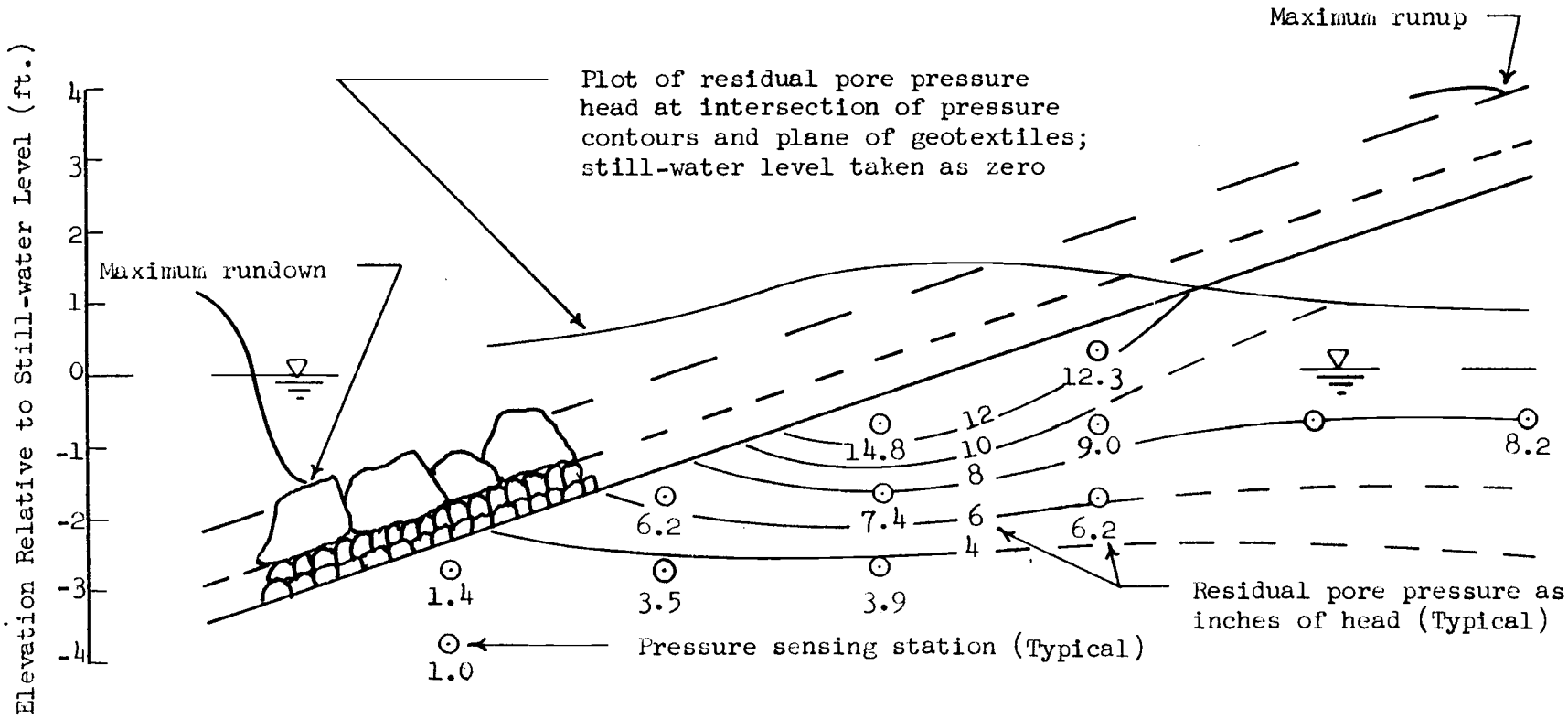

Figure 4.9. Pattern of residual pore pressures in core of structure with high permeability geotextile under a 36-inch high, 3.95 second wave

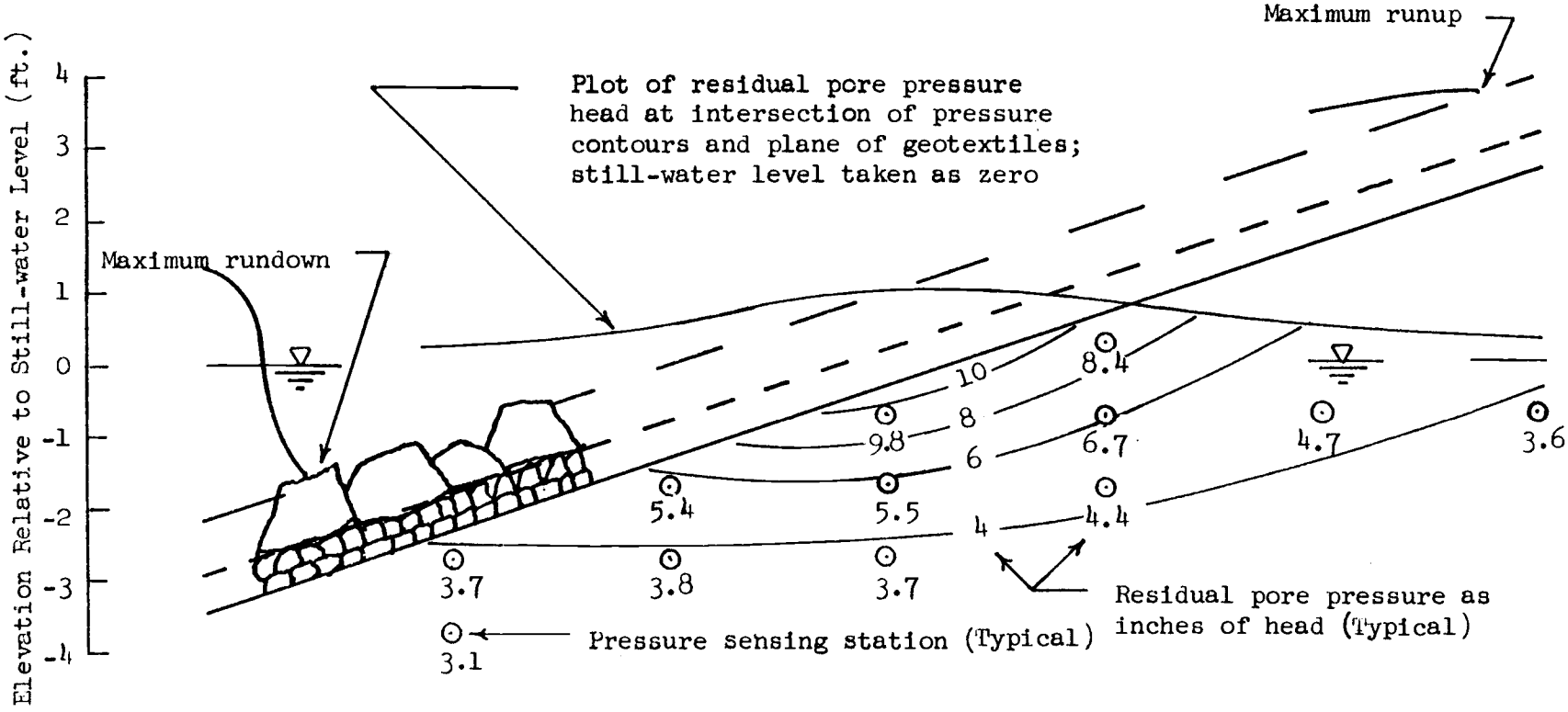

Figure 4.10. Pattern of residual pore pressures in core of structure with an impermeable membrane under a 36-inch high, 3.95 second wave

under the highly permeable fabric. The situation is reversed higher on the slope. Since the upper slope residuals are always the highest, the result is that highest downslope residual pressure gradients are observed under the most permeable fabric. The differences in response among the fabrics diminished rapidly with distance into the slope. At Station 5 at a depth of 2.5 ft (0.76 m) below the geotextile/still-water intersection, there is virtually no difference in residual pressure among the different fabric cases. Thus, the effect of geotextile permeability on residual pore pressure is limited to a reduction in downslope pore pressure gradient associated with a reduction in fabric permeability, and this effect occurs only near the surface of the core.

The magnitude of dimensionless residual pressure does not appear to be related to wave height in any consistent way. The general tendency appears to be one of remaining relatively constant as wave height changes. The one notable exception to this general lack of trends is the case of the transducer at Station 2 under the highly permeable fabric and under wave loadings with period of 3.95 sec and longer. In this case, the residual is negative for very small waves and increases into the same range as the other fabrics as wave height increases.

4.3c Magnitude of Transient Pressure Amplitude

The dimensionless transient pressure amplitude shows very consistent trends. Figures 4.11 through 4.18 illustrate these trends. As wave length increases, the magnitude of dimensionless transient pressure amplitude also increases for all transducers and

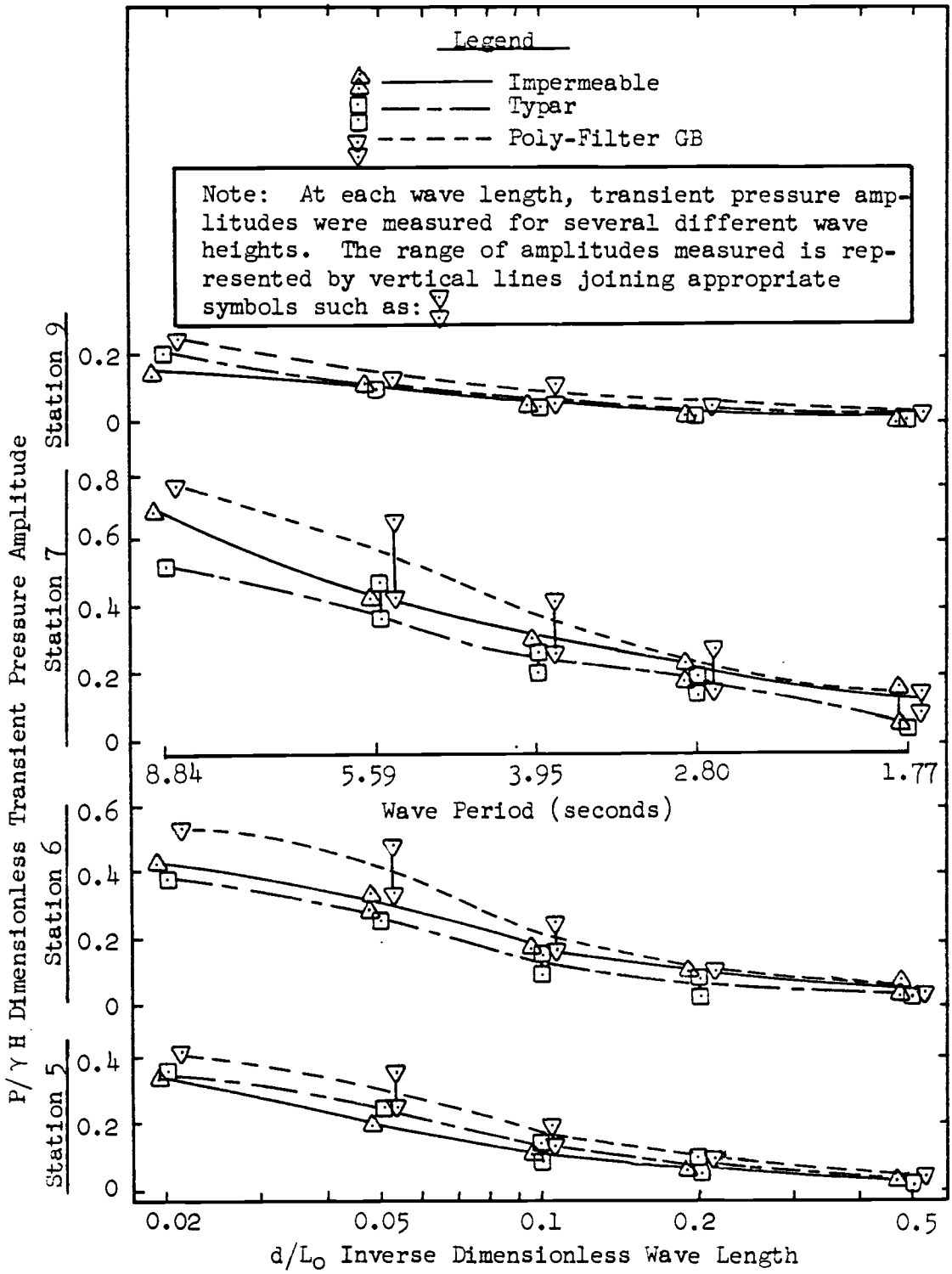

Figure 4.11. Dimensionless transient pressure amplitude as a function of inverse dimensionless wave length for Stations 5, 6, 7, and 9

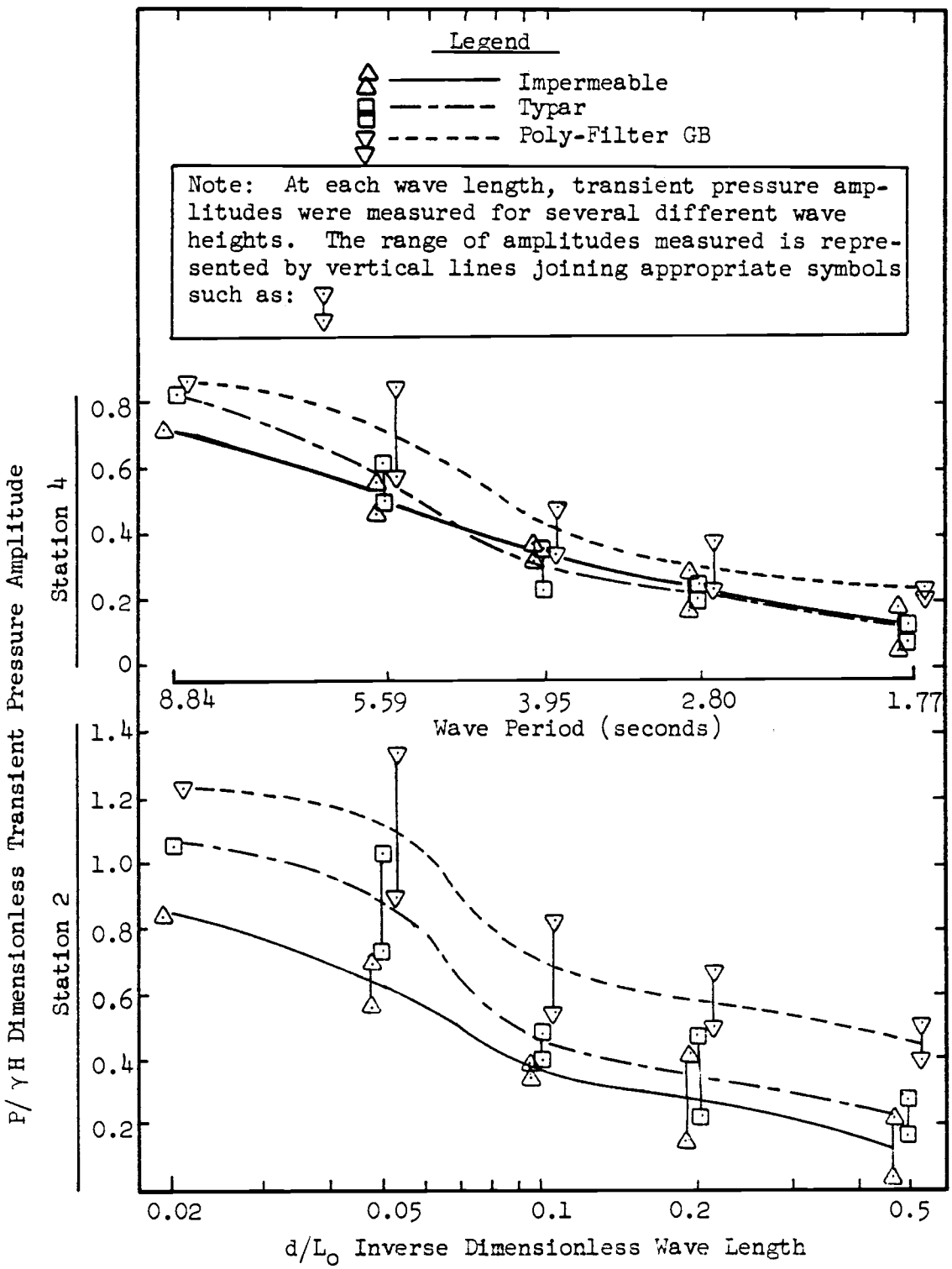

Figure 4.12. Dimensionless transient pressure amplitude as a function of inverse dimensionless wave length for Stations 2 and 4

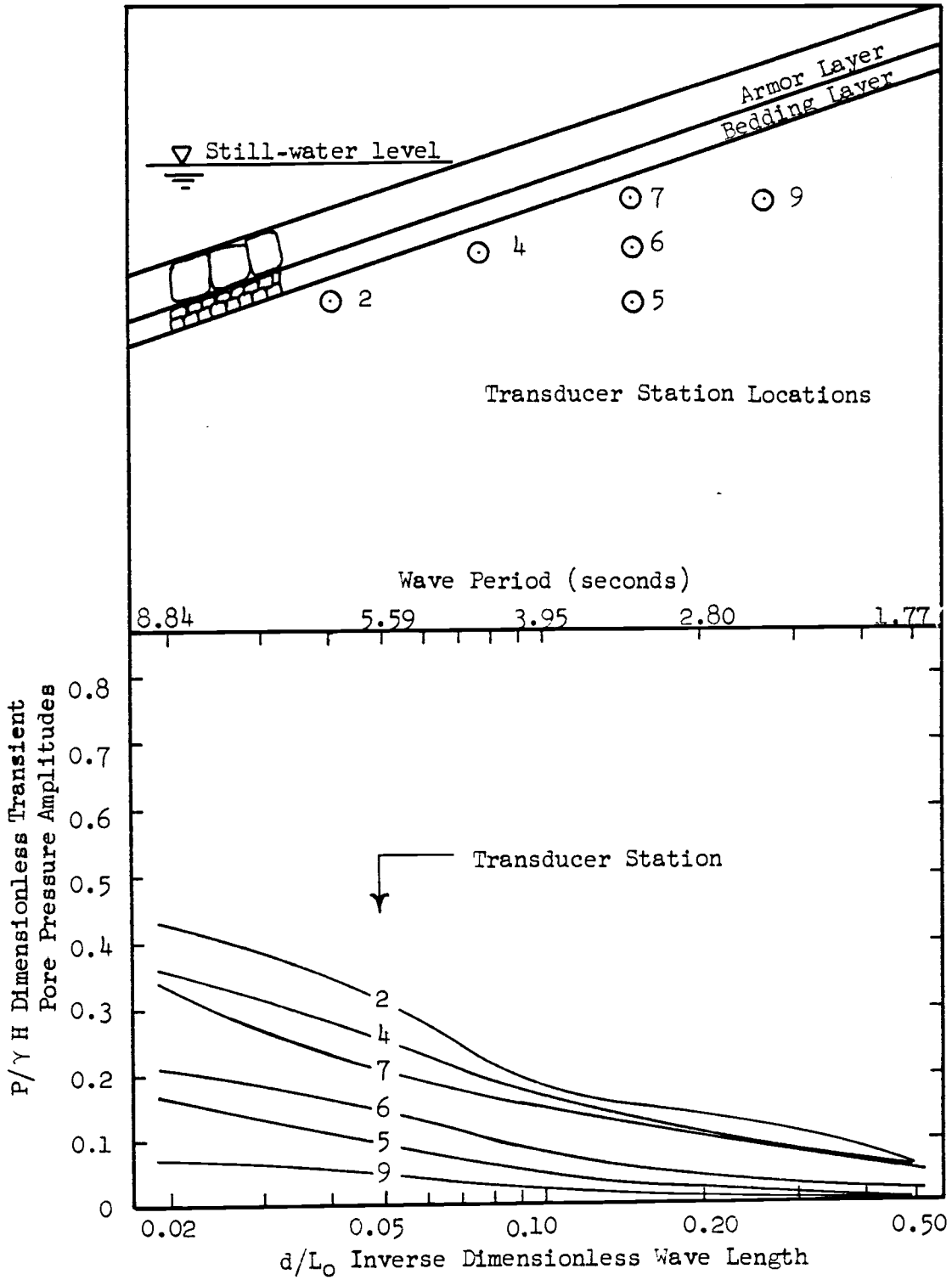

Figure 4.13. Dimensionless transient pressure amplitude as a function of inverse dimensionless wave length and location in the structure with an impermeable membrane

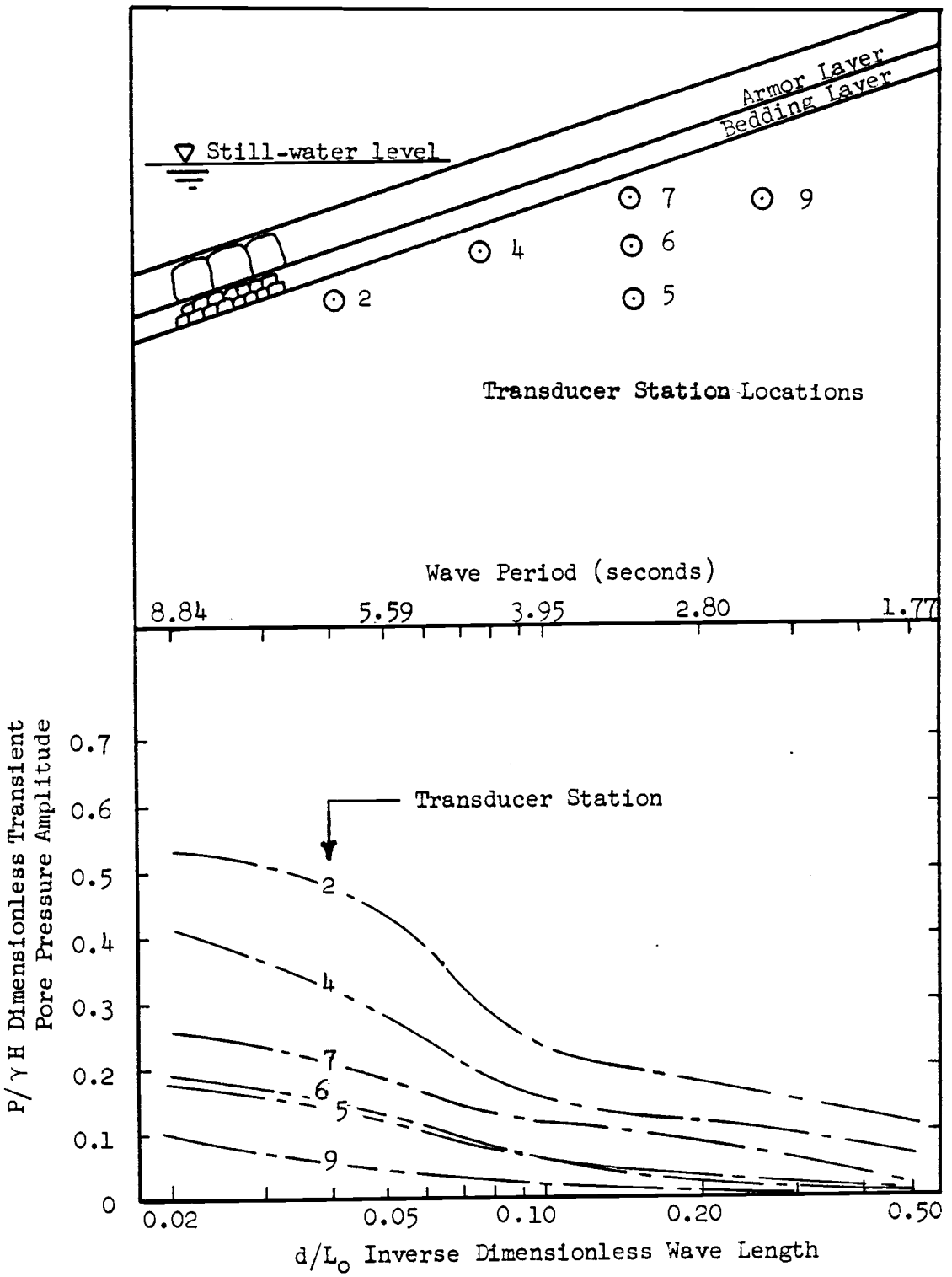

Figure 4.14. Dimensionless transient pressure amplitude as a function of inverse dimensionless wave length and location in the structure with Typar, low permeability geotextile

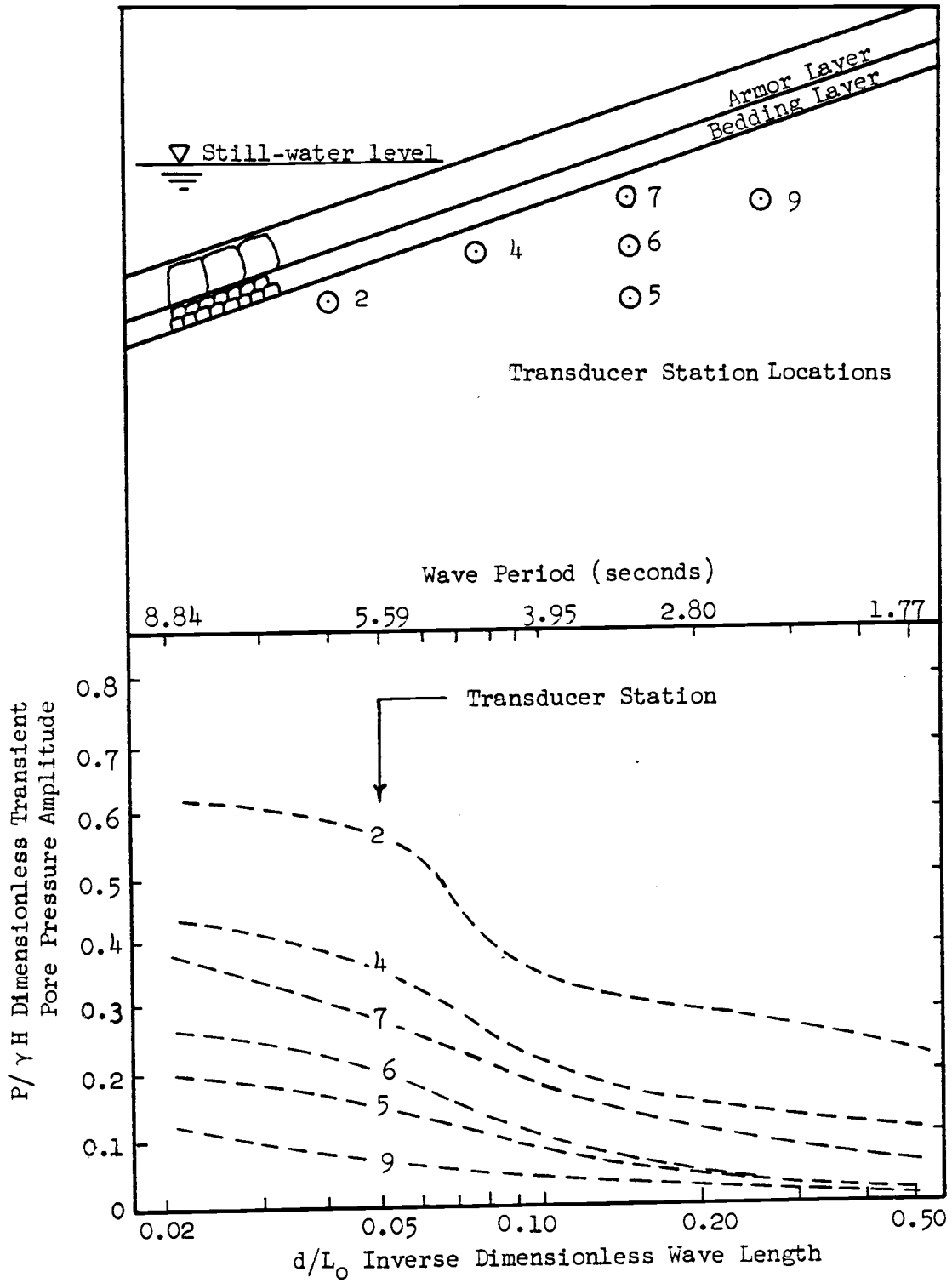

Figure 4.15. Dimensionless transient pressure amplitude as a function of inverse dimensionless wave length and location in the structure with Poly-Filter GB, high permeability geotextile

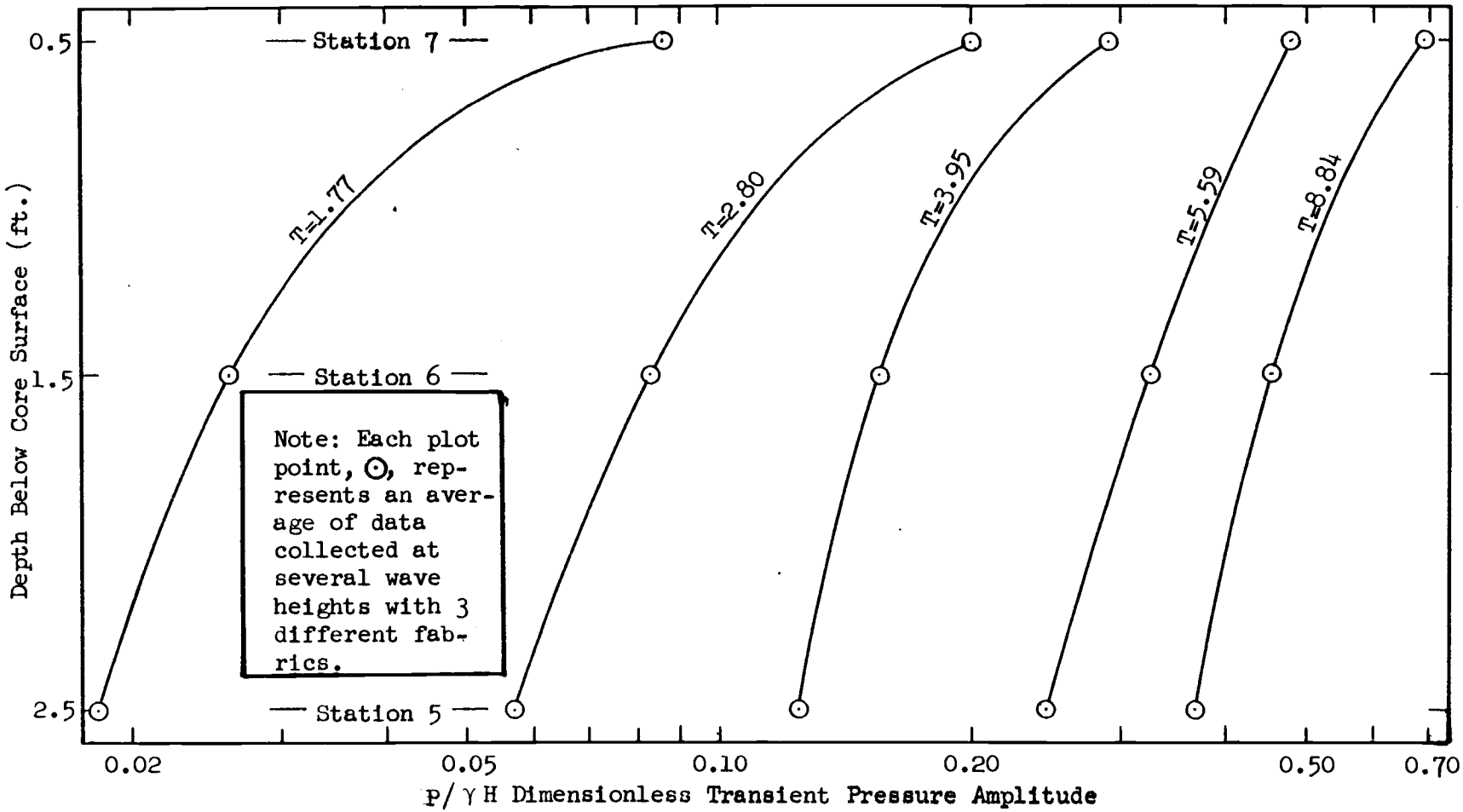

Figure 4.16. Dimensionless average transient pressure amplitude as a function of depth below the core surface at Stations 5, 6, and 7

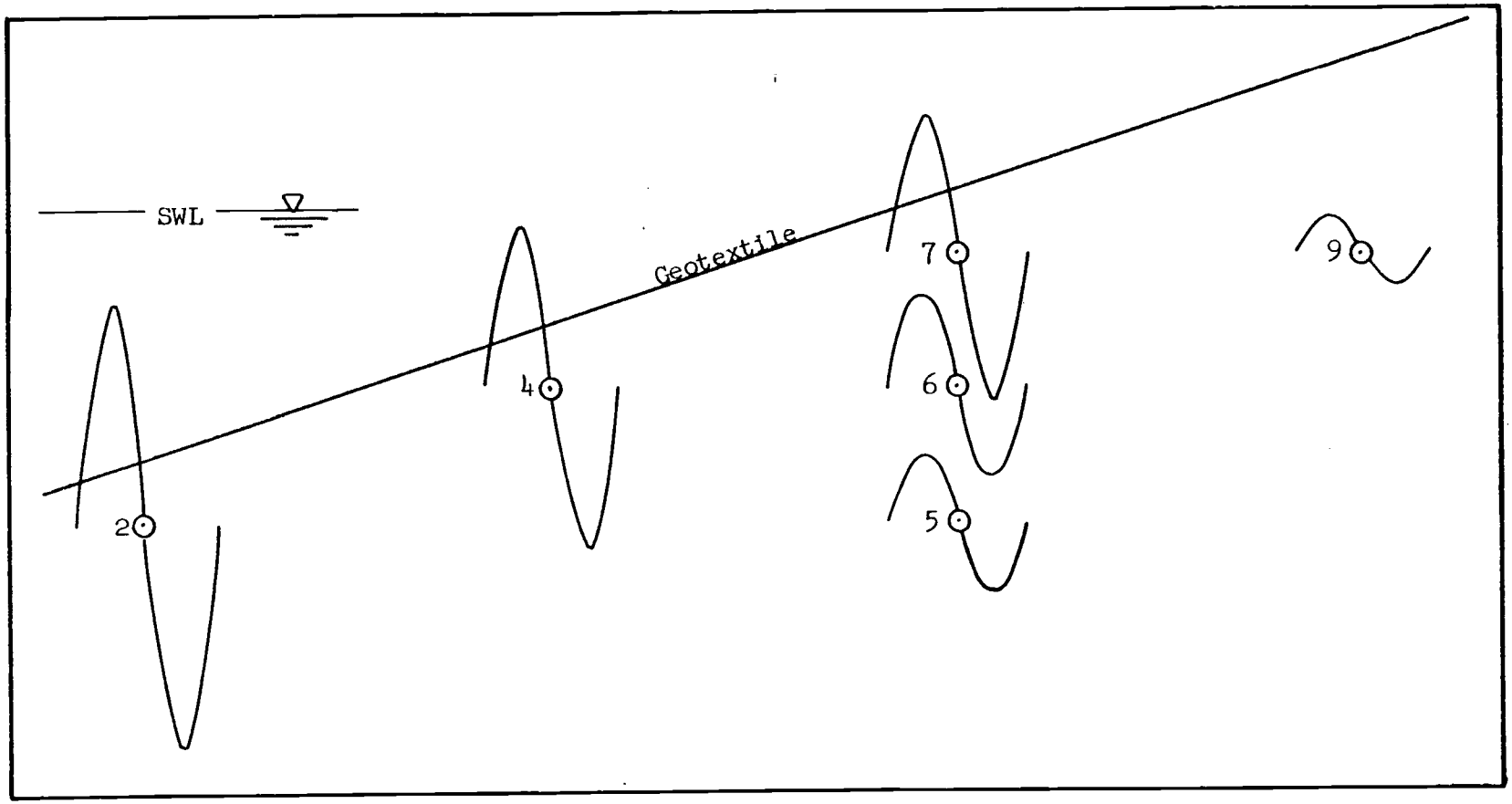

Figure 4.17. Idealized representation of transient pressure amplitude as a function of position in the structure core

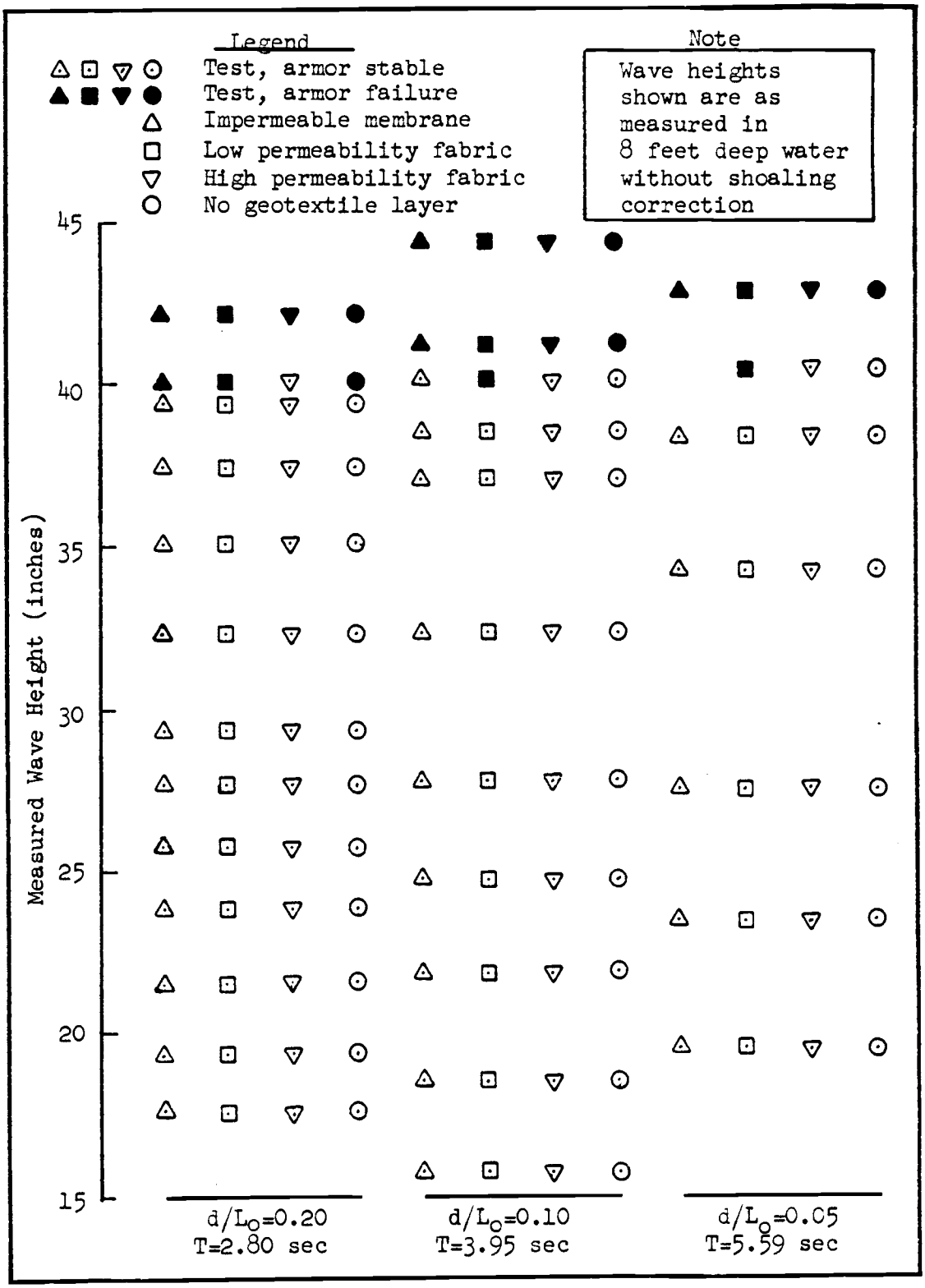

Figure 4.18. Wave height causing initial failure of armor as a function of wave period and geotextile permeability

for all geotextile cases. The dimensionless magnitude at the near-surface Stations 2, 4, and 7 is consistently the greatest for the most permeable case under small waves. This difference tends to disappear as wave height increases. The low permeability case and the impermeable case show no consistent trend relative to each other, with the impermeable fabric resulting in the lowest magnitude at Station 2 and the Typar the lowest at Stations 6 and 7. Figure 4.16 shows that the most pronounced transient responses are nearest the core surface decreasing rapidly with distance into the core. The largest magnitude transient response occurs at Station 2, the near-surface station lowest on the slope. The response progressively decreases at progressively higher near-slope stations. This result is idealized in Figure 4.17.

4.4 Results: Armor Unit Stability

Figure 4.18 demonstrates the failure envelope established during the Phase II experiment. Initial failure of the armor occurred at virtually the same wave height regardless of wave period and regardless of geotextile used. In some cases, the armor failed under a wave at one wave period which was then followed by a wave of smaller height at a different period. Even though failure had been initiated, the armor would remain stable when under attack by the smaller wave.

Interestingly, smaller stones appeared to find appropriate stable environments in the interstices of the larger rocks. These smaller stones would remain in these stable spots until such time

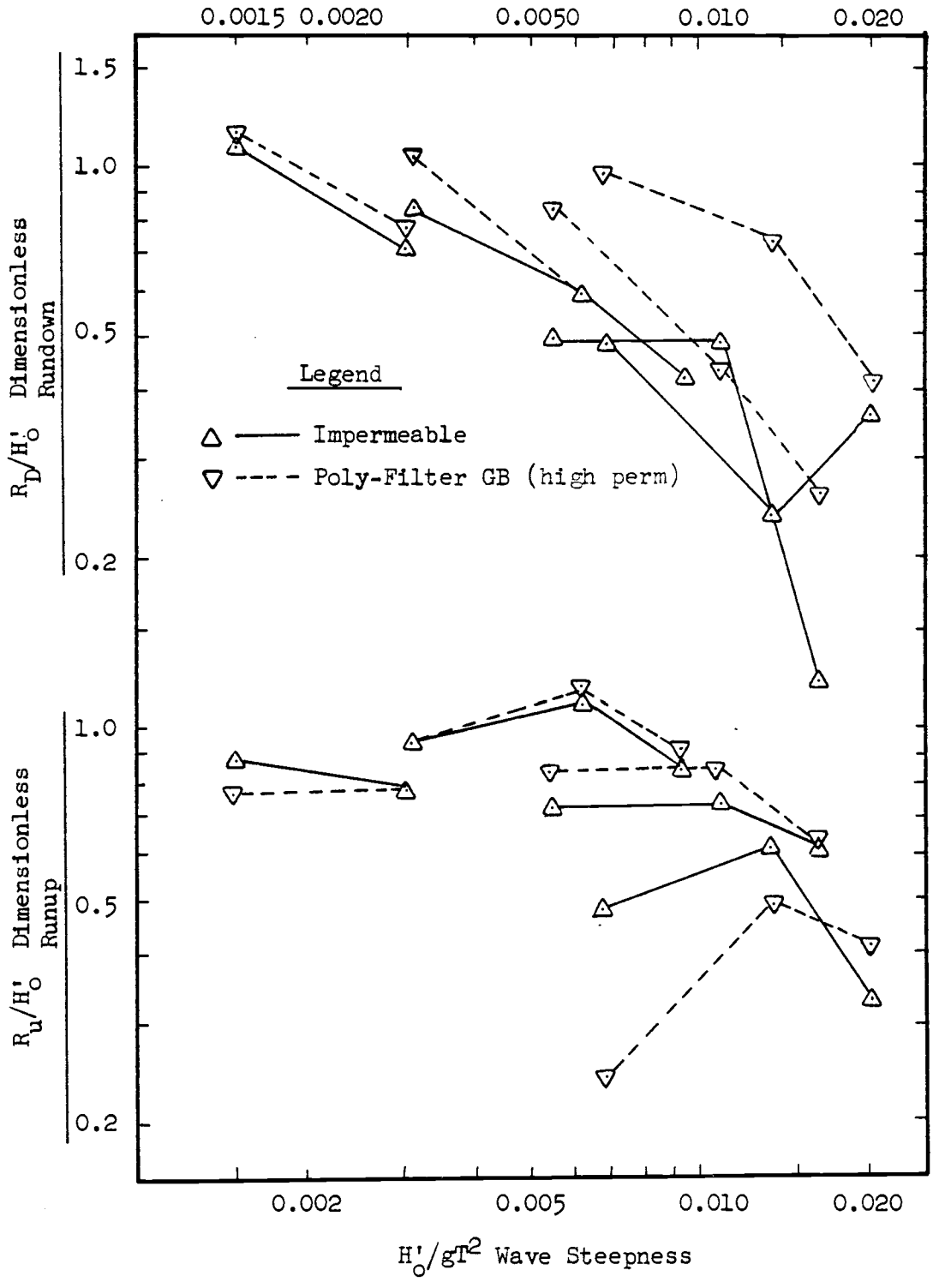

Figure 4.19. Phase I dimensionless runup and rundown as a function of wave steepness for impermeable membrane and highly permeable Poly-Filter GB

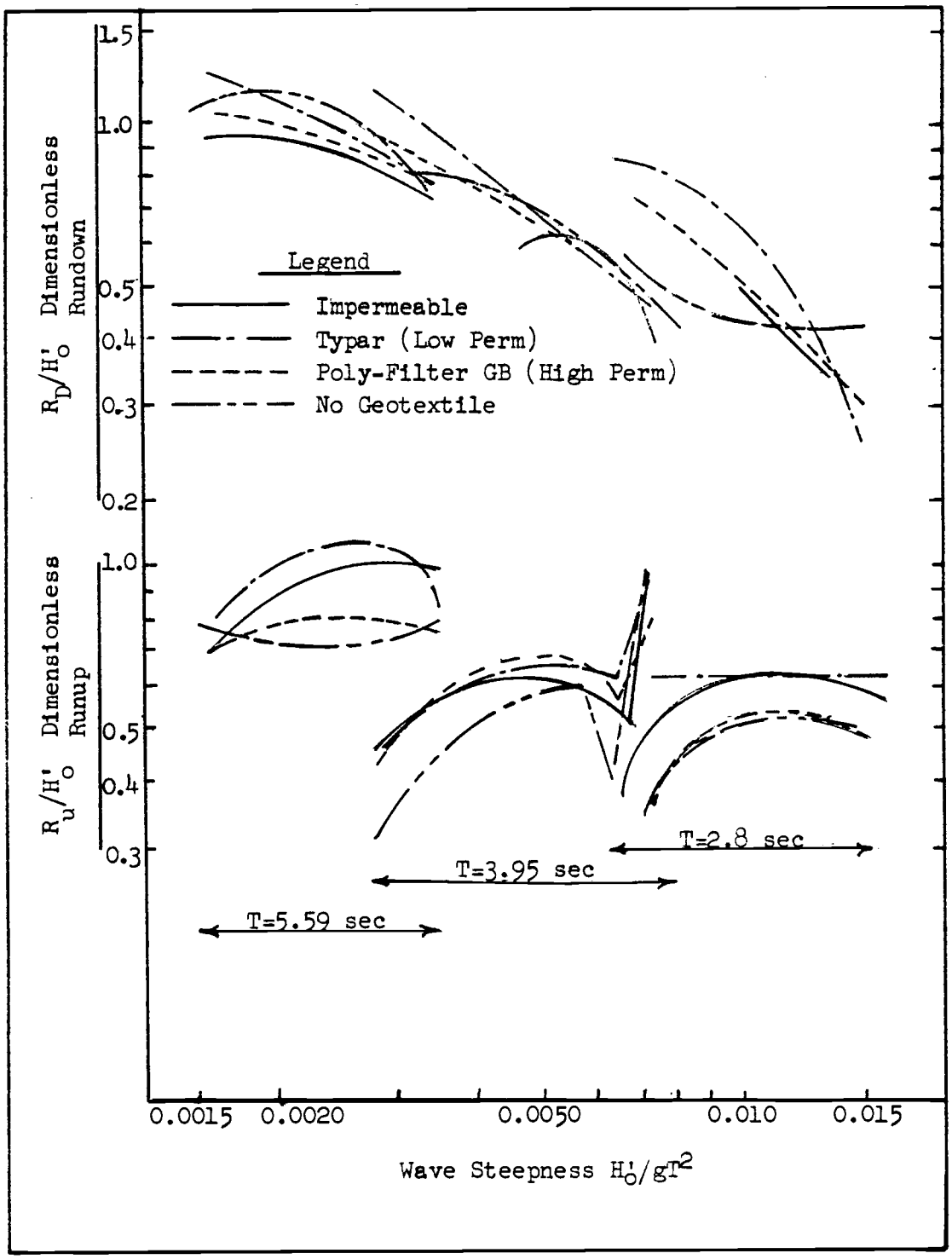

Figure 4.20. Phase II runup and rundown as a function of wave steepness at various geotextile permeabilities

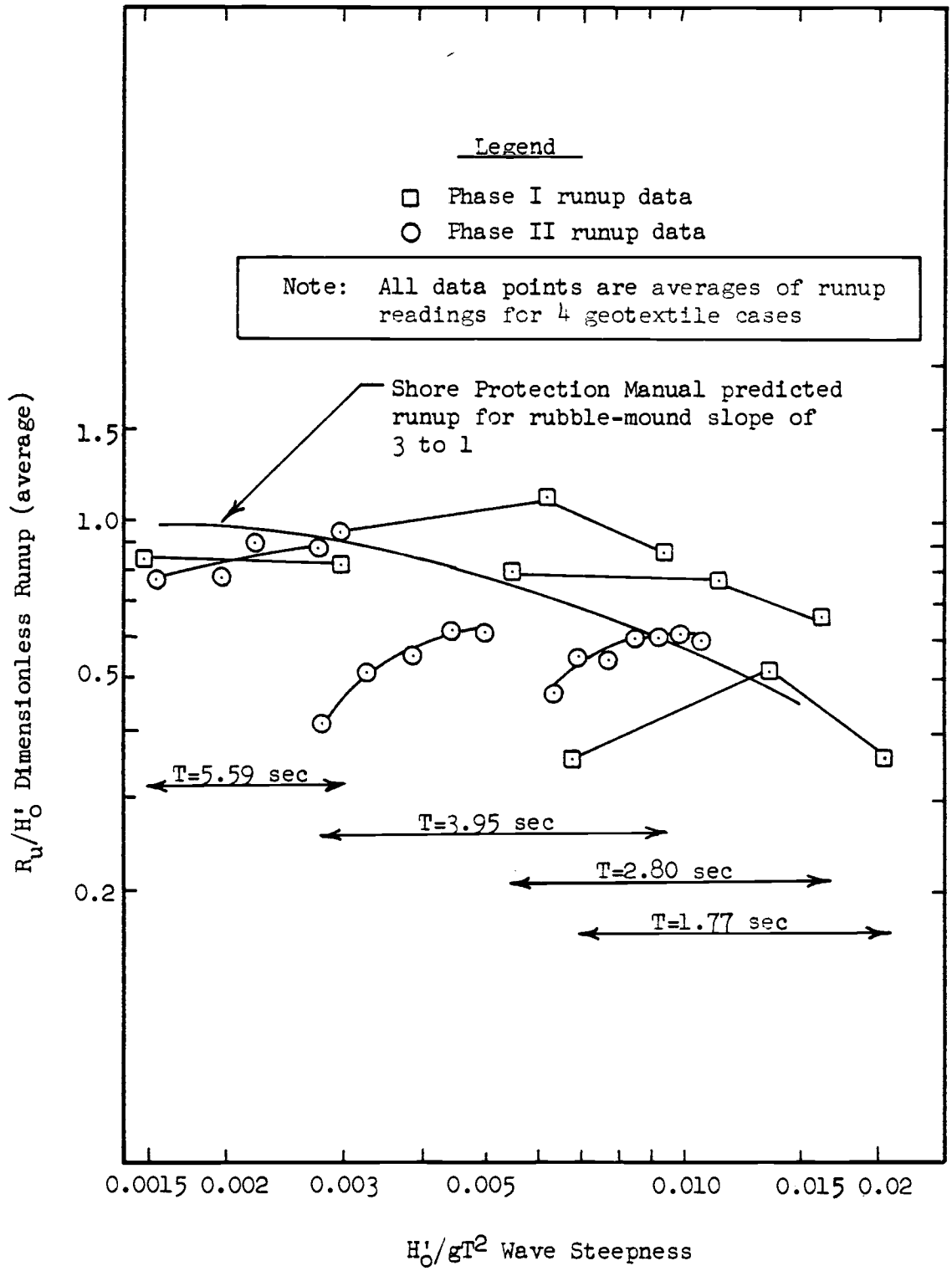

Figure 4.21. Average dimensionless runup as a function of wave steepness for Phase I and Phase II

as the nominal size rock began to move.

A Hudson's stability coefficient was computed for the graded stone armor based on the actual 44 lb (20 kg) median size and a 40 in (1.02 m) failure wave. The computed stability coefficient of 9 was much higher than that which was anticipated for this armor.

4.5 Runup and Rundown

Runup and rundown are plotted as a function of wave steepness in Figures 4.19, 4.20, and 4.21. Included on the runup plots in Figure 4.21 is a plot of predicted runup for permeable 3 to 1 slopes from the U.S. Army Corps of Engineers, Shore Protection Manual (1977). The runup pattern corresponds well to the pattern predicted by the Corps of Engineers. The prismatic armor of Phase I showed slightly higher runup than predicted, and the graded rubble of Phase II slightly lower than predicted runup.

The runup pattern for the prismatic armor compares well with results by Sollitt and DeBok (1976) for the same material. As in the Sollitt and DeBok investigation, the dimensionless runup increases with increasing wave steepness for a given wave period and decreases with a decrease in wave period.

During Phase II, runup on the slopes with the less permeable Typar in place, and with the impermeable membrane in place, appeared to be very modestly greater than runup on the Poly-Filter GB and no-fabric slopes for the 2.8 sec and 5.59 sec period waves. Results were virtually the same for all fabrics for the 3.95 sec waves in both Phase I and Phase II. In Phase I, runup did not vary

in a consistent way with geotextile permeability. At the longer wave lengths, the results were approximately the same for all geotextile cases, but at the shorter wave lengths, results showed apparently higher runup for the impermeable fabric case at the 1.77 sec period and apparently lower runup for the impermeable case at the 2.8 sec period.

5.0 DISCUSSION OF LARGE-SCALE TEST RESULTS

5.1 Residual Pore Pressures

5.1a A Model for Residual Pore Pressure Generation

The residual pressures show a very consistent pattern within the slope, peaking at the still water level intersection with the surface of the core and becoming smaller both upslope and downslope of that point. The peak magnitude of this pressure expressed in terms of hydraulic head is on the order of 1/2 the wave height. Pressures of this magnitude may have a significant effect on the stability of both the core material and the armor of a rubble structure.

There are several different descriptive models which might explain the pattern of residual pressures within the core. Seed and Rahman (1978) proposed a model for wave-induced pore pressures in ocean floor deposits. In this model, the pore pressures are a response to the cyclic shear stresses within the soil which result, in turn, from the wave-generated cyclic pressure loadings on the soil surface. Although the face of shore protection structure is not horizontal and is not entirely submerged as in the ocean floor, the wave loading on the slope is cyclic and undoubtedly results in cyclic shear stresses within the core of the structure.

A second way of descriptively modeling the residual pore pressure pattern is as a response to an average flow pattern. The water transported onto the slope by the attacking waves can be thought of as being delivered by a large source pouring onto the

slope in the vicinity of the intersection with the still water level. This source water in the model then flows down through the slope and exits somewhere lower down on the slope or near the toe. Such an average flow into the slope would generate pressure gradients with equipotential lines similar to those in Figures 4.9 and 4.10.

A third descriptive model takes into consideration the fact that a substantial amount of the water downrushing from a spent wave never reaches down to the elevation on the slope corresponding to the wave trough before being overrun by the next onrushing wave. As this water rushes downslope, some of it must travel a tortuous, turbulent path through the upper layers of the rubble, and that portion flowing over the rubble is also slowed in its retreat by friction with the rough surface. Thus, even at minimum drawdown, a moving layer of water still lies on the slope. Often a portion of this layer lies above still water level. This moving layer of water has a considerable velocity through the highly porous rubble armor and exerts both static and kinetic hydraulic pressure loads on the surface of the structure core. Therefore, the average hydraulic load on the surface of the core during a wave cycle is greater than the hydraulic load imposed by the still water situation. At least a portion of this load is transmitted to the pore fluid in the core. This third model perhaps serves best as an explanation of the water source of the second model. Without the through-the-core flow proposed in the second model, the third model

cannot account for the attenuation of residual pressure with distance into the core.

The experimental results cast doubt on the utility of the second and third models. One would expect that higher rates of flow into the slope would result from higher fabric permeabilities. These higher flows would, in turn, result in a higher seepage pressure near the theoretical source. At transducer Station 7, nearest the theorized "source," the residual is, in fact, greatest for the case of the highest permeability fabric. However, the impermeable geotextile case also shows a considerable residual pressure at this source position. Since any flow into the core is blocked by the impermeable membrane, the residual pressure in this case must be due to a different mechanism.

Perhaps the best model of the residual pressure generation is a combination of the three models mentioned. Such a combination of the cyclic shear mechanism and the flow-through-the-core mechanism of generation of residual pressures accounts for several of the experimental results observed and is not in conflict with any of the results. The fact that residuals at Station 7 are higher in the case of the higher permeability fabric, and lower at Station 2 for this same case, can be explained in terms of an average circulating flow entering near Station 7 at the still water level and exiting in the vicinity of Station 2 near or below minimum rundown. The existence of residuals in the case of an impermeable boundary can, in turn, be explained as a response to cyclic shear stresses as in the Seed-Rahman ocean floor model. The resulting

descriptive model is one of cyclic shear-generated pore pressures modified by a superimposed pattern of seepage pressures resulting from an average circulating flow condition in the core.

During the experiment, a rise in the elevation of the average phreatic surface was observed. This fits well with the combination model. However, in the impermeable membrane case, the source of water to fill the pore volume between the original still water phreatic surface and the raised phreatic surface must be other than the face of the structure. In this case, the rise could possibly be due to flow upward in response to cyclic-shear-generated pore pressures, the extent of the upward migration of the phreatic surface being limited by the balancing gravity gradient. The pore water flowing upward would be replaced by leakage into the toe of the slope or around the edges of the membrane. This type of mechanism accounts for the slower rate of rise in the impermeable case.

5.1b Implications for Armor Stability

Residual pressures generated by cyclic shear stresses are not transmitted beyond the boundaries of the core material. As explained by Seed and Rahman (1978), the total stresses within the soil structure do not change in response to the residual pore pressure buildup, but there is a reduction of the effective stress, equal in magnitude to a concurrent increase in pore fluid pressure. This type of redistribution of stress within the core can only affect the armor units if the core material experiences reduced effective stress or liquefies to the extent that the armor sinks into the core. Alternatively, this can be called a "flowing

out" of the liquefied core material. If a geotextile with pores small enough to retain the core material is in place between the core and the armor, the armor would, in effect, be "floating" on a deformable bed. This situation could lead to reduced armor stability.

5.1c Implications for Core Stability

A reduced effective stress condition or liquefaction of the core material can occur if the pore pressures within the core rise severely or become equal to the total stress in the core. The presence of armor units contributes to the total stresses within the core so that the pore pressures must be correspondingly larger to cause liquefaction or dangerously reduced effective stresses. Seed and Rahman (1978) observed in their computer model that an overlying 2 ft thick layer of material not susceptible to liquefaction would prevent liquefaction of the underlying liquefaction-susceptible ocean floor. Their model does not include an impermeable membrane between the underlying and overlying materials, and did provide for drainage at that boundary. In their model, dissipation of pore pressures by drainage at the sea floor surface over the duration of the storm was very important in preventing dangerously high residual pressures in the underlying sands.

The experimental results of this present study suggest that free drainage of the surface of the core material is not important to the magnitude of the pore pressure rise in the core of a rubble shore protection structure. In fact, lower residual pressures resulted in the undrained surface case than in the drained case.

It is possible that the drainage provided by leakage around the edges of the impermeable membrane and at the toe of the slope were sufficient to prevent development of an "undrained" case. At the same time, the impermeable boundary would be sufficient to prevent the circulating flow necessary to cause flow-associated gradients or "seepage pressures."

The study by Seed and Rahman (1978) suggests that permeability of the material of the core is a critical factor in determining the magnitude of residual pore pressures developed in response to wave loading. In their computer model, a permeability between 2×10^{-3} cm/sec (3.3×10^{-5} ft/sec) and 10^{-3} cm/sec (6.6×10^{-5} ft/sec) was the critical permeability. At higher permeability, the pore pressures do not reach sufficient magnitude to cause liquefaction because of the influence of drainage. This permeability is between that of clean sands and very fine sands on a permeability scale [Terzaghi and Peck (1967)]. If one were building a breakwater with a sand core or backfilling behind a seawall or revetment structure, the permeability of the core or backfill material should be equivalent to that of a clean coarse sand in order to avoid excessive buildup of residual pore pressures. However, the permeability of a fabric used in constructing such a structure does not appear to be crucial to stability of the underlying material.

The danger of liquefaction or severely reduced effective stress, is located near the surface of the core material. Residual pore pressure response is very sensitive to a change in the permeability of the sand when the permeability value is near that criti-

cal value resulting in liquefaction. Only moderate increases in permeability result in drastically reduced maximum residual pore pressures.

5.2 Transient Pore Pressure Amplitudes

5.2a Comparison to Ocean Floor Models

Several models are available for predicting transient pore pressure response in the soils beneath the surface of an ocean floor loaded with wave-induced cyclic pressures. These models are well summarized by McDougal (1981). The most sophisticated of these models treat the bottom as being porous, deformable, and compressible. The Biot equations for flow in a porous medium are typically employed as the basis for derivation of these analytical models. The cyclic pressure loading is usually taken from linear wave theory.

These models all predict a decay of transient pore pressure amplitude with depth. This decay is usually predicted to be exponential with depth and frequency dependent. A typical representation of the decay in a seabed of infinite depth is given by Finn, Siddharthen and Martin (1980), as follows:

$$p = p_o e^{-\lambda z}$$

where: p = pressure amplitude at a point below the ocean floor

z = depth of the point below the floor

λ = the wave number.

The wave number, λ, is inversely proportional to wave length, so less attenuation of the pore pressure response within the soil is experienced under longer waves.

Both of these phenomena, a decay of transient pressure amplitude with depth and an increase in amplitude with increasing wave length, were observed in the pore pressure response within the core of the rubble structure. As shown in Figure 4.16, the decay with depth was less than an exponential decay which would have given a straight line on the semi-logarithmic plot. McDonald (1981) has shown that, on a flat ocean floor, the decay should be hyperbolic for a seabed of finite depth.

The similarity in results in the core of the structure with those predicted by models for soils beneath ocean floors is not surprising. In both situations, a cyclic hydraulic pressure load is transmitted to the soil, although the load cannot be described by a simple mathematical model in the case of the rubble structure. Another similarity results because of the water retained on the slope in the armor and bedding layers. Due to the retained water, the surface of the core is usually continuously submerged in the critical stability area near the still water level.

Of course, there are significant differences between the rubble structure and ocean floor environments. Characteristics of the rubble structure environment which are not common to the ocean floor include: (1) the water surface at the interface between sea and air, (2) rotation of the flow axes relative to gravity, and (3) partial saturation of the rubble structure core. Each of these

differences seriously complicates the flow and pressure phenomena associated with waves. To date, no comprehensive analytic model has been developed to describe the interaction of water and soil in such a complicated environment.

However, the similarity in pore pressure response in the two different situations holds promise for future researchers. The decrease in transient pressure amplitude with increase in height on the structure slope is reasonable considering the corresponding reduction in the amplitude of water surface fluctuation.

The effect of geotextile permeability on the rubble core pore pressures was similar to that observed by McDougal (1981) for the ocean floor situation. McDougal's analytic model predicted progressively decreasing transient pressure response below geotextiles of progressively decreasing permeability; however a geotextile with a permeability of the same order or greater than the soil permeability responded as hydraulically transparent. McDougal's experimental results did not show the expected change in response in the ocean floor situation for an imperable membrane. McDougal offers the following explanation supported by additional laboratory investigation. Dynamic pore pressures are transmitted by small, cyclic deflections of the geotextile which is loose and compliant. The transmission of pressures by fabric deflection result in an "apparent" permeability. Interestingly, the Phase I experimental results show that, for the rubble structure core, especially near the surface of the core, the transient pore pressure amplitude is greater under the more permeable Poly-Filter GB geotextile than under the

Typar or the impermeable membrane. The reason that the geotextile in the rubble structure did not show the same "apparent" permeability as in the ocean floor situation may be that the partial saturation of the upper part of the rubble structure core allows for flows through the geotextile of a larger magnitude than could be represented by a compliant deflection of a geotextile. Also, the heavier armor burden on the geotextile may preload the geotextile, reducing it's flexibility.

5.2b Implications for Structure Stability

The transient pore pressures are a response to the wave pressure loading. The pressure gradient is always decreasing away from the slope so these pressures are not transmitted to the armor units. The concern for structure stability is, once again, one of possible reduced effective stress or liquefaction of the core material. The effect of the transient pore pressure is very dependent on the phase relationship with the wave-induced pressure load at the surface of the core. If the pore pressure response is in phase with the surface loading, it is no more than an expected expression of the increase in total stress with no reduction in effective stress. This phase relationship was not measured during the experiment. No transducers were placed at the core surface. However, only very minor phase lag was observed with the 2 ft (0.6 m) increase in depth from pressure Station 7 to Station 5. Intuitively, one would expect the pressure response near the surface to be instantaneous, that is, in phase with the loading pressure. In the case of in-phase response, transient pore pressures do not

reduce effective stress in the soil,and will not contribute to liquefaction.

Although the transient pore pressures probably do not reduce the effective stress between soil grains, the shear stresses induced in the soil by the wave loading could affect the structural stability. Without an analytic model, the nature of those shear stresses remain unknown. Experimental investigation of shear stresses would require determination of effective stress within the soil by measurement of total stress from which pore presure could be subtracted. Total stress measurements in a dynamic situation have historically proved unreliable, and no attempt was made to measure total stress during either phase of the experiment. A model with uncoupled pore stress and effective stress similar to the ocean floor analysis in Finn, Siddharthan and Martin (1980) may prove to be a suitable subject of investigation for future researchers.

5.3 Armor Stability

The results of the Phase II investigation of armor stability were different than expected. It was anticipated that the lower the permeability of a geotextile was, the greater would be the reduction in the armor stability. The reduction of armor stability could be attributed to two factors. First, high normal forces result from the fluid acceleration associated with the stagnation pressure of a wave plunging onto the slope. This stagnation pressure was expected to be more severe for lower fabric perme-

abilities. Second, previous investigations have reported higher runup for lower permeability cores, and higher runup has correlated with reduced armor stability.

During Phase II, no reduction in armor stability was noted with a reduction in geotextile permeability. During Phase I and Phase II, runup was did not vary with geotextile permeability in any consistent way. A plausible explanation for the observed results is that, since the permeability of the core material was several orders of magnitude less than the permeability of the armor, the core was, in comparison, virtually impermeable regardless of the geotextile used. Even with no geotextile on the slope, any flow in the core is insignificant in comparison to the considerable flow within the armor and bedding layers and the very large flow above the armor layer. This high contrast in permeabilities is to be expected for any rubble structure in which a geotextile is used to separate materials, since the reason for using the geotextile is the excessive contrast in particle sizes between the separated layers.

Another surprising result was that the stability of the armor did not appear to be sensitive to wave period or Iribarren's number. The failure height of 42 in (107 cm) under the 5.59 sec wave was at an Iribarren's number of 2.2 which is within the range of 2 to 3 considered by Günbak (1979) to be critical to stability. The failure heights for wave periods of 2.8 and 3.95 sec occurred at Iribarren's numbers of 1.6 and 1.2, respectively, which are outside the critical range. In contrast to expected results,

the wave heights for failure in these cases were 41 and 40 in (104 and 102 cm), respectively; heights lower than that in the longer period wave. However, if shoaling is taken into account and deep-water wave heights calculated, the expected results are obtained. The deep-water height of the longest failure wave is 41 in (104 cm) and that of the two shorter failure waves was 44 in (112 cm).

5.4 Runup and Rundown

The runup and rundown results were well behaved, and similar to the results observed by other investigators. The observations lend credence to the typical nature of the experimental structure. The higher runup in the case of the prismatic armor relative to the graded random armor was expected. The hand-placed prismatic armor layer was thinner and presented a smoother surface than a typical rubble armor layer.

The apparent absence of a consistent trend to increasing runup with decreasing geotextile permeability supports the proposed descriptive model. Evidently the contrast in permeability between the core material and the armor and bedding materials is so great that any flows within the core are small and insignificant in comparison to the flow in the overlying layers. A further decrease in core permeability resulting from an impermeable geotextile on the face of the core would thus eliminate only an insignificant flow, and would not noticeably affect the runup.

5.5 Credibility of Results

The results obtained from the experiment are applicable to full scale protection structures. Errors due to scale effects were avoided by conducting the experiment on a structure of nearly prototype size.

The credibility of the pore pressure response results is supported by the constancy of the basic pattern of residual pressures and of the basic pattern of transient pressure amplitudes observed in the core. These basic patterns remained very much the same for all waves and for all geotextiles tested. Furthermore, the changes to the basic residual pressure pattern in response to changes in geotextile permeability were very consistent over the entire range of waves considered.

The uniformity of the pore pressure response was verified during a four-hour continuous attack of the Phase I structure by a Case 6-C wave. After stabilizing during the first few waves, the residual pore pressures and transient pressure amplitudes remained essentially constant during the entire test period.

The patterns of residual pore pressures as measured by the pressure transducer array were validated by the simultaneous pore pressure measurements made with the piezometer array. The piezometer array produced residual pressure patterns of the same shape and magnitude as the coincidental transducer array.

Identification of the failure condition for riprap stability was subjective rather than quantitative. However, there was an easily observed contrast between the failure and the non-failure

conditions. Only minor adjustments of armor stones occurred during attack by waves smaller than the failure wave in substantial contrast to the continuing major movements of the nominal size armor during attack by the failure wave.

The wave sequence used for testing was such that shorter period non-failure waves were applied to the slope following application of the longest period failure wave. Although the slope had been disturbed by the long period wave, that disturbance did not result in a failure of the armor when under attack by the subsequent shorter period waves which were smaller than failure size. This result demonstrated that the initial failure did not fatally injure the armor layer and did not invalidate subsequent armor stability results.

The runup measurements correlated well with those given in the Shore Protection Manual (1977) and with those by Sollitt and DeBok (1976). The favorable correlation of runup data with previous data developed by others demonstrates the conventional, non-radical nature of the flow conditions on the test structure.

As transient components of head became moderately large, measurement of head in the piezometers became difficult and very time consuming. However, sufficiently accurate measurements could be made with the piezometers to validate and extend the pattern of residual pore pressures observed in the transducer array. Fortunately, those piezometer measurements needed for extension of the transducer data were, for the most part, at locations deeper in the core of the structure where the transient components of pore pres-

sure response were not as great and the water level in the piezometers was more stable and, thus, more easily and accurately measured. Although piezometers proved to be a poor choice of instrumentation for quantitatively precise measurements, they did enable a simple, direct measurement of head within the core which was used to validate the electronic output of the more sophisticated transducers.

The boundary conditions at the bottom and sides of the test structure may have had some effect on the experimental results. However, several noteworthy observations made during the course of the experiment suggest that these effects were minimal.

A comparison of Phase I and Phase II pore pressure response reveals no change in the nature of the response. During Phase II, the pressure transducer was located on the centerline of the structure in contrast to the Phase I location at a point one quarter of the tank width from one side. If flow around the edges of the geotextile significantly affected the pore pressure response, one could expect a difference in the nature of response at one location as compared to the other. The similarity in results between Phase I and Phase II also suggests that the boundary condition at the toe of the slope was not important to the results. The core material at the toe of the slope below the false bottom was sealed off by an impermeable membrane in Phase II, but was not sealed in Phase I.

The armor stability did not appear to be affected by the edge boundary condition. Armor stones next to the wave tank walls were observed to become unstable at the same wave height as those

located near the centerline of the revetment structure.

5.6 Implications for Design

Adequate permeability is recommended by authorities as a primary criterion to be applied in selection of a geotextile for use in rubble shore protection structures. Designers have been concerned that clogging of a fabric incorporated in a structure will result in severely reduced permeability which will, in turn, result in reduced structural stability.

Results of this experiment have shown that, for the test structure, reduction in geotextile permeability had no adverse effects on the stability of the structure. Residual pore pressure within the core did not rise as geotextile permeability was decreased, implying that effective stress was not reduced. Therefore, stability of the core was in no way reduced. No reduction in armor stability was observed as a result of decreasing geotextile permeability. These results show that incorporation of a geotextile as a separator between core and overlying material in no way reduces stability of a rubble shore protection structure similar to the test structure. Therefore, this type of structure may be designed by the same procedures as though the geotextile were not included. However, the weight of the overlying material must remain sufficient to prevent liquefaction or dangerously reduced effective stress. As long as the weight of material overlying the core is the same, a design with a geotextile may be the same in all respects as a design with a graded aggregate filter. Of course,

the designer is freed from the constraints of gradation of the material overlying the core when a geotextile separator is employed.

5.7 Applications Beyond the Scope of the Experiment

A consideration of the qualitative model presented in Section 5.1 enables a application of the experimental results to some situations outside the scope of the experiment. In other cases, further research is necessary to extend the experimental results and identify the effects of geotextile permeability on structural stability.

5.7a Changes in Armor Material

A variety of materials are commonly used as armor for revetments. These materials include large, gravel-filled geotextile bags, concrete units with unique geometries, interlocking concrete blocks, and concrete blocks linked together by cables. The results of this experiment are directly applicable to all armor layers constructed of individual units that act independently except for friction between the units and also have a layer permeability considerably greater than that of the core material.

Gravel-filled bags can conform to neighboring bags and may result in a layer with a relatively small percent of open area and a permeability of the same order as the core material. It is possible that low geotextile permeability, less than that of the core material, might affect structural stability in such a case with low contrasts between the core and armor permeabilities. Further

experiments are necessary in order to determine geotextile permeability effects for this case.

Interlocking concrete or cable-connected concrete blocks derive stability from their connection to adjacent blocks, and the layer of blocks acts more or less as a continuous blanket. Localized lift and drag forces are spread out over an area of the blanket rather than concentrated on individual units. These types of armor systems typically present a smooth, relatively impervious surface to the attacking waves with the relatively small percentage of open area limited to the joints between blocks. Flow within the block armor layer is much less volumous and different in nature than flow within a random armor layer. Because of these considerable differences, further experimental research is necessary to define the effect of geotextile permeability on the stability of interlocking concrete block systems. Future research should investigate the effect on these structures both with and without bedding layers.

5.7b Bedding Layer Changes

The bedding layer used in this investigation was not changed throughout the entire experiment. However, eliminating beding from the structure or changing the relative permeability of the bedding layer should not cause a drastic change in geotextile permeability effects.

The most serious changes associated with elimination of a bedding layer are those resulting in mechanical stress being

applied to the geotextile. Since rubble armor tends to move slightly under even relatively mild wave conditions, the geotextile can be subjected to abrasion. Also, large armor units have correspondingly large gaps between points of contact with the fabric. The geotextile bridging across the gap may "stretch" and "balloon" into the void. However, provided the geotextile survives these mechanical stresses, there should be no significant change in the circulating flow or the cyclic shear stresses within the core. In a structure with no bedding layer, the geotextile separates two layers of highly contrasting permeability just as it did in the experimental structure. The pore pressure response to changes in geotextile permeability should be very similar to that with the bedding layer in place. Consequently the experimental results should be directly applicable to the no-bedding case.

A bedding layer of very low permeability would restrict the flow of water into the core from above and reduce the tendency for circulating flow. Since the difference in pore pressure response beneath geotextiles of different permeabilities is due to corresponding differences in circulating flow, those differences would be reduced in the case of a low permeability bedding layer. Cyclic shear stresses in the core should not be affected by bedding permeability. Also, since the high permeability contrast between layers would be moved to a position above the geotextile layer, there is no reason to suspect that geotextile permeability would assume a significance to armor stability that was not observed when the high contrast was located at the geotextile layer.

5.7c Changes in Core Material

The experiment was conducted using an uncompacted granular core material with a permeability several orders of magnitude less than that of the armor and bedding layers. Core materials with less contrast in permeability or a very loose or very dense packing might differently react to changes in geotextile permeability.

A decrease in the permeability of the core material would exaggerate the difference between core and armor permeabilities. The small effects of geotextile permeability on pore pressures within the core and on armor stability would become even less apparent since the hydraulic visibility of the geotextile would be reduced by the presence of a lower permeability core. On the other hand, as the core permeability approaches the permeability of the armor layer, the significance of geotextile permeability to circulating flow within the core is greater. Further research is required to define the effects of geotextile permeability in the case of highly permeable cores. However, layers of similar permeabilities would also have similar particle sizes, and it is unlikely that a geotextile separator between such layers would serve useful function.

Relative density of the core material is an important parameter in the Seed-Rahman model of cyclic shear induced pore pressures. A core material of low relative density would have a greater tendency to densify under cyclic loading and would therefore have higher residual pore pressures and a greater tendency to drain at the surface. In the case of a low density core, the

effects of geotextile permeability might be different than those observed during the experiment described herein. Consequently the experimental results should not be extended to the case of a low density core. However, the experimental results are directly applicable to the case of a high density, compacted core. The cyclic shear-induced pore pressures would continue to be virtually unaffected by geotextile permeability, and effects of geotextile permeability on circulating flow in the core do not in any way depend on the relative density of the core.

5.7d Landside Source of Water or Overtopping

The permeability of the geotextile will affect the drainage of the face of the revetment structure relative to a landside source of water. Water on the land side of the structure could be from ground water or from the surface infiltration of overtopping waves. In either case, the affect of geotextile permeability on pore pressures within the core could be evaluated using conventional flow net techniques. In the case of wave overtopping, assumptions would have to be made regarding the rate of infiltration resulting from the overtopping waves.

5.7e Shallow Toe of Structure

Rubble revetment structures have been constructed at locations where the toe of the structure is near or above the still-water level during portions of the tidal cycle. The wave loading on the structure in these cases is considerably different than in the

experiment. The most important difference is that the toe of the slope, which is an important boundary, with discontinuities in slope and in material cross-section, is now placed in the location at which rubble structure failure is most commonly initiated. In this situation, varying the permeability of a geotextile used in the cross-section of the structure might result in significant changes in stability of the structure. The experimental results do not necessarily apply to the case of a shallow toe. Further research would be required to evaluate geotextile permeability effects for this condition

5.7f Variation in Slope Angle

The 3 to 1 slope of the experimental revetment is near the shallow end of the range of slopes commonly used in rubble shore protection structures. However, a steepening of structure slope would produce no basic qualitative change in the cyclic shear loading and circulating flow pattern within the core. One might expect that a change in geotextile permeability will have the same effects for a steeper sloping revetment as for the experimental revetment.

5.7g Variation in Wave Environment

Considerable controversy exists as to whether or not an attack on a rubble structure by a random spectrum of waves can be effectively modeled by a uniform series of waves. It is of interest to note that whether waves are regular or random, they still generate

cyclic shear stresses within the soil and create the "wave setup" condition which would provide the source for the theorized circulating flow within the core. Therefore, it appears reasonable to extend the experimental results presented herein to random wave loading conditions.

Long period waves were not directly investigated in the experiment. However, variations in water level at a rate similar to tidal fluctuations were applied to the experimental revetment during filling and draining of the wave tank. The wave tank filled and drained at about one ft/hr and under those conditions, the water level in the core kept pace with the exterior water level regardless of geotextile permeability. Destabilizing forces on the structure were not generated by these slow water level fluctuations.

The effect of geotextile permeability on structural stability of a revetment subject to wave periods on the order of several minutes to an hour could be analyzed using flow net techniques. In the case of these intermediate period waves, cyclic shear stresses can be assumed to occur at a rate too slow to result in generation of residual pore pressures. Circulating flow need only be considered in these cases.

6.0 CONCLUSIONS

To determine the effect of geotextile permeability on rubble structure stability, wave tank tests were conducted on a large-scale rubble revetment with a sandy gravel core and a geotextile on the surface of the core material. The structure was reconstructed and retested several times, each time with a geotextile layer of a different permeability. Pore pressure patterns within the core and stability of armor stone on the face were monitored.

A descriptive model combining circulating flow and cyclic-shear-induced pore pressures is proposed as a means of explaining the pore pressure response. A qualitative analysis of the experimental results leads to the following conclusions.

1) For the conditions investigated in this study, low permeability or impermeability of a geotextile separator between rubble structure armor units and an underlying soil does not cause a significant increase in the magnitude of "residual" (mean accumulated) wave-induced pore pressure within the core. This conclusion applies to the specific structure tested and is theorized to apply to structures in which the core material has a permeability several orders of magnitude less than the permeability of the armor and bedding layers. Such a contrast in permeabilities is expected in most situations for which a geotextile separator would be appropriate. Since residual pore pressures are not increased by decreasing geotextile permeability, stability of the core material is not reduced.

2) A decrease in permeability of a geotextile separator between armor and core materials of high contrasting permeabilities does not result in an observable decrease in stability of rubble armor units. This is true for the case of an impermeable membrane as well as one of low permeability. Evidently, destabilizing forces on the armor units associated with flows within the slope are not significant in comparison with the forces from the flows within the armor layer itself. Similarly, destabilizing forces associated with stagnation of plunging waves apparently do not increase significantly as the permeability of a core, already of a low permeability relative to the armor and bedding layers, is further reduced or eliminated by inclusion of a geotextile.

3) For many rubble structures similar to the experimental structure, permeability is not a suitable criterion for selection of a geotextile separator between the core and the armor. For these structures, geotextile clogging is also not of concern.

4) Because an impermeable geotextile in a rubble structure similar to the test revetment does not reduce the armor stability and does not cause a reduction of effective stress in the core, the design of such structures may be the same as though an aggregate filter were employed. That is, as long as the weight of material overlying the core is the same, the incorporation of a geotextile separator will not reduce the stability of the structure, regardless of the geotextile permeability.

BIBLIOGRAPHY

1. Barrett, R.J., (1966), "Use of Plastic Filters in Coastal Structures," Proceedings the 10th International Conference on Coastal Engineering, ASCE, Vol. 2, Chapter 63.

2. Bell, J.R. and R.G. Hicks, et al., (1980), Evaluation of Test Methods and Use Criteria for Geotechnical Fabrics in Highway Applications, Interim Report, Federal Highway Administration Report No. FHWA/RD/021.

3. Bruun, P., (1970), discussion of "Damage Functions of Rubble Mound Breakwater," Journal of the Waterways and Harbors Division, Vol. 96, No. WW2, ASCE.

4. Bruun, P. Günbak, (1976), "New Design Principles for Rubble Mound Breakwaters," Proceedings the 15th Conference on Coastal Engineering, Vol. 3, Chapter 142, ASCE.

5. Bruun, P. and P. Johannesson, (1976), "Parameters Affecting Stability of Rubble Wounds," Journal of the Waterways, Harbors, and Coastal Engineering Division, Vol. 102, No. WW2, ASCE.

6. Carver, R.D., (1980), Effects of First Underlayer Weight on the Stability of Stone-armored, Rubble-mound Breakwater Trunks Subjected to Nonbreaking Waves with No Overtopping; Hydraulic Model Investigation, Technical Report HL-80-1, U.S. Army, Corps of Engineers.

7. Cedergren, H.R., (1974), Drainage of Highway and Airfield Pavements, John Wiley and Sons, Inc., New York, N.Y.

8. Dean, R.G., (1974), Evaluation and Development of Water Wave Theories for Engineering Applications, Vol. 1 and Vol. 2, Special Report No. 1, U.S. Army Corps of Engineers, Coastal Engineering Research Center, Fort Belvoir, VA.

9. Dunham, J.W. and R.J. Barrett, (1974), "Woven Plastic Cloth Filters for Stone Seawalls," Journal, Waterways, Harbors, and Coastal Engineering Division, Vol. 100, ASCE.

10. Finn, W.D. Liam and K.W. Lee, (1979), "Seafloor Stability Under Seismic and Wave Loading," Proceedings, Soil Dynamics in the Marine Environment, ASCE, National Convention and Exposition, Boston, MA, Preprint 3604.

11. Finn, W.D., Liam, R. Siddharthan, and G.R. Martin, (1980), "Wave Induced Instability in Ocean Floor Sands," Preprint, Annual Convention and Exposition, ASCE, Hollywood, Florida.

12. Font, J.B., (1968), "The Effect of Storm Duration on Rubble Mount Breakwater Stability," Proceedings, the 11th Conference on Coastal Engineering, London, England, Vol. II, Chapter 50, ASCE.

13. Günak, A.R., (1979), Rubble Mound Breakwaters, Repott 1-1979, Division of Port and Ocean Engineering, The Norwegian Institute of Technology, The University of Trondheim, Trondheim, Norway.

14. Haliburton, T.A., J.D. Lawnmaster, and B.C. McGuffey, (1981), Use of Engineering Fabrics in Transportation-Related Applications, draft of a handbook prepared for the Office of Development, Federal Highway Administration, Contract No. DTFH61-80-C-00094.

15. Heerten, G., (1980), "Long Term Experience with the Use of Synthetic Filter Fabrics in Coastal Engineering," Proceedings, the 17th Conference on Coastal Engineering, Sydney, Australia, Vol. 3, Chapter 131, ASCE.

16. Losada, M.A. and L.A. Gimenez-Curto, (1980), Mound Breakwaters Under Wave Attack, Report No. SR-1-80, Department of Oceanographical and Ports Engineering, University of Santander, Santander, Spain.

17. McDougal, W.G., (1981), Ocean Wave-Soil-Geotextile Interaction, thesis presented to Oregon State University in partial fulfillment of the requirements for the degree of Doctor of Philosophy.

18. Rankilor, P.R., (1981), Membranes in Ground Engineering, John Wiley and Sons Ltd., New York, N.Y.

19. Saville, T., (1966), "Rock Movement in Large-Scale Tests of Riprap Stability Under Wave Action," Proceedings, the 10th Conference of Coastal Engineering, Tokyo, Japan, Vol. 2, Chapter 56, ASCE.

20. Seed, H.B. and M.S. Rahman, (1978), "Wave-Induced Pore Pressure in Relation to Ocean Floor Stability of Cohesionless Soils," Marine Geotechnology, Vol. 3, No. 2.

21. Sigurdsson, G., (1962), "Wave Forces on Breakwater Capstones," Journal of the Waterways and Harbors Division, Vol. 88, No. WW3, ASCE.

22. Sollitt, C.K. and D.H. DeBok, (1976), "Large Scale Model Tests of Placed Stone Breakwaters," Proceedings, 15th International Conference on Coastal Engineering, Vol. 3., ASCE.

23. Sowers, G.D., (1979), Introductory Soil Mechanics and Foundations: Geotechnical Engineering, Fourth Edition, MacMillan Publishing Co., Inc., New York, N.Y.

24. Terzaghi, K. and Peck, R.B., (1967), Soil Mechanics in Engineering Practice, Second Edition, John Wiley and Sons, Inc., New York, N.Y.

25. Thomsen, A.L., P.E. Wholt, and A.S. Harrison, (1972), "Riprap Stability on Earth Embankments Tested in Large-and Small-Scale Wave Tanks: Technical Memorandum 27, U.S. Army Corps of Engineers.

26. U.S. Army Corps of Engineers, (1977), "Plastic Filer Fabric," CW 2215.

27. U.S. Army Corps of Engineers, (1977), Shore Protection Manual.

Appendix

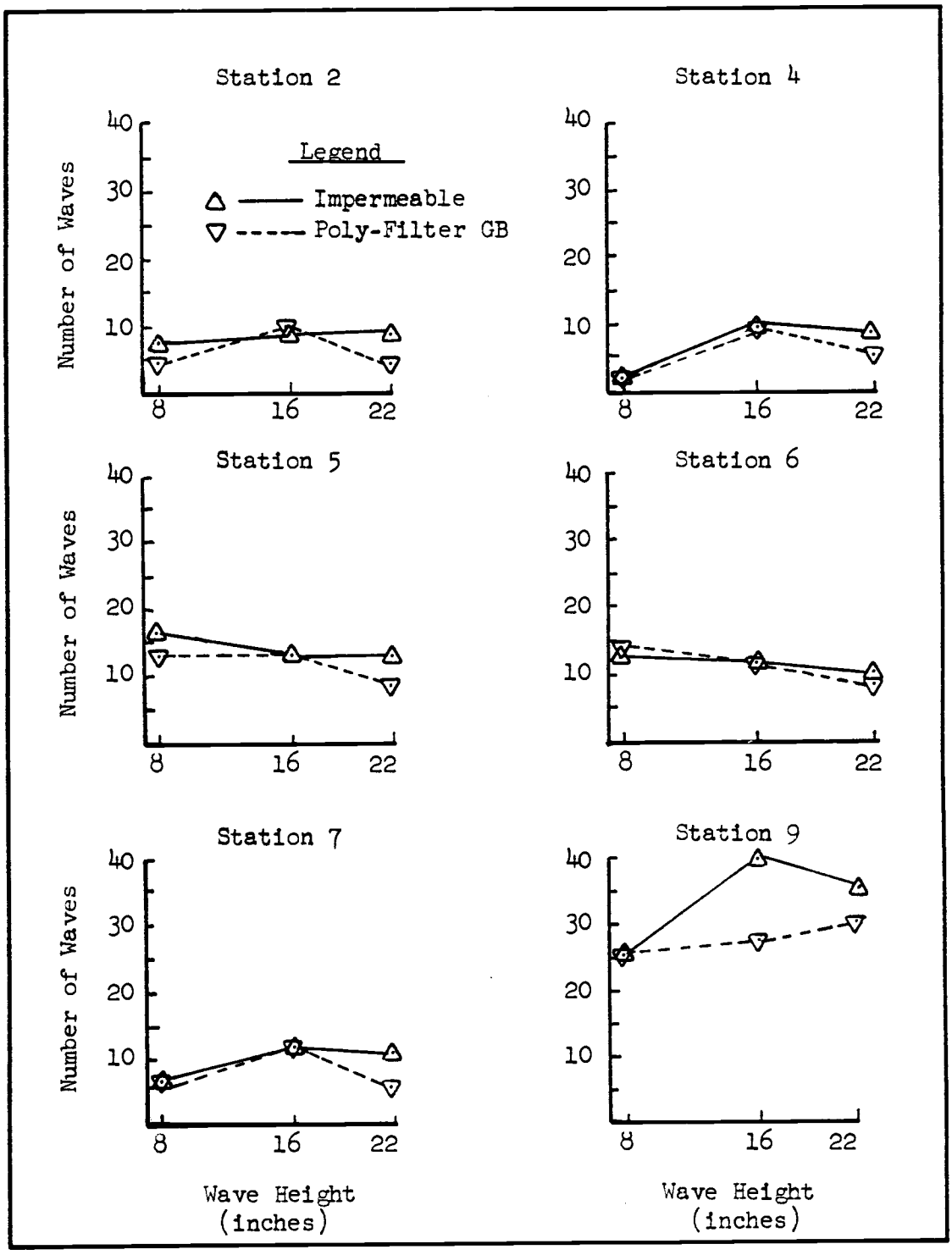

Figure A.1. Number of waves required to build residual pressure at wave period of 1.77 seconds

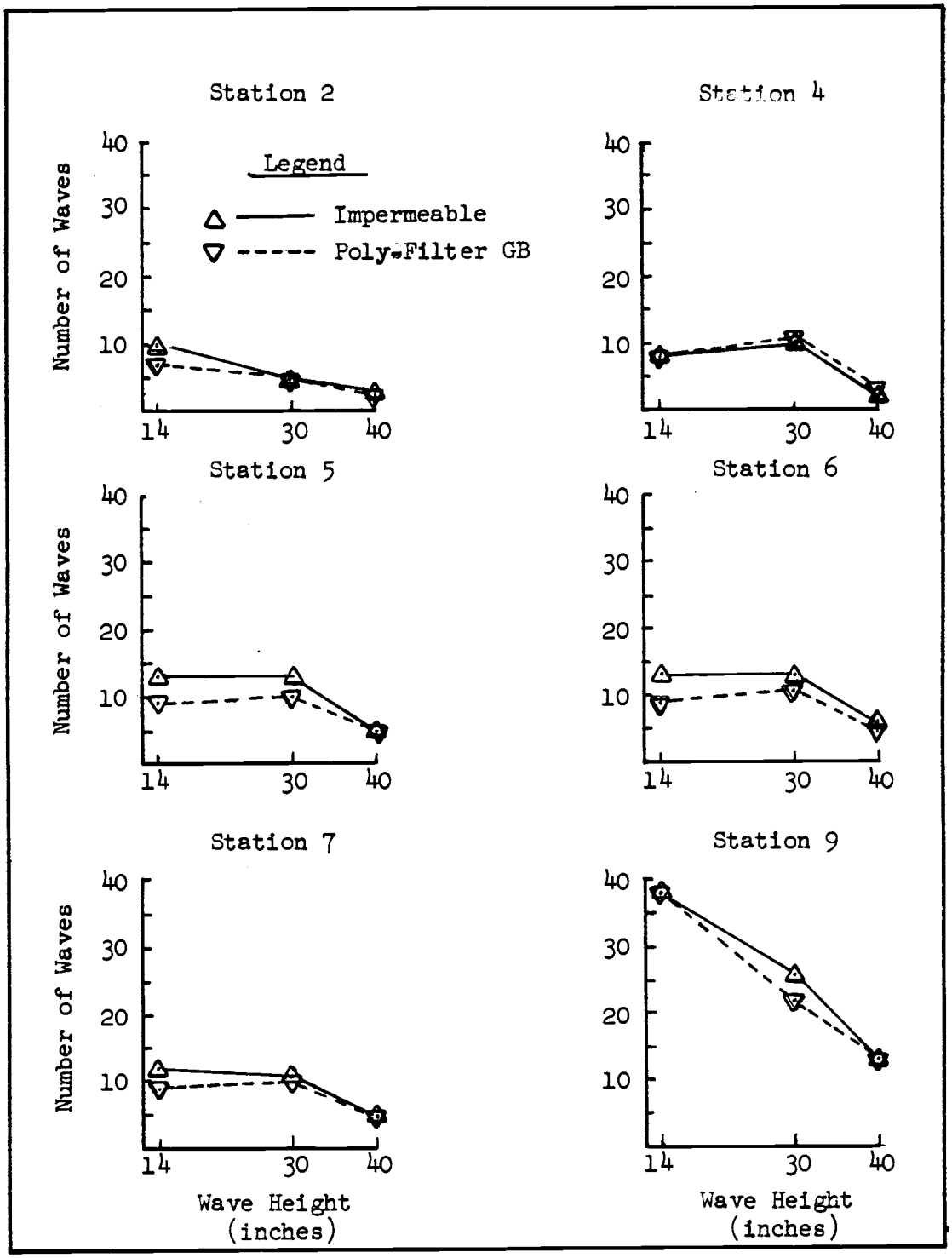

Figure A.2. Number of waves required to build residual pressure at wave period of 2.80 seconds.

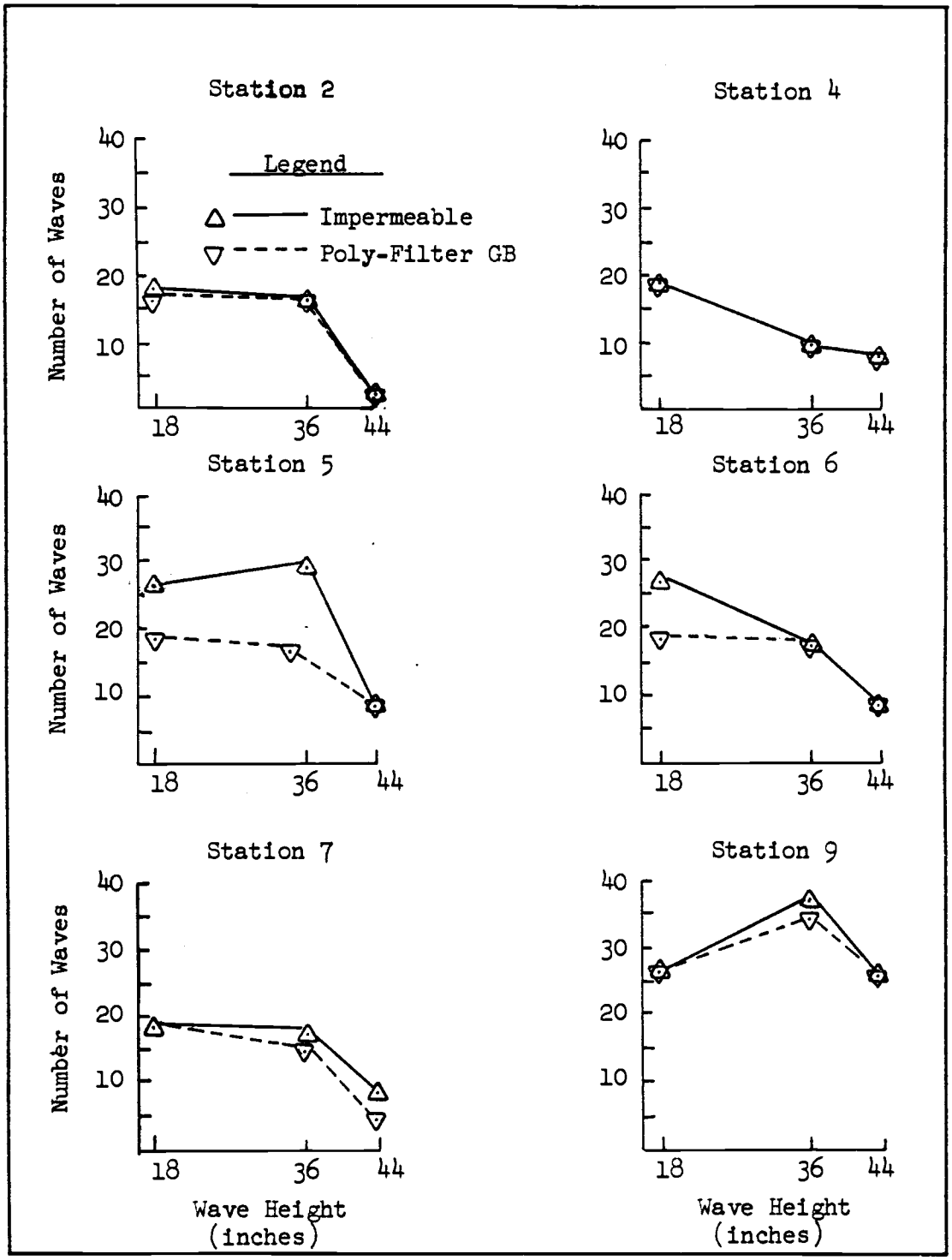

Figure A.3. Number of waves required to build residual pressure at wave period of 3.95 seconds

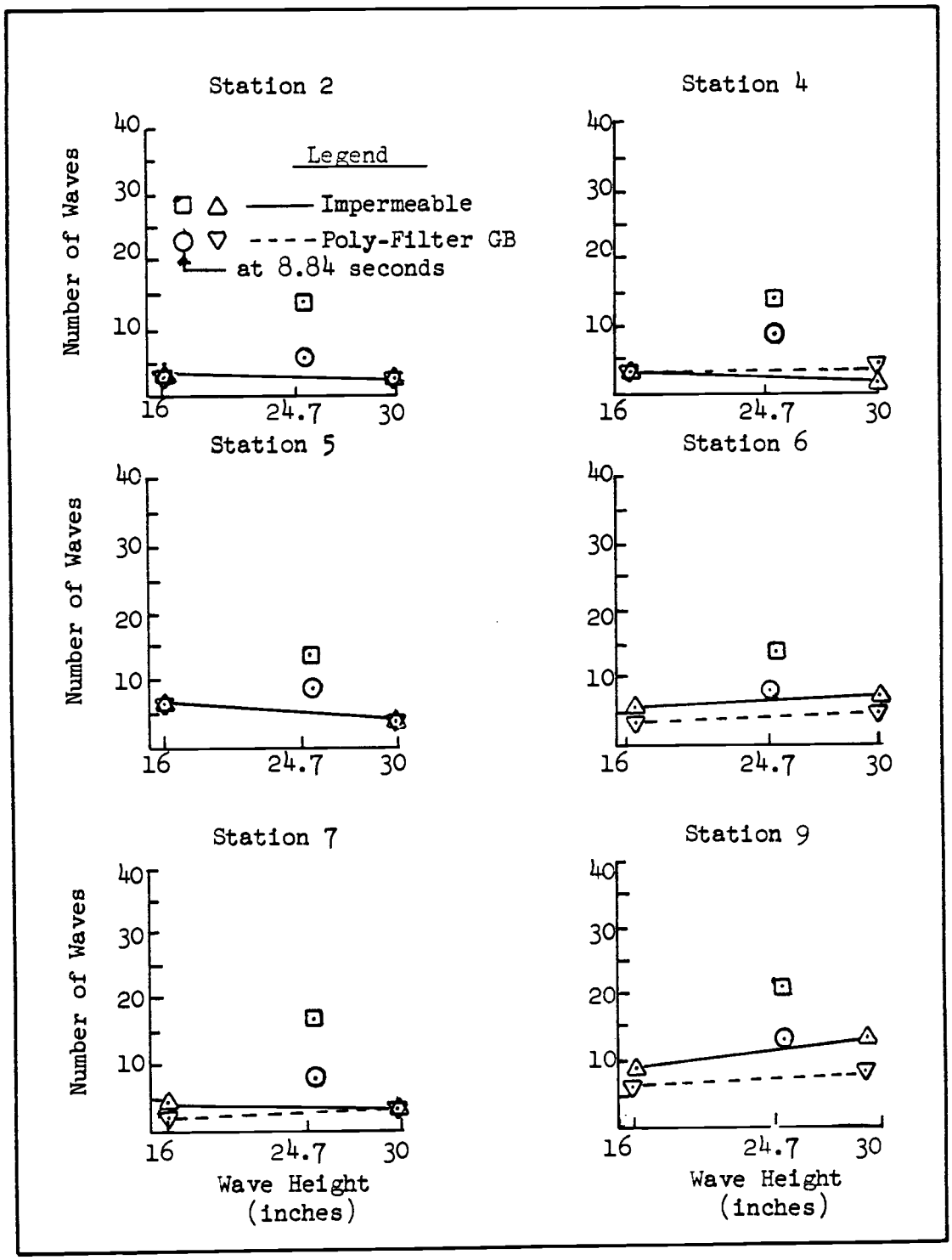

Figure A.4. Number of waves required to build residual pressure at wave periods of 5.59 and 8.84 seconds

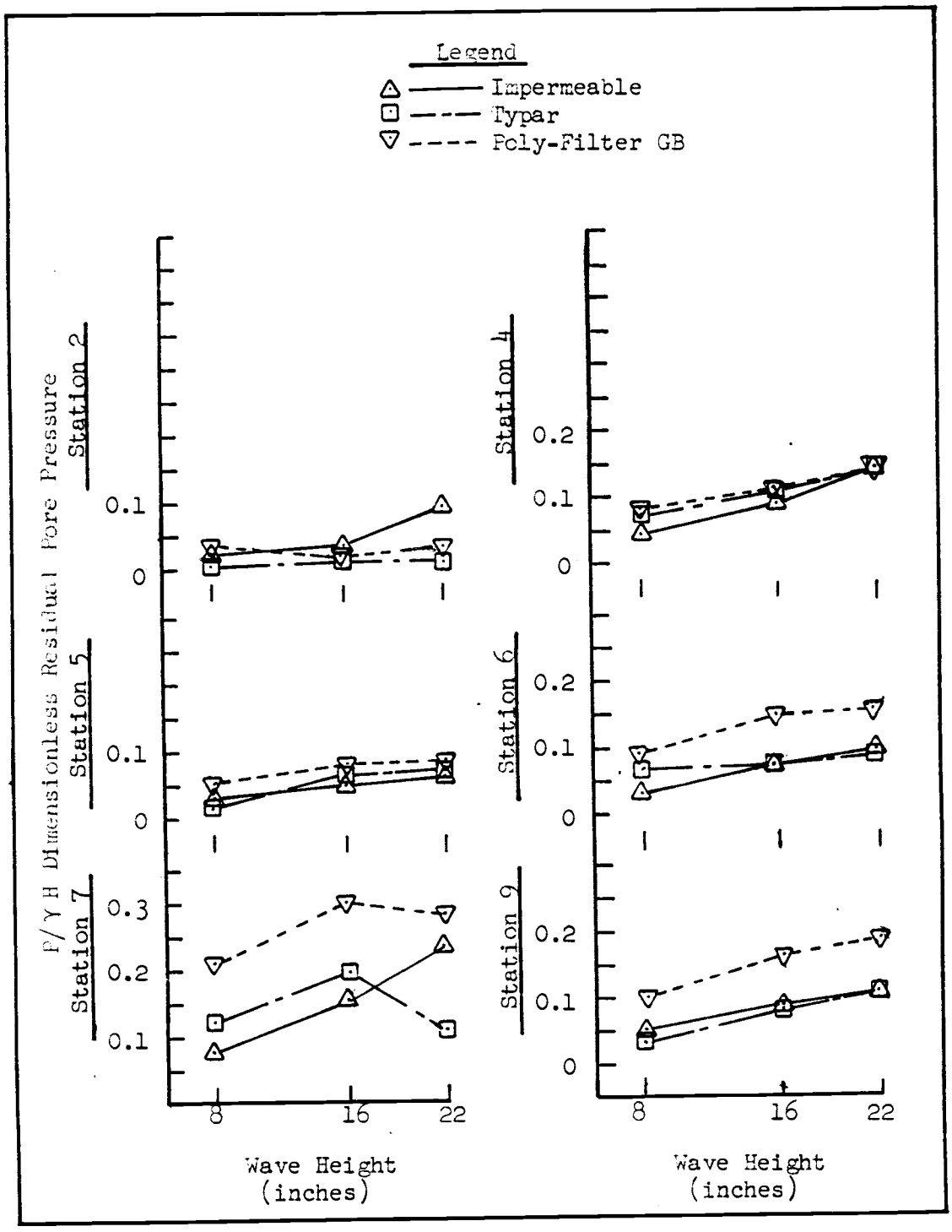

Figure A.5. Dimensionless residual pore pressure as a function of wave height, at wave period of 1.77 seconds

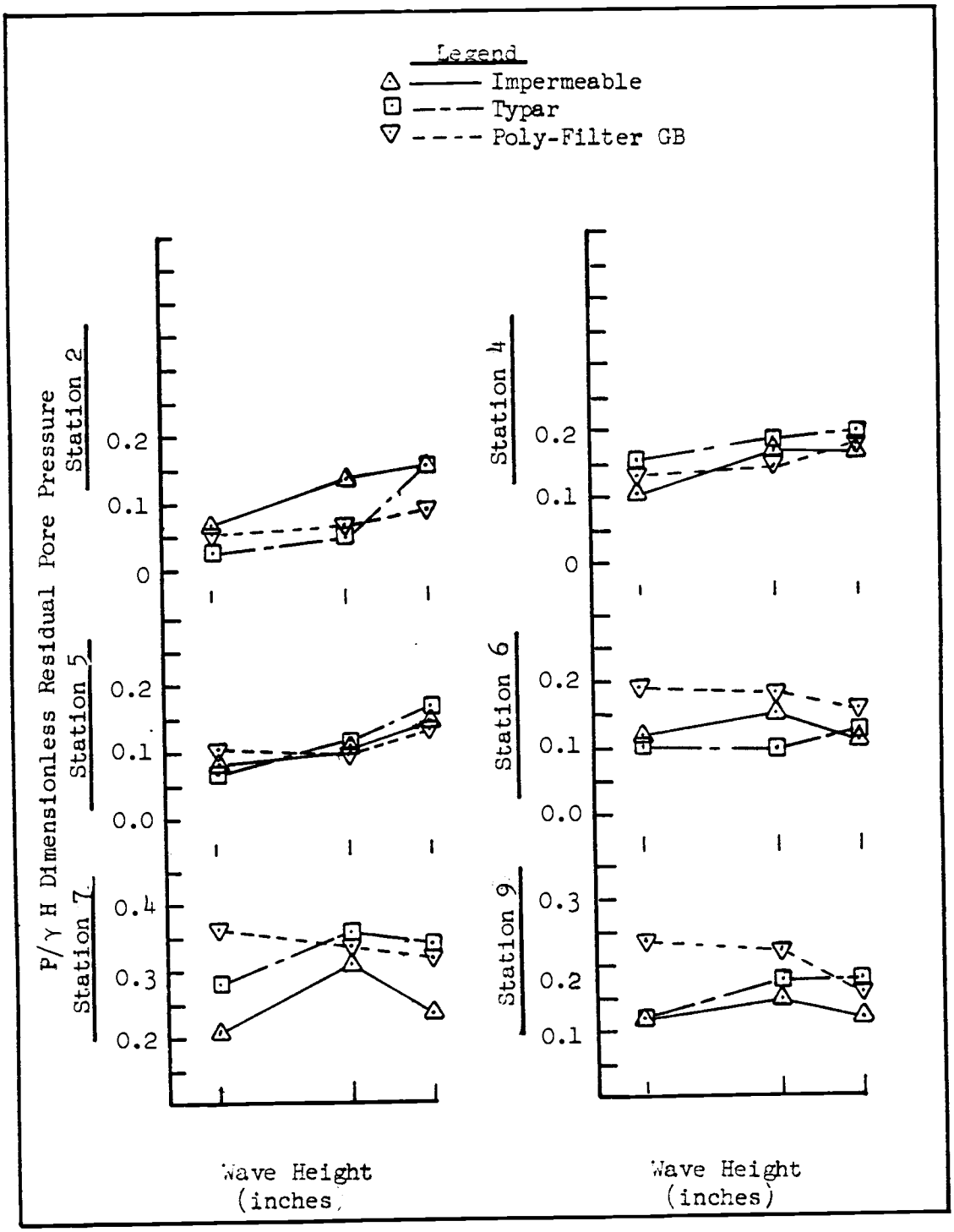

Figure A.6. Dimensionless residual pore pressure as a function of wave height, at wave period of 2.80 seconds

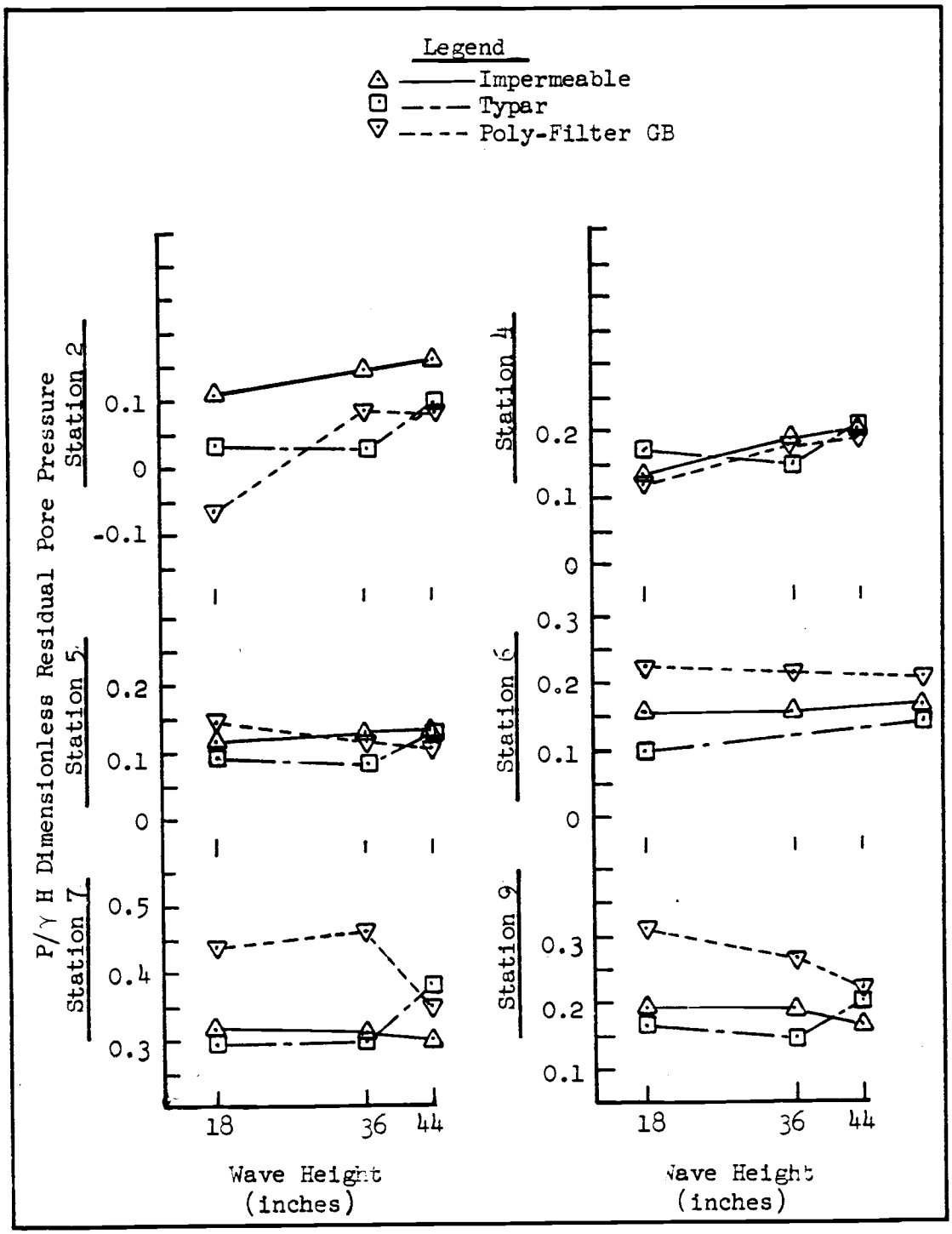

Figure A.7. Dimensionless residual pore pressure as a function of wave height, at wave period of 3.95 seconds

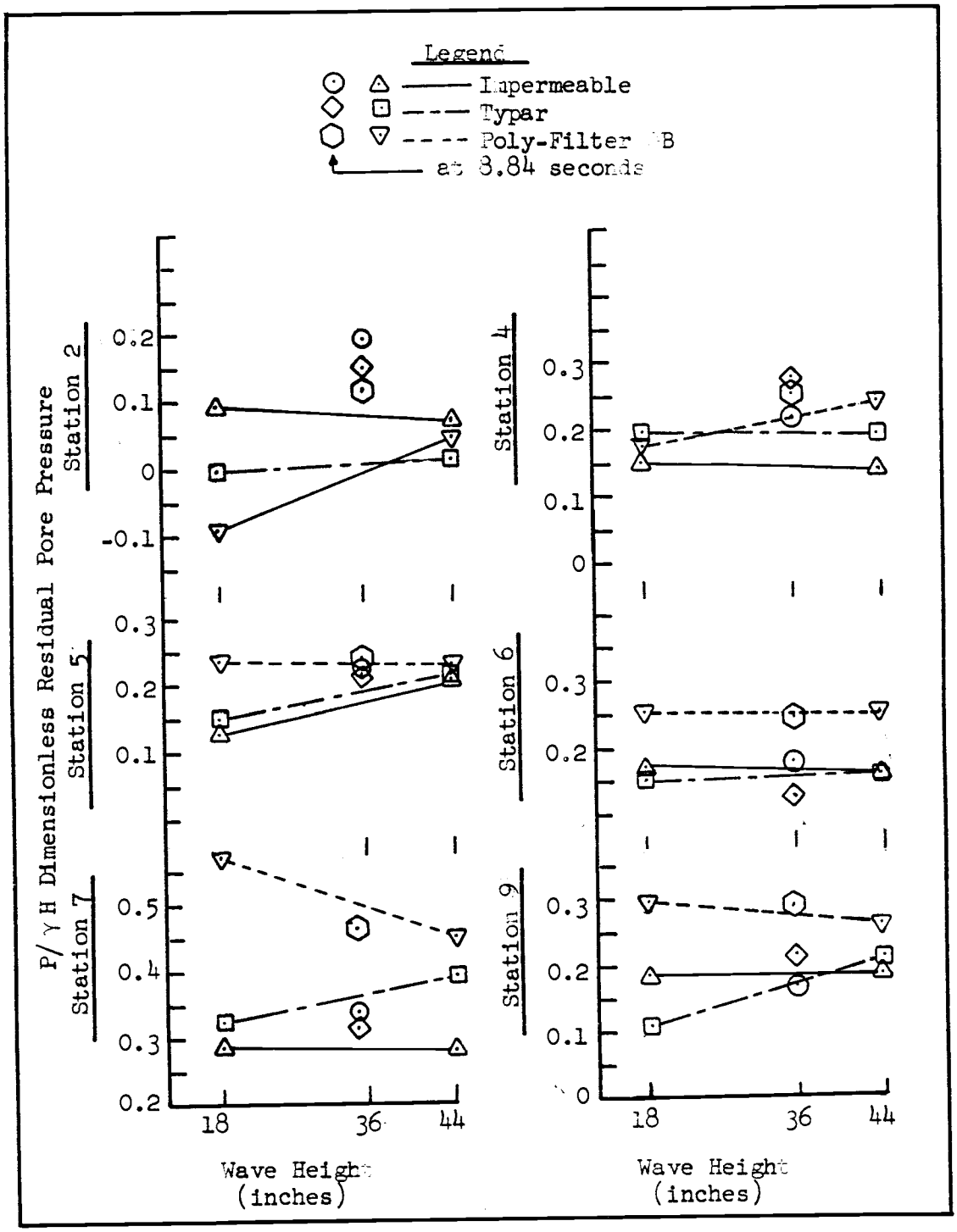

Figure A.8. Dimensionless residual pore pressure as a function of wave height, at wave periods of 5.59 and 8.84 seconds

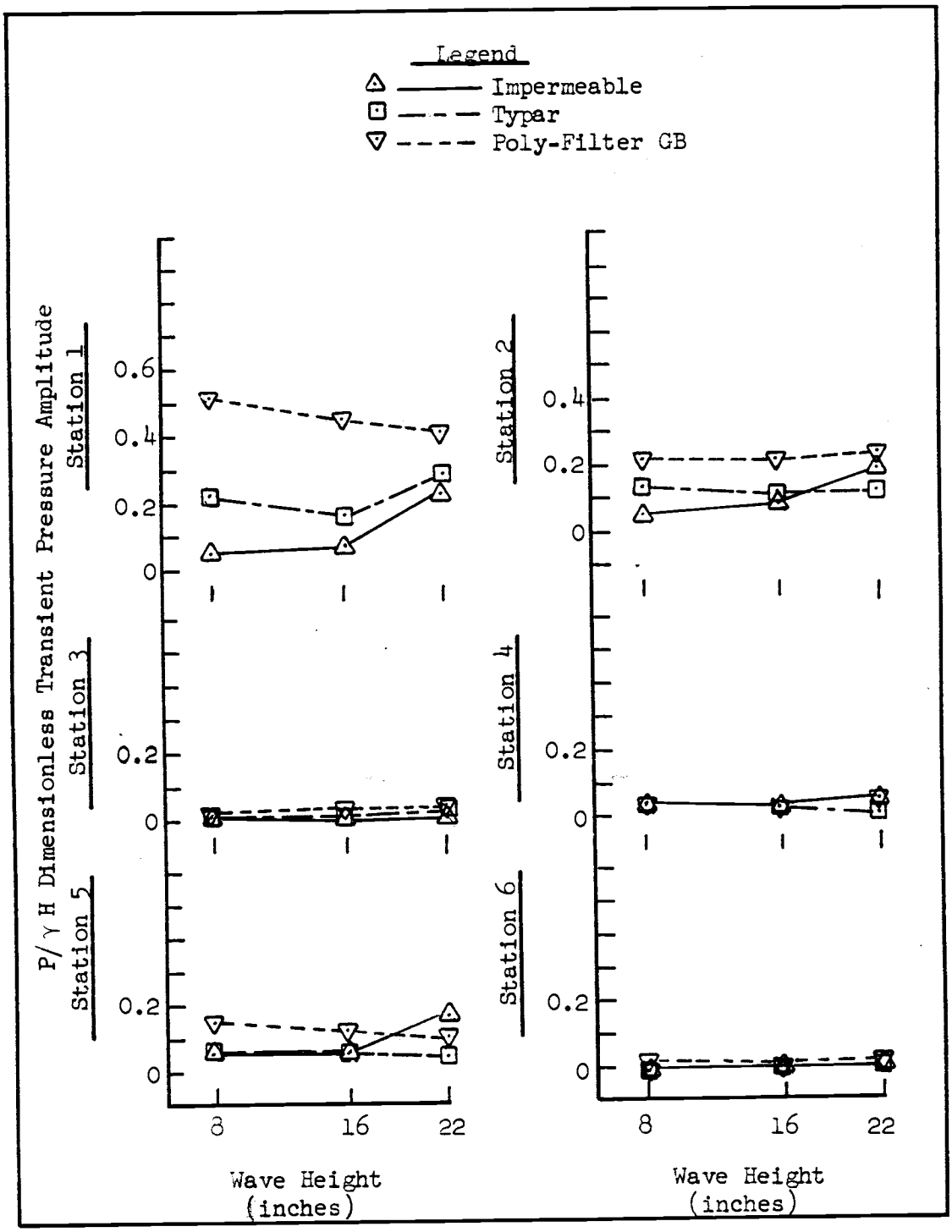

Figure A.9. Dimensionless transient pressure amplitude as a function of wave height, at wave period of 1.77 seconds

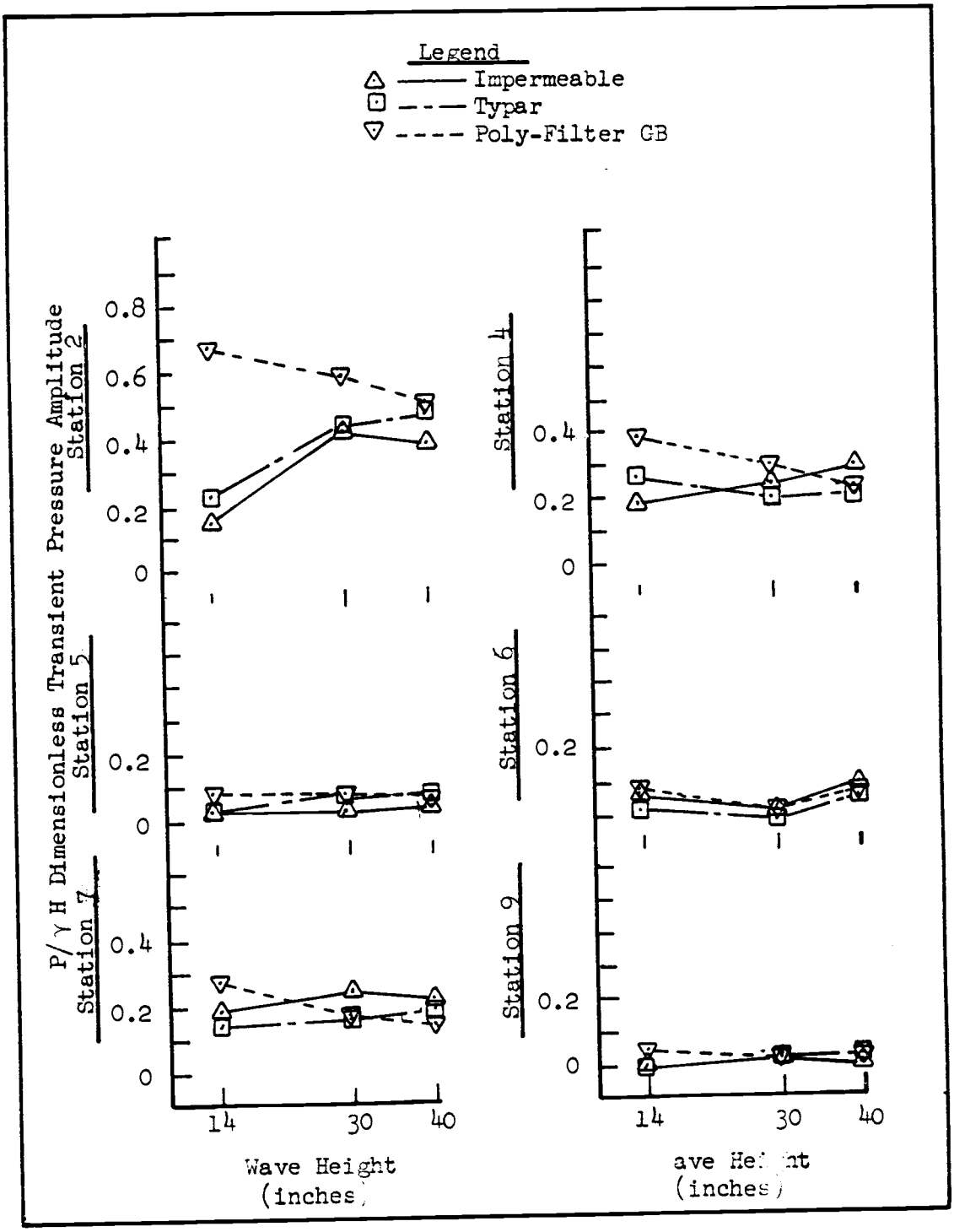

Figure A.10. Dimensionless transient pressure amplitude as a function of wave height, at wave period of 2.80 seconds

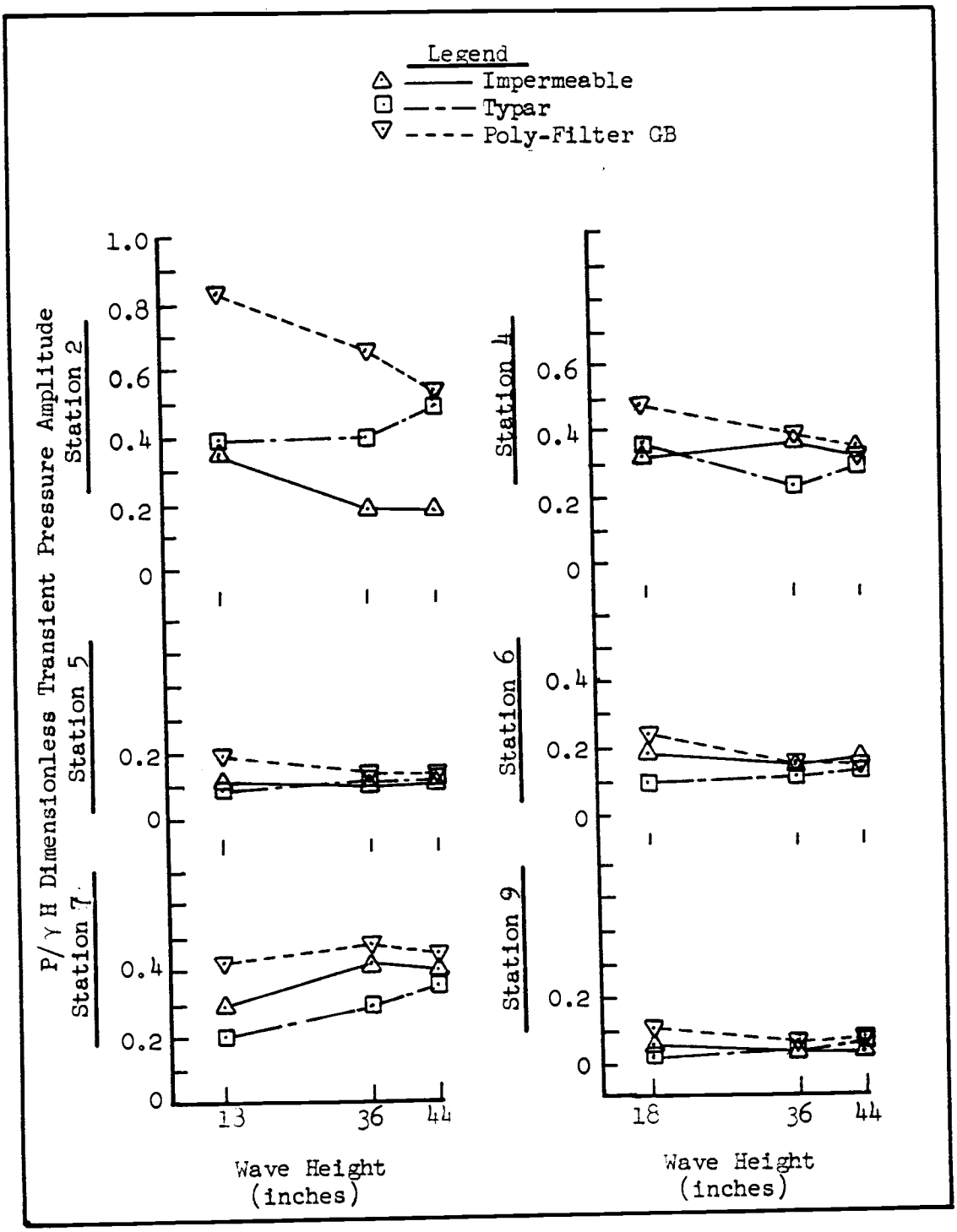

Figure A.11. Dimensionless transient pressure amplitude as a function of wave height, at wave period of 3.95 seconds

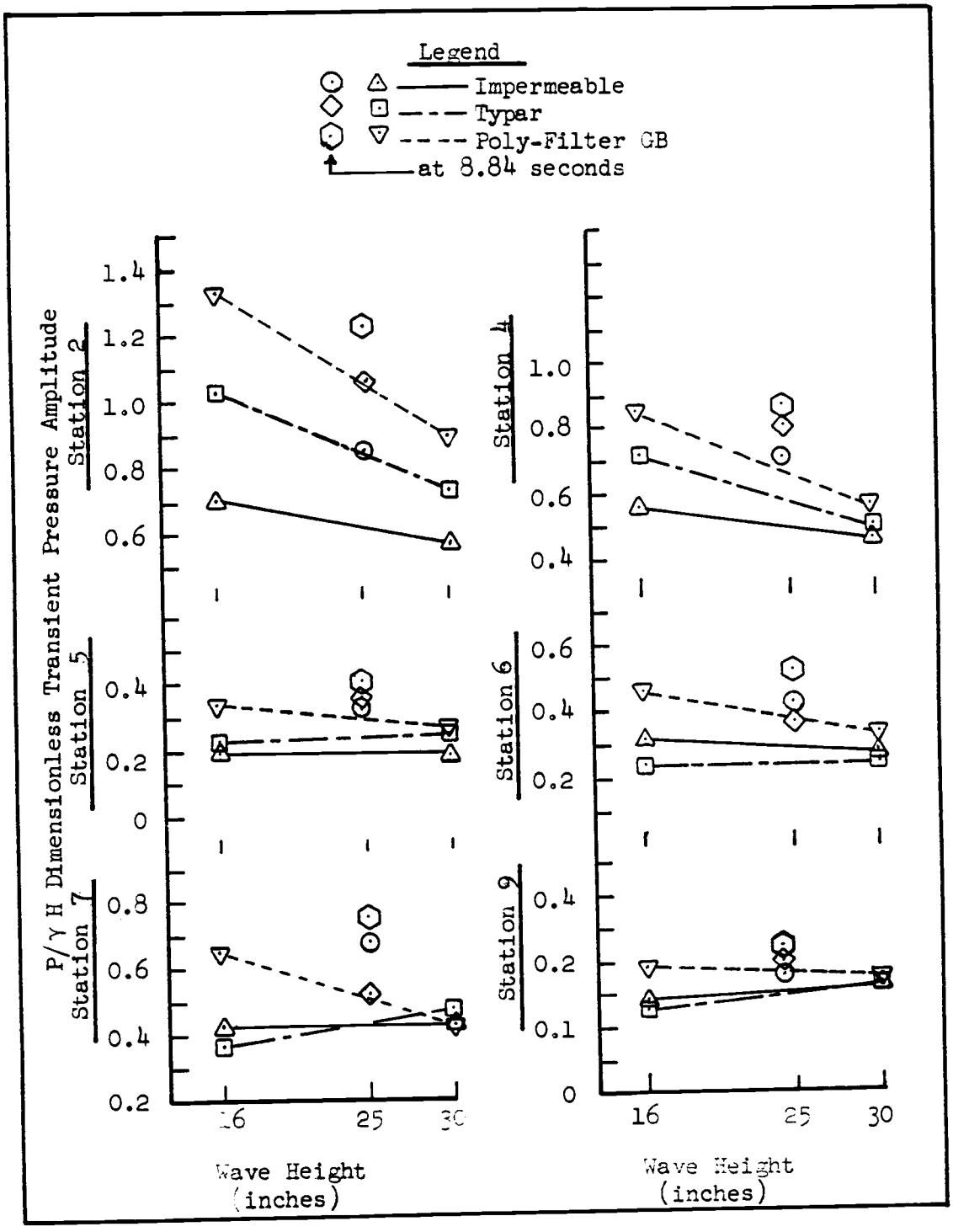

Figure A.12. Dimensionless transient pressure amplitude as a function of wave height at wave periods of 5.59 and 8.84 seconds